Fall 2014

In Silico-Guided Design of Novel-Scaffold Therapeutics Targeting the Dopamine D3 Receptor

Debesai Gaim Hailemicael

Follow this and additional works at: https://dsc.duq.edu/etd

IN SILICO-GUIDED DESIGN OF NOVEL-SCAFFOLD THERAPEUTICS

TARGETING THE DOPAMINE D3 RECEPTOR

A Thesis

Submitted to the Graduate School of Pharmaceutical Sciences

Duquesne University

In partial fulfillment of requirements for

the degree of Masters of Sciences

By

Debesai Hailemicael

December 2014

IN SILICO-GUIDED DESIGN OF NOVEL-SCAFFOLD THERAPEUTICS

TARGETING THE DOPAMINE D3 RECEPTOR

By

Debesai Hailemicael

Approved July 25, 2014

_____

Christopher K. Surratt, Ph.D.
Professor of Pharmacology
(Committee Chair)

Jeffry Madura, Ph.D.
Professor of Chemistry
(Committee Member)

_____

Dr. Rehana K. Leak, Ph.D.
Assistant professor of Pharmacology
(Committee Member)

J. Douglas Bricker, Ph.D.
Dean, Mylan School of Pharmacy and the
Graduate School of Pharmaceutical
Sciences
Professor of Pharmacology-Toxicology

ABSTRACT

IN SILICO-GUIDED DESIGN OF NOVEL-SCAFFOLD THERAPEUTICS TARGETING THE DOPAMINE D3 RECEPTOR

By

Debesai Hailemicael

December 2014

Thesis supervised by Dr. Christopher K. Surratt

Computational methods in drug discovery reduce research time and costs, and only now can be applied to certain psychiatric conditions due to recent breakthroughs in determining the 3D structures of relevant drug receptors in the brain. A new computational technique, *de novo* fragment-based drug design (DFDD), was evaluated employing a dopamine D3 receptor (D3R) crystal structure. Three DFDD approaches – scaffold replacement, ligand building, and MedChem Transformations – were assessed in replacing structural portions of eticlopride, a D2/D3R-specific antagonist, to generate compounds of novel drug scaffold. Pharmacological characterization of the compounds determined their binding affinities at target brain receptor. Analogs of scaffold replacement-generated compounds displayed moderate D3R affinity, suggesting that this DFDD method could be an important drug design tool. The findings support the addition of *in silico* approaches to conventional drug discovery, toward creation of new

therapeutics for depression, anxiety, schizophrenia, addiction and other disorders of the central nervous system.

ACKNOWLEDGEMENT

It is my pleasure to thank those people who made this thesis possible.

In particular I am most grateful to my research advisor, Dr. Christopher K. Surratt, for his patience, understanding, caring, continual guidance and help that made this thesis possible. I am indebted to him not just for his scientific contributions but also for his motivating words, encouraging spirit, personal guidance, financial support and friendship.

I would like to thank my thesis committee members, Drs. Jeffry D. Madura, Rehana K. Leak and Christopher K. Surratt, for their valuable time in extending guidance towards my completing the M.S. program in pharmacology at Duquesne University.

I wish to express my sincere appreciation to Deborah Willson, Jackie Farrer, Mary Caruso, and Nancy Hosni for their unconditional support in administrative affairs. My thanks goes to all my colleagues in the Graduate School of Pharmaceutical Sciences for their help and advice which made my stay at Duquesne University a most pleasant experience. I would like to thank the Graduate School of Pharmaceutical Sciences for both admission and financial support, without which I could not have accomplished my goal of earning a Masters in Pharmacology.

Finally, I would like to pay tribute to the constant support of my family and my friends for their timely direction and emotional support during this experience.

TABLE OF CONTENTS

LIST OF TABLES

LIST OF FIGURES

LIST OF ABBREVATIONS

DFDD   *De novo* fragment-based drug design

D3R   Dopamine D3 receptor

SERT   Serotonin transporter protein

VS   Virtual screening

CADD   Computer-aided drug discovery

MOE   Molecular Operating Environment

MAT   Monoamine transporter protein

GPCRs   G protein-coupled receptors

SBP   Secondary binding pocket

OBS   Orthosteric binding site

TM   Transmembrane

IL   Internal loop

EL   External loop

DA   Dopamine

5-HT   5-hydroxytryptamine (serotonin)

TCAs   Tricyclic antidepressants

MAOIs   Monoamine oxidase inhibitors

SSRIs   Selective serotonin reuptake inhibitors

HTS   High-throughput screening

SAR   Structure activity relationship

HEK293   Human embryonic kidney cells

CHAPTER ONE

1   INTRODUCTION

1.1   Study overview

Depression is a mental disorder characterized by the loss of pleasure, low self-esteem, hopelessness, low energy, and poor concentration, affecting millions around the world. It is a common disabling disorder that considerably downgrades the quality of life, inflicting huge economic costs to individuals and society. Depression pathophysiology is not yet fully understood (Connolly and Thase, 2011). Many classes of antidepressants have been developed since the serendipitous discovery of the first generation of antidepressants: tricyclic antidepressants (TCAs) and monoamine oxidase inhibitors (MAOIs) (Howland, 2010). However, even the current antidepressants continue to carry severe drawbacks: delayed onset of action, intolerable adverse effects, and low efficacy (Bosker et al., 2004; Han et al., 2014; Kessler, 2012; Rosenzweig-Lipson et al., 2007; Manosso et al., 2013). Even the popular selective serotonin reuptake inhibitors (SSRIs) have many intolerable adverse effects. SSRIs adverse effects are due to ubiquitous synaptic increases in serotonin, leading to indiscriminate activation of serotonin receptors, of which there are 14. Most of these adverse effects can be attributed to the $5\text{-HT}_{2A/2C}$ and 5-HT_3 serotonin receptor subtypes. Therefore, drugs that inhibit the serotonin transporter (SERT) and additionally block the 5-HT_{2C} and 5-HT_3 receptors could eliminate most of the adverse effects while retaining antidepressant efficacy (Artigas, 2013).

Developing successful new antidepressants using traditional high-throughput screening (HTS) and knowledge-based structure-activity relationship (SAR) approaches are, however, expensive. It is reported that the addition of computational methods could reduce drug discovery costs of \$0.8 to \$1.2 billion by 50% (Geldenhuys et al., 2006). HTS is laborious, time-

consuming, expensive and broad-targeted while computational methods are fast, cheap, and with less human workload (Acharya et al., 2011). Computational drug design approaches are commonly divided into three categories based on the use and availability of a 3D structure of a target molecule: structure-based, ligand-based, and hybrid (structure/ligand) based drug design (Acharya et al., 2011; Palmeira et al., 2012; Pratuangdejkul et al., 2008; Wilson and Lill, 2011). Computational approaches employ different methods according to the stage of drug design and the challenges faced to identify or optimize lead compounds. The most widely used approaches are de novo fragment based drug design (DFDD) and virtual screening (VS) of chemical libraries. DFDD is more advantageous over VS because it creates a novel ligand with guided physicochemical, pharmacokinetic, and pharmacodynamics properties (Hartenfeller and Schneider, 2011; Loving et al., 2010; Pirard, 2011). Such methods will be used to generate new antidepressant candidates with guided properties.

As proof-of-concept regarding the newer DFDD methods, this study took advantage of a recently published crystal structure of the dopamine D3 receptor complexed with the D2/D3 antagonist eticlopride. This crystal structure allowed development of a computational model that was employed with three DFDD methods, scaffold replacement, MedChem transformation, and ligand building, toward generating novel-scaffold D3 receptor ligands. After fine-tuning these DFDD methods with the well-characterized D3 system, the methods will next be applied to serotonin transporter and receptor proteins implicated in depression, for development of novel antidepressant lead compounds.

1.2   Statement of the problem

The currently used antidepressants have major limitations: delayed onset of action, severe adverse effects, and incomplete remission of symptoms (Penn and Tracy, 2012; Trivedi et al., 2006; Uher et al., 2011).   Only 50% of patients show resolution of symptoms and 30% of population fail to respond to current antidepressants (Al-Harbi, 2012; Berton and Nestler, 2006; Judd, 2001; Kulkarni and Dhir 2009; Pacher et al., 2001).   Such major drawbacks limit the popularity of the current antidepressants and promote the search for new avenues of treatment.

However, the high cost of successful development of novel antidepressants is prohibitive (Khanna, 2012; Janero, 2012; Paul et al., 2010). Fortunately, costs could be considerably reduced if a crystal structure-based homology model of a drug target protein is available that can virtually simulate a native protein environment. Such models allow virtual screening or ligand building of novel scaffolds that can serve as lead compounds (Kar and Roy, 2013; Singh and Singh, 2010). DFDD methodology is an example of such *in silico* drug design approaches that can create novel structures from a known active ligand (Hartenfeller and Schneider, 2011; Mauser and Guba, 2008; Schneider and Fechner, 2005). The **objective** of this study is to refine and evaluate DFDD methods (scaffold replacement, MedChem transformations, and ligand building) via generating novel D3R ligands.

The **hypothesis** of this study is that new de novo fragment-based *in silico* guided drug design methodologies can be used to create unique scaffold D3R ligands, thereby providing tools for rational design of antidepressant drugs.   The recently crystalized high resolution D3R receptor is used as a proof of concept to refine and evaluate the novel methods. Refinement and evaluation is performed by generating new structures of ligands using eticlopride that was cocrystalized with D3R. *Specific aim 1* of this study was to prepare, refine and use a D3R model

3

to generate eticlopride and novel-scaffold ligands via scaffold replacement, MedChem transformation, and ligand building of eticlopride. *Specific aim 2* was to pharmacologically characterize the ligands generated via scaffold replacement, MedChem transformation, and ligand building at D3R stably expressing HEK293 cells.

D3R/eticlopride cocrystal structure

Protein preparation and refinement

D3R/eticlopride model binding pocket

Scaffold replacement of eticlopride

MedChem transformation of eticlopride

Ligand building of eticlopride

Generation of huge number of hit compounds

London dG score and visual inspection

Top hits/their analogs

Pharmacological characterization

Method refinement

D3R antagonists

Method evaluation

Apply DFDD to proteins implicated in depression

Fig 1.1: Scheme showing the general picture of the current study.

The **overall goal** of this study is to identify *in silico* guided drug design methodology that can rapidly and cheaply generate novel ligands to be used as lead compounds. This was performed by evaluating Molecular Operating Environment (MOE) – DFDD methods in generating novel D3R ligands. The study covered four experiments: (a) Scaffold replacement of eticlopride within the D3R binding pocket (b) MedChem transformation of eticlopride within the D3R binding pocket. (c) Ligand building of eticlopride within the D3R binding pocket (**Figure 1.1**). (d) Pharmacological characterization of hit compounds or commercially available analogs using HEK293 cells stably expressing the D3R.

1) Scaffold replacement of eticlopride at D3R. Structurally, eticlopride can be divided into three moieties: aryl, methyl amide linker, and an ethyl pyrrolidine that has an ionizable tertiary amine (**Figure 1.2**). These discrete portions of the drug can be systematically replaced using a pool of over one million fragments. With each replacement a hit compound was generated and ranked based on its virtual affinity (London dG score), visual inspection, and structural novelty
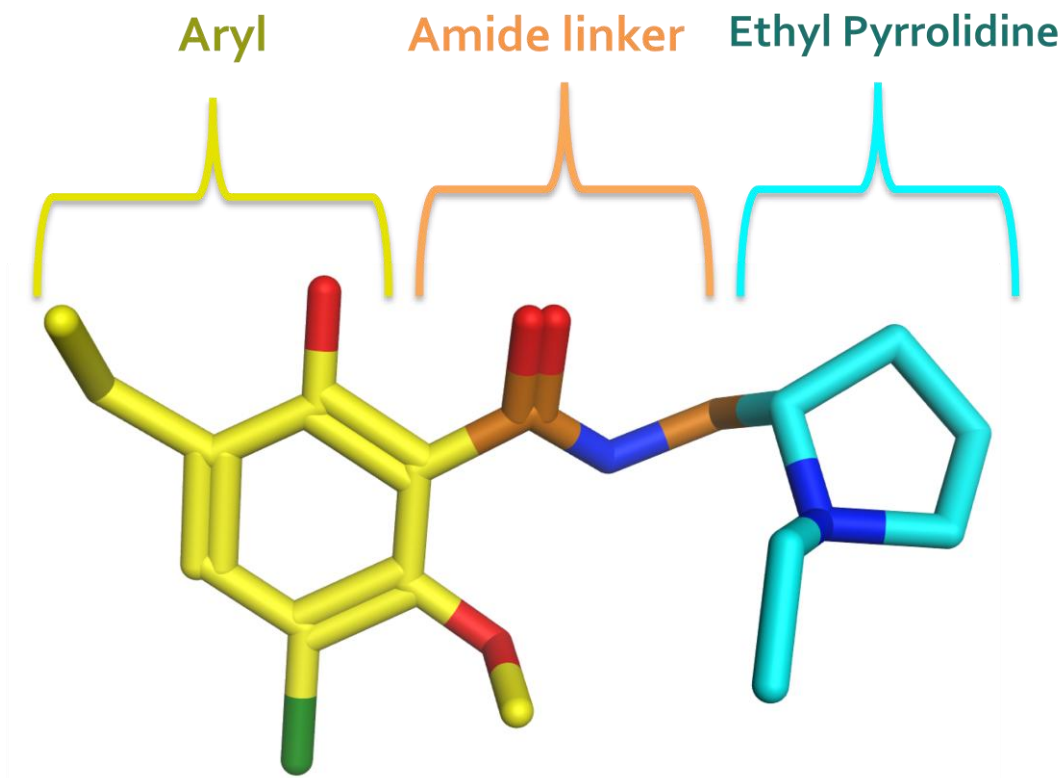
Fig 1.2: The three structural parts of eticlopride used for scaffold replacement: aryl

(green), methyl amide (orange), the aryl (yellow), and ethyl pyrrolidine (cyan) are shown.

2) <u>MedChem transformation of eticlopride at D3R.</u> With this method, the same three segments

of eticlopride were replaced using medicinal chemistry rules of transformations in six different

ways:

3) <u>Ligand building of eticlopride at D3R.</u> Eticlopride was divided into two aryl and methyl

amide ethyl pyrrolidine segments (**Figure 1.3**). With either portion as a starting fragment, the

ligand building method searches the fragment pool to reconstruct the molecule from within its

D3R pocket.
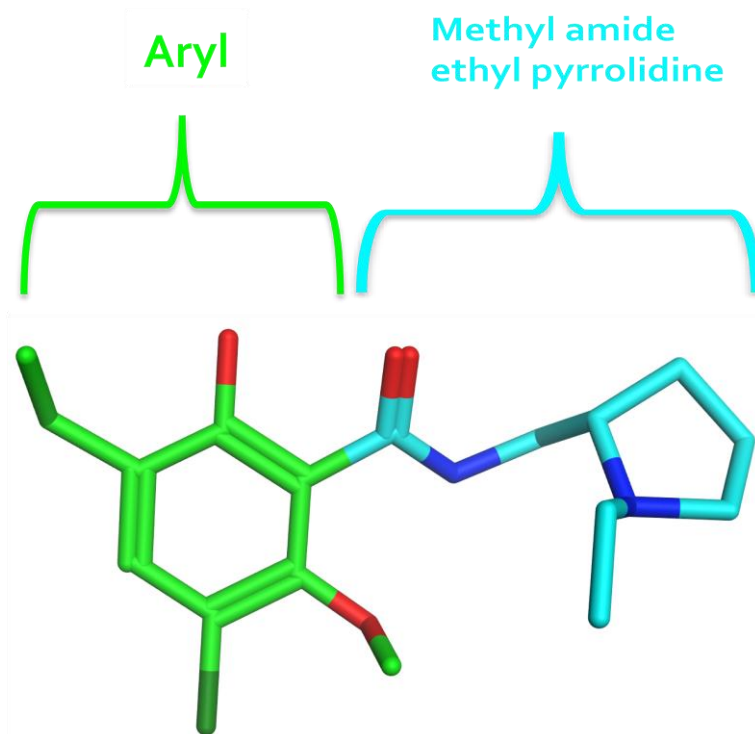
Fig 1.3: The two parts of eticlopride that were deleted. They were deleted and attempted generating them from the undeleted part subsequently. The two parts are shown: the Aryl group (green), and methyl amide ethyl pyrrolidine (cyan).

4) <u>Pharmacological characterization of hit compounds and their analogs</u>. To test the validity of each ligand discovery method, hit compounds or their analogs may be selected, purchased and tested for in vitro binding affinity at the D3R. First, each compound is screened via one-point membrane binding assay using stably expressing D3R HEK 293 cell membranes, to evaluate the ability of the hit to inhibit binding of a radiolabeled D3R ligand. Hits that show at 10 micromolar final concentration a significant inhibition of radioligand binding are then more fully characterized via the membrane binding assay to generate Ki values.

The **overall rational** of this study is that once DFDD methods: scaffold replacement, MedChem transformation, and ligand building are known to be promising methods in generating

novel D3R ligands, such methods can be applied to monoamine transporters (MATs) and 5-HT$_{2A/2C}$ and 5-HT$_3$ receptors to generate potential lead antidepressants that can possibly overcome the current antidepressants severe drawbacks.

1.3   Literature Review

1.3.1   Currently used antidepressant drugs

The first antidepressants, the tricyclic antidepressant (TCA) imipramine and the monoamine oxidase inhibitor (MAOI) and antibiotic iproniazid, were serendipitously discovered over 50 years ago, opening avenues for intensive research in the treatment and etiology of depression (Baldessarini, 1989; Feighner, 1999; Lopez et al., 2009). In the 1960s, identification of their mechanisms of action lead to the postulation of the monoamine hypothesis of depression (Slattery et al., 2004). TCA and MAOI antidepressants exert their effects by increasing synaptic levels of one or more monoamine neurotransmitters. Many antidepressants from the two drug classes were introduced to the market. The second landmark discovery that reformed the treatment of depression was the introduction of fluoxetine in the 1980s, the first marketed selective serotonin reuptake inhibitor (Lopez et al., 2009; Wong et al., 2005). In the last decade, the development and advent of antidepressants significantly increased with drugs that produce their pharmacological effect at monoaminergic systems and beyond (Feighner, 1999; Gumnick and Nemeroff, 2000).

The first line of antidepressants, TCAs and MAOIs, possesses numerous adverse effects and toxic reactions in overdose or in combination with other drugs due to their additionally targeting cholinergic, histaminergic and adrenergic receptors (Gartlehner et al., 2011; Lakatos and Rihmer, 2005; Penn and Tracy, 2012). Development of antidepressants without such adverse effects is possible by designing new ligands that selectively bind to MATs. Consistent with this, the second generation of antidepressants was developed to avoid the adverse effects, increase rate of onset and enhance efficacy, although limited success has been achieved. Even though the naming of the generation depends on the timing of the antidepressant reaching the

market and not structural characteristics, newer generations are reported to be more selective for one or more monoamine transporters (Nishida et al., 2009; Pinder, 1997; Westenberg, 1999). Current antidepressants show full resolution of symptoms for less than 50% of patients, and still suffer from delayed onset of action and many adverse effects. Consequently, new avenues of non-monoamine targeted antidepressant development are under intense research. Such targets include non-monoamine proteins, neuropeptides, and hormone receptors (Bosker et al., 2004; Bourin et al., 2002; Chaki et al., 2006). Potential fast-acting antidepressants have been suggested from preclinical and preliminary clinical trials. These are the NMDA antagonist ketamine, the muscarinic acetylcholine receptor antagonist scopolamine, and the 5-HT2c receptor antagonist SB242084 (Drevets and Furey, 2010; Furey and Drevets, 2006; Lapidus et al., 2014; Murrough et al., 2013; Opal et al., 2013). The identification of fast-acting potential antidepressants is an important advance in the drug development field. Logically, even though depression treatment alternatives and safety have increased significantly since the serendipitous discovery of the first generation antidepressants, the current collection of antidepressants still bears limitations of efficacy and tolerability. Such drawbacks demand immediate attention for development of new antidepressants that overcome these alarming problems.

1.3.2   Computational methods of antidepressant drug discovery

The drug discovery and development path of a novel drug is an uncertain, slow, laborious, expensive, and interdisciplinary process that takes an average of 14 years and a cost of 0.8 to 1.0 billion dollars from concept to clinic (Adams and Brantner, 2006; Dickson and Gagnon, 2004; Ou-Yang et al., 2012; Schacter et al., 1992). Recent advances in HTS and combinatorial chemistry have reduced the labor and time by synthesizing and screening large libraries of compounds (Lahana, 1999; Liu et al., 2004; Maehr, 1997; Mayr and Bojanic, 2009) .

Even though the tools for drug discovery such as HTS have improved and the investment for new drug discovery has significantly increased, the success rate has been very low (Ramesha, 2000; Shekhar, 2008). Drug discovery efforts are exploring new avenues to reduce time and costs while increasing success rates, and one such avenue is computer aided drug discovery (CADD). This method combines computer software, algorithms and the 3D structure of a target in the drug design process. Because of the large quantities of compounds available and the requirement to examine these huge libraries as well as related drug design information in a short period of time, CADD is an appropriate tool to analyze, store, and manage these digital repositories (Song et al., 2009). CADD advancement in the last decade has accelerated lead compound identification and optimization, and is changing the pharmaceutical research approach in drug discovery. It is also reported to reduce drug design costs by 50% (Rester 2008; Taft et al., 2008; Talele et al., 2010).

CADD has considerable advantages over the traditional HTS drug discovery approach of robotic assays of a collection of drug-like compounds for biological activity. These advantages are i) less prior drug design knowledge is needed ii) higher hit rates, iii) lower costs and workload without affecting lead discovery success, and iv) less preparation, development, and validation are required (Sliwoski et al., 2014; Warren et al., 2006). CADD is most successful when a 3D structure of the target protein is available either a crystal structure or homology model. CADD has helped in the drug discovery of compounds that have made their way to the market for the treatment of many diseases. Examples include the 1998 fibrinogen antagonist tirofiban (Hartman et al., 1992; Kobayashi and Naito, 2000), the 1995 carbonic anhydrase inhibitor dorzolamide (Kobayashi and Naito, 2000; Vijayakrishnan, 2009), and the 1981 antihypertensive captopril (Talele et al, 2010).

CADD can be broadly classified into ligand-based, structure-based, or hybrid (structure/ligand)-based categories. When the 3D structure of a target protein is available and employed, the method is known as structure-based drug design. The basic concept in this approach is that a compound that favorably interacts with and fits into the protein's ligand binding pocket is considered to have biological activity in that protein (Sliwoski et al., 2014). In contrast, the ligand-based method uses "model" ligand information alone to predict the activity of candidate ligands; activity is predicted based on the similarity to established active ligands, without the knowledge of the target protein structure. A pharmacophore feature is created from the "model" ligands that have the same biological activity, selecting common spatial orientation features that are necessary for biological activity (Aparoy et al., 2012; Jain, 2004; Lundstrom, 2009; Martin et al., 1993; Martin, 1992). The hybrid (structure/ligand)-based approach employs the ligand-based method in the context of a target protein (Immadisetty et al., 2013).

The two most important methods in computational drug design are DFDD, and virtual screening (VS).

1.3.2.1 De novo fragment drug design

DFDD is a computational approach that generates novel chemical structures by replacing, building, and/or mutating a known active ligand as well as assembling fragments to guide the generation of drug-like compounds with defined physical, chemical and biological activities. Since its introduction in 1991, DFDD is getting greater attention as alternative to HTS from the pharmaceutical industry and academia (Erlanson, 2012; Krueger et al., 2009; Mauser and Guba, 2008). HTS searches for a lead compound out of the available 10^{60-100} drug-like and chemically feasible compounds to find the favorable lead compound. The comprehensive search of such "chemical space" is time-consuming, expensive and laborious. However, this challenge

can be overcome by using DFDD, systematically building or creating novel virtual structures thought to have biological activity at a specific target protein (Lipinski and Hopkins, 2004; Schneider, 2002). Even though DFDD started as a structure-based approach, it was strengthened with the ligand-based approach and is now most effective when the hybrid (structure/ligand)-based approach is employed. Unlike VS, DFDD does not search to fish out biologically active compounds from a database of compounds, but "creates" new chemical scaffolds. As with CADD, DFDD, if used within a protein structure, invents new hypothetical virtual structures that fit the receptor binding pocket within a specified space (Hartenfeller et al., 2012). Such methods were developed to solve the problem of generating novel structures and lead optimization by employing medicinal chemistry rules and algorithms (descriptor filters) that could guide the design of chemicals that are accessible and display the desired pharmacokinetic and pharmacodynamics properties (Kutchukian and Shakhnovich, 2010).

Recently, DFDD approaches were able to develop hit compounds that were synthetically accessible and with modest potency. An example is the design of human polo-like kinase 1 (PIK1) inhibitors using "design of genuine structures" (DOGS) software (Schneider et al., 2011; Spankuch et al., 2013). Despite the considerable success of DFDD, it has significant challenges to overcome: generating chemical structures that are invalid or non-drug like, and poor synthetic plausibility (Honma, 2003; Liu et al., 2007). This challenge is the reason why very few de novo synthesis packages have been exposed to extensive practical evaluation (Mauser and Guba, 2008; Hartenfeller et al., 2012). To partially overcome DFDD drawbacks, medicinal chemistry knowledge about the returned hits (chemical space) should be incorporated as algorithms whenever possible. This current study has applied DFDD to generate novel D3R ligands using MOE software packages (scaffold replacement and MedChem transformations).

1.3.2.2 Scaffold replacement ("Scaffold hopping")

Scaffold replacement is a method that is employed to design novel chemical structures via replacing a part (scaffold) of a biologically active ligand while keeping the remaining chemical structure. The notion of "scaffold replacement" was first introduced and coined in 1999 by Schneider and colleagues to generate molecular structures with similar functions but with very different chemical backbones (Schneider et al., 1999). Scaffold replacement was developed to discover novel chemical structures starting from a well-known compound by changing the central structure of the compound (Cramer et al., 2004). And it was also developed to modify the physiochemical and pharmacokinetic properties of lead compounds that are identified by HTS or VS (Sun et al., 2012). To perform a scaffold replacement, a known bioactive ligand and a known target are essential; however, for a new target, HTS and possibly VS are the only promising approaches to generate target specific active lead compounds. Therefore, it is unwise, ineffective and costly to use HTS for screening huge databases using a known ligand-protein complex structure (Hopkins and Groom, 2002; Pang 2007; Russ and Lampel, 2005; Sun et al.,2012). Scaffold replacement is not limited to structure-based drug discovery but can also be used in ligand-based drug design. The technique has been effectively applied in many drug discovery projects; at least 200 PubMed citations are associated with scaffold replacement (Lloyd, 2013).

Several methods of scaffold replacement have been proposed and employed in novel drug design, one of which is the MOE scaffold replacement package, an extension of CAVEAT scaffold hopping software (Lauri and Bartlett, 1994). This program replaces a scaffold by selecting the bonds that link the scaffold (linkers) and the remaining part of the known ligand (R-groups). Such selection is defined by exit vectors that separate the selected scaffold and the

retained R-group. The selected scaffold is then replaced by fragments that satisfy the bond length and angle, hybridization, and chemical nature of the R-groups to form a covalent bond between the new fragment and the retained R-groups (**Figure 1.4**). Scaffold replacement is performed using fragment databases that are formed by decomposition of synthesizable compounds into synthesizable fragments that can retrosynthesize compounds that could be accessible.

Scaffold replacement in MOE was first performed by the developers of MOE software, Chemical Computing Group (CCG) (Deschenes et al, 2007; Grimshaw, 2010). Grimshaw evaluated whether MOE scaffold replacement could predict the structure of a clinical candidate (BRIB-976) from its initial hit ligand (1-(3-(*tert*-butyl)-1-methyl-1*H*-pyrazol-5-yl)-3-(4-chlorophenyl) urea). The scaffold replacement was performed by deleting the chlorophenyl group of the initial hit and generating new structures by growing the retained part. The study was successful in showing that scaffold replacement of the initial hit could generate similar structures to that of the clinical candidate. Nevertheless, three pharmacophore features were used to guide the resulting hits. The generated potential hits were structurally similar to BIRB-976 but their *in vitro* binding affinities were not determined and compared with the parent compound and BIRB-976.
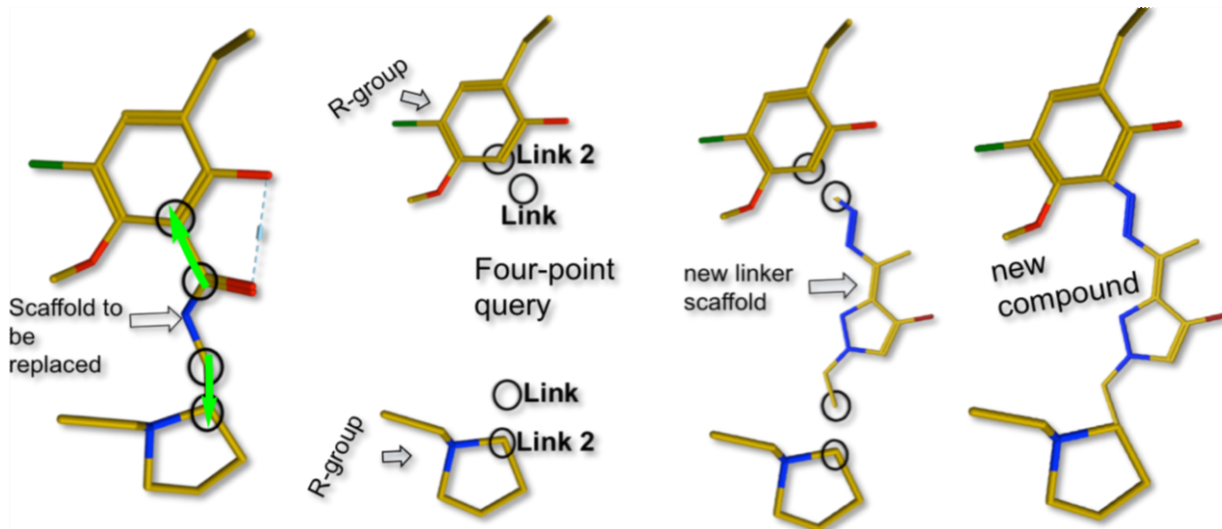
Fig 1.4: The molecular workflow of scaffold replacement: Example of eticlopride amide linker scaffold replacement. Eticlopride has two R-groups and an amide linker (scaffold) to be replaced, and two exit vectors (green arrows). The (**Linker, linker2**) feature is employed to preserve the aryl R-group and the (**Linker, Linker3**) feature is used to retain the pyrrolidine ring R-group. Linker is a vector site that connects the scaffold and R-groups. A four-point query is created to replace the scaffold. Searching the database of fragments generates a new compound.

1.3.2.3 MedChem transformation

MedChem transformation is an approach used to generate novel chemical structures using virtual "medicinal chemistry rules" on a known biologically active compound. In a nutshell, it can be defined as the mutation of a portion of a biologically active compound to generate new structures or improve physicochemical, pharmacokinetic, potency and anti-

toxicological properties. Lead optimization demands medicinal chemistry knowledge, and at times, searching of large databases. Once a lead compound is identified, chemists propose promising structures using SAR, generate libraries of small molecules, or hybridize the lead compound via its coupling to structures that are known to have desired properties and activities. Such methods are expensive, time-consuming and dependent on the experience of the chemist. To overcome these challenges, automated virtual medicinal chemistry transformation rules can be used. The transformation rules used are medicinal chemistry drug design common rules collected from many years of experience in drug discovery programs (Segall et al., 2009; Stewart et al., 2006; Therrien et al., 2012). Transformations could include functional group changes, bioisostere replacement, ring closing or opening, and partial structure replacement to generate novel structures. Transformations could run in multiple iterations to generate large and completely dissimilar structures to the parent compound; the MOE MedChem transformations program allows a maximum of 50 iterations. The smaller the number of transformation iterations, the smaller the structural change of the parent compound. For successful use in drug discovery projects, MedChem transformation should generate diverse, novel, accessible, and stable structures (Khedkar, 2010; Segall et al., 2011). The main limitation of this method as with any other DFDD is that generated compounds may not be synthesizable, drug-like, or stable. MedChem transformations could be performed as a bioisosteric replacement that maintain certain properties, or a ring replacement that modifies the properties of the parent compound. With MOE MedChem transformation any part of a parent compound could be replaced and transformed by either growing a small fragment or mutating a known bioactive compound.

1.3.3   The eticlopride-dopamine D3 receptor structure complex

Dopamine, an endogenous catecholamine, has extensive effects in neurons as a neurotransmitter and in non-neuronal tissues as an autocrine or paracrine agent. In the CNS, dopamine binds to its receptors to regulate locomotion, learning, working memory, cognition, and emotions (Chien et al., 2010; Drozak and Bryla, 2005). The D3R has been linked to schizophrenia, Parkinson's disease and addiction (Newman, et al., 2012; Hackling and Stark, 2002). There are five dopamine receptor subtypes, all G protein-coupled receptors (GPCRs) and named D1 through D5. From a sequence homology and G protein coupling, the five subtypes can be classified as "D1-like" (D1R and D5R), which couple to stimulatory G proteins, or "D2-like" (D2R, D3R and D4R), which couple to inhibitory G proteins (Sokoloff et al., 1990).

The dopamine D3 receptor was of interest in the present studies because of its recent cocrystallization with the D2R/D3R-specific antagonist, eticlopride (Feng et al., 2012; Hackling and Stark, 2002). The determination of the eticlopride-D3R structure was essential not only for combating disorders where D3R is implicated, but to evaluate and refine computational methods before applying them to target proteins. Given the good (3.2 Å) resolution of the D3R structure and its being a GPCR, a receptor class serving as the target for more than 30% of FDA-approved drugs (Overington et al., 2006). The eticlopride-D3R complex is an ideal tool for evaluation, refinement and validation of computational methods.

Like essentially all GPCRs, the D3R has seven transmembrane helices (TM1- TM7), three intracellular loops (IL1 - IL3) and three extracellular loops (EL1 - EL3). The crystal structure of the D3R indicated that eticlopride binds within the orthosteric-binding site (OBS), encircled by the upper halves of TMs 3, 5, 6 and 7. Dopamine is also reported to bind in the OBS, and this pocket is responsible for the efficacy and potency of D3R ligands. A secondary

binding pocket (SBP) is also found, enclosed by TMs 1, 2, 3, 7 and ELs 1 and 2 (**Figure 2.5**). The SBP is thought to be important for differentiating D2R and D3R ligands (Newman et al., 2012).

The presence of eticlopride helped with the stabilization of D3R receptor crystal structure by providing high thermostability. This substituted benzamide was originally developed as a potential antipsychotic drug and contributed to a better understanding of CNS dopamine receptor functions. Eticlopride is currently being used only for research purposes because it causes severe adverse effects (Martelle and Nader 2008; Giuliani and Ferrari 1997). Eticlopride has three- to six-fold greater affinity for D2R over D3R, with Ki values of 0.23 ± 0.05 nM and 0.78 ± 0.36 nM at MN9D cells, respectively (Tang et al., 1994). The eticlopride-D3R complex was used in this study to refine and evaluate the DFDD methods before applying them to depression-related brain targets
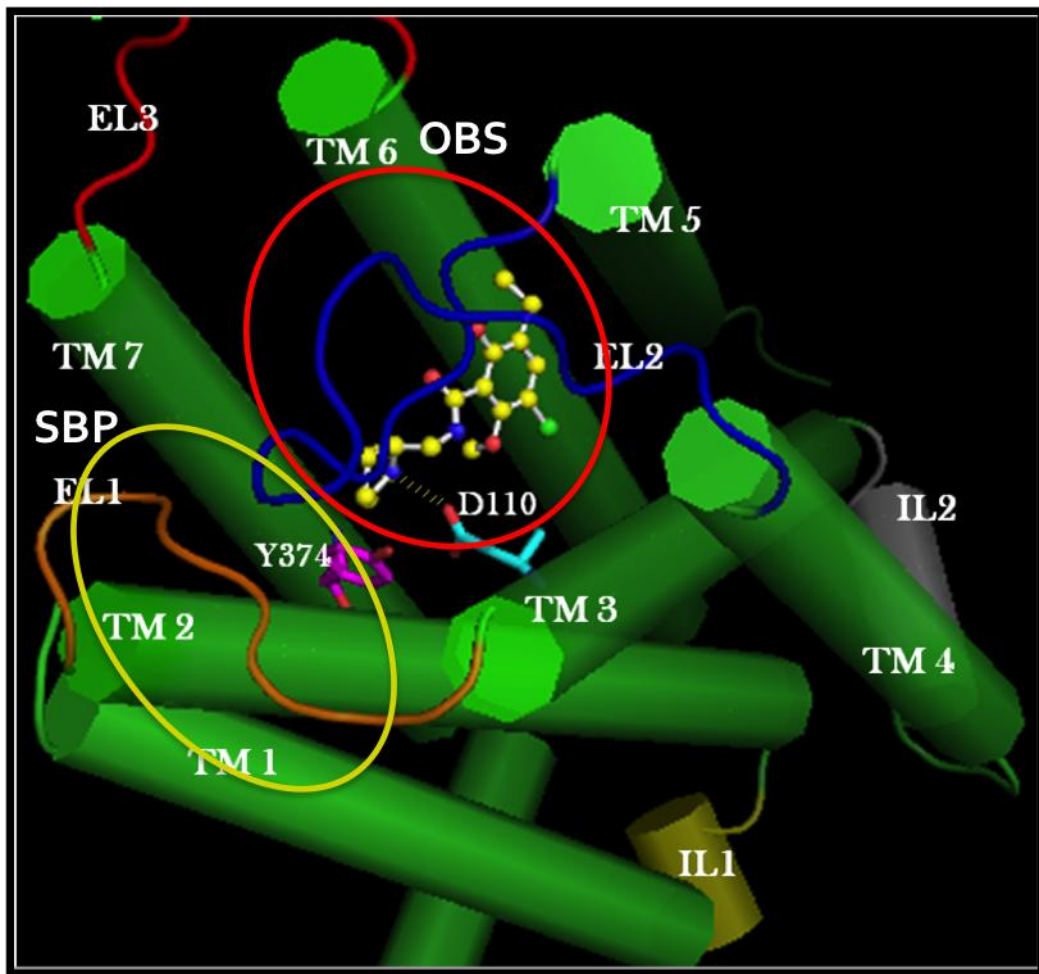
Fig 1.5: D3R structure and binding pockets. The seven transmembrane helices (green cylinders annotated TM 1 - 7) are shown, as are the extracellular (EL1, orange; EL2, blue; EL3, red) and intracellular (IL1, yellow; IL2, gray) loops. Eticlopride (yellow, ball-and-stick) is bound in the OBS (red circle) and forms an ionic interaction with the TM3 Asp-110 side chain. The SPB is also delineated (yellow circle) by TMs 1, 2, 3 and 7.

To summarize, currently used antidepressant drugs are largely effective in alleviating depression symptoms but have number of drawbacks; improved antidepressants are needed. However, CNS drug development costs are beyond the reach of pharmaceutical companies and academic labs. Methods that reduce the cost of CNS drug discovery are essential to attain this goal. Computational methods have been reported to identify and optimize lead compounds cheaper and faster. Novel DFDD-based computational methods have been designed to identify and develop lead compounds using virtual medicinal chemistry rules that save time, cost and personnel resources. Scaffold replacement, MedChem transformations, and ligand building are such methods, and were employed in the present study. Before applying these DFDD methods to target proteins such as the SERT, NET, 5-HT$_{2C}$R, 5-HT$_{2C}$R and 5-HT$_3$R in generating superior antidepressant lead compounds; methodology proof-of-concept was investigated using a well-characterized system, the D3 dopamine receptor. Using a recently crystallized eticlopride-D3R complex as template, structural fragments of the drug eticlopride were replaced or manipulated while within the antagonist binding pocket of the D3R crystal structure model, using the scaffold replacement, MedChem transformations, and ligand building methods.

CHAPTER TWO

2. MATERIALS AND METHODS

2.1 Materials and Equipment

2.1.1 Facilities

Laboratories - Mellon Hall of Science, Room 408, 414, 416, 456, 457 and 459

2.1.2 Cell lines

Human embryonic kidney 293 cells stably expressing wild type human D3R
Dr. Robert Luedtke, University of North Texas Health Sciences Center, Fort Worth, Texas

2.1.3 Chemicals and Drugs

Acetic acid, glacial
Fisher Scientific, Pittsburgh, PA

Ampicillin, sodium salt
Acros, Carlstad, NJ

Compressed carbon dioxide
Air Products, Pittsburgh, PA

Calcium chloride
Sigma-Aldrich Co., St. Louis, MO

Dimethylsulfoxide (DMSO)
Sigma Chemical Co., St. Louis, MO

D-(+)-Glucose
Sigma-Aldrich Co., St. Louis, MO

Dulbecco's Modified Eagle Medium (DMEM)
Thermo Scientific, Logan, UT

Dulbecco's Phosphate Buffered Saline (DPBS), Ca/Mg-free
Cambrex Bioscience Inc., Walkersville, MD

EDTA
Sigma-Aldrich Co., St. Louis, MO

Ethanol, 200 proof
Pharmaco Products Inc., Brookfield, CT

Ethanol, HPLC grade
Acros, Carlstad, NJ

Eticlopride HCl
Sigma-Aldrich, Inc., Allentown, PA

Fetal bovine serum
Thermo Scientific, Logan, UT

HBSS/modified
Hyclone, Logan, UT

[^{3}H]-Spiperone
Perkin Elmer, Foster City, CA

G-418 sulfate
Clontech Laboratories Inc., Mountain View, CA

Isopropanol (DNase, RNase and protease free)
Fisher Scientific, Pittsburgh, PA

L-Glutamine
Invitrogen, Carlsbad, CA

Penicillin-Streptomycin
Gibco-BRL, Grand Island, NY

Trypsin-EDTA, 10X
Gibco-BRL, Grand Island, NY

Penicillin-Streptomycin
Toronto Research Chemicals Inc., North York, ON Canada

Potassium chloride
Sigma-Aldrich Co., St. Louis, MO

Potassium phosphate, monobasic
Sigma Chemical Co., St. Louis, MO

Sodium Chloride
Sigma-Aldrich Co., St. Louis, MO

Sodium Hydroxide
Fisher Scientific, Pittsburgh, PA

Sodium Hydroxide, 2N solution
Fisher Scientific, Pittsburgh, PA

Sodium Hydroxide, 12N solution
Fisher Scientific, Pittsburgh, PA

Tris-EDTA buffer (DNase, RNase and protease free)

Acros, Carlstad, NJ

Tris-HCl salt
Sigma Chemical Co., St. Louis, MO

Triton X-100
Acros, Carlstadt, NJ

2.1.4   Materials

Cell culture flasks, 75cm^2
Corning Inc., Teterboro, NY

Cell culture grade water
Hyclone, Logan, UT

Cell culture plates (10, 25cm)
Fisher Scientific, Pittsburgh, PA

Centrifuge tube, 15ml
Corning Inc., Horseheads, NY

Centrifuge vials, 1.5ml
Corning Inc., Horseheads, NY

Culture tubes, disposable
Fisher Scientific, Pittsburgh, PA

Eppendorf microcentrifuge tubes, 1.5 ml
Fisher Scientific, Pittsburgh, PA

Falcon tubes, 14ml
Fisher Scientific, Pittsburgh, PA

Falcon tubes, 50ml
Fisher Scientific, Pittsburgh, PA

Filter unit, sterile
Millipore, Billerica, MA

Parafilm
Fisher Scientific, Pittsburgh, PA

Pasteur pipettes, disposable
Fisher Scientific, Pittsburgh, PA

Pipette tips, disposable Redi-Tips TM (1, 10, 200, 1000 µl)
Fisher Scientific, Pittsburgh, PA

Polypropylene tubes
Fisher Scientific, Pittsburgh, PA

Respirator
Fisher Scientific, Pittsburgh, PA

Scintillation vials
Fisher Scientific, Pittsburgh, PA

Serological pipettes, sterile disposable (5, 10, 25 ml)
Fisher Scientific, Pittsburgh, PA

Syringes, sterile (10 ml)
Fisher Scientific, Pittsburgh, PA

Tissue culture plates, sterile (6 well, 24 well)
Fisher Scientific, Pittsburgh, PA
Sarstedt Inc., Newton, NC

Whatman GF/B filter
Schleicher and Schuell, Keene, NH

2.1.5   Equipment

Analytical balance
Mettler Inc., Toledo, OH

Bottletop dispenser
Brinkmann Instruments Inc., Horseheads, NY

Cell culture incubator
Forma Scientific, Worcester, MA

Centrifuge Model 228
Fisher Scientific, Pittsburgh, PA

Centrifuge Model 5415 C
Eppendorf Scientific Inc., Hauppauge, NY

Confocal laser microscope, Leica TCS-SP2
Leica Microsystems Inc., Exton, PA

Dispensing Eppendorf pipetter (50 ml)
Brinkmann Instruments Inc., Hauppauge, NY

Isotemp incubator
Fisher Scientific, Pittsburgh, PA

Lab freezers and refrigerators
Forma Scientific, Worcester, MA

Liquid Scintillation Analyzer
Packard Instruments Co., Meriden, CT

Millipore Milli-Q and Elix
Millipore Corporation, Billerica, MA

Mixer (Style: 37600)
Thermolyne Corporation, Duqubue, IA

NapFLOW Laminar airflow unit
Fisher Scientific, Pittsburgh, PA

ORBIT Shaker
Lab-line Instruments Inc., Melrose Park, IL

pH meter AB15
Fisher Scientific, Pittsburgh, PA

Pipet-aid
Drummond Scientific Co., Broomall, PA

Pipetman (P-2, P-10, P-20, P-100, P-200, P-1000)
Mettler Toledo Company, Woburn, MA

Universal Vacuum System UVS 400
Savant Instruments Inc., Holbrook, NY

UV-Visible spectrophotometer, DU 530
Beckman Instruments Inc., Fullerton, CA

Vacuum pressure pump
Barnant Co., Lake Barrington, IL

Vertex-2 Genie
Scientific Industries Inc., Bohemia, NY

Water bath, 180 series
Precision Scientific, Winchester, VA

Water bath, Iso TEMP 205
Fisher Scientific, Pittsburgh, PA

Weighing scale
Denver Instruments Co., Denver, CO

2.1.6 Computer software

Adobe Acrobat Reader 7.0
Adobe Systems Inc., San Jose, CA

Adobe Acrobat Writer
Adobe Systems Inc., San Jose, CA

ChemBioDraw 13.0
CambridgeSoft Corporation, Cambridge, MA

GraphPad Prism 6.0
GraphPad Software, San Diego, CA

Microsoft Office Word & Excel Mac 2011
Microsoft Corporation, Seattle, WA

Molecular Operating Environment 2010.06 /2013.08
Chemical Computing Group, Montreal, Canada

PyMOL
The PyMOL Molecular Graphics System, Version 1.5.0.4 Schrödinger, LLC.
University of California, Los Angeles

2.2 Methodology and procedure

2.2.1 Computational methods

2.2.1.1 Scaffold replacement.

This technique is employed to develop novel structures via replacing the central portion ("scaffold") of a known ligand while keeping its remaining parts (R-groups). The scaffold is replaced in hopes of generating ligands with more selective biological activity and fewer adverse/side effects (Sourial, 2007) (**Figure 2.1**). Scaffold replacement in MOE occurs within the receptor binding pocket and is based on the CAVEAT software (Lauri and Bartlett, 1994), which requires at least two bonds connecting the scaffold to the R-groups of a known ligand.
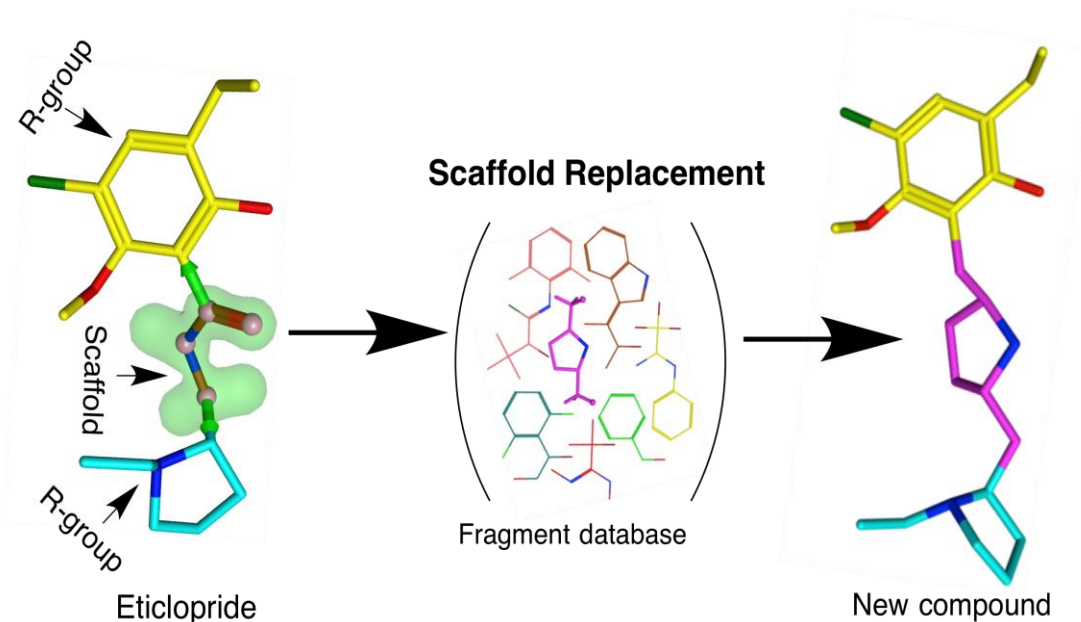
Figure 2.1 Scaffold replacement of the amide linker of eticlopride. Eticlopride, a D3R-selective antagonist, has two R-groups (yellow and cyan) to be retained and an amide linker (green cloud) to be replaced. MOE searches a virtual fragment database to generate new potential ligands.

The method uses fragments to replace the identified scaffold, and when the bond length, angle, geometry and hybridization of the retained R-groups and the fragments to replace the scaffold match, a new structure is formed. Moreover, MOE scaffold replacement allows the user to create pharmacophore features based on an approach called Recore (Maass et al., 2007). Pharmacophore features can be created to specify key portions of the ligand that must be retained, as well as to guide specific interactions between the generated structures and the receptor. Generated structures that clash with the walls of the receptor pocket are eliminated; a volume inclusion or exclusion component may be used to specify the space accessible to the generated structures. To generate drug-like structures, MOE scaffold replacement allows use of QuaSAR descriptor filters, pharmacophore features and Model files. The detailed and technical aspects of scaffold replacement are reported elsewhere (Grimshaw, 2010; Sourial, 2007). The general procedure of scaffold replacement is depicted below (**Figure 2.2).**
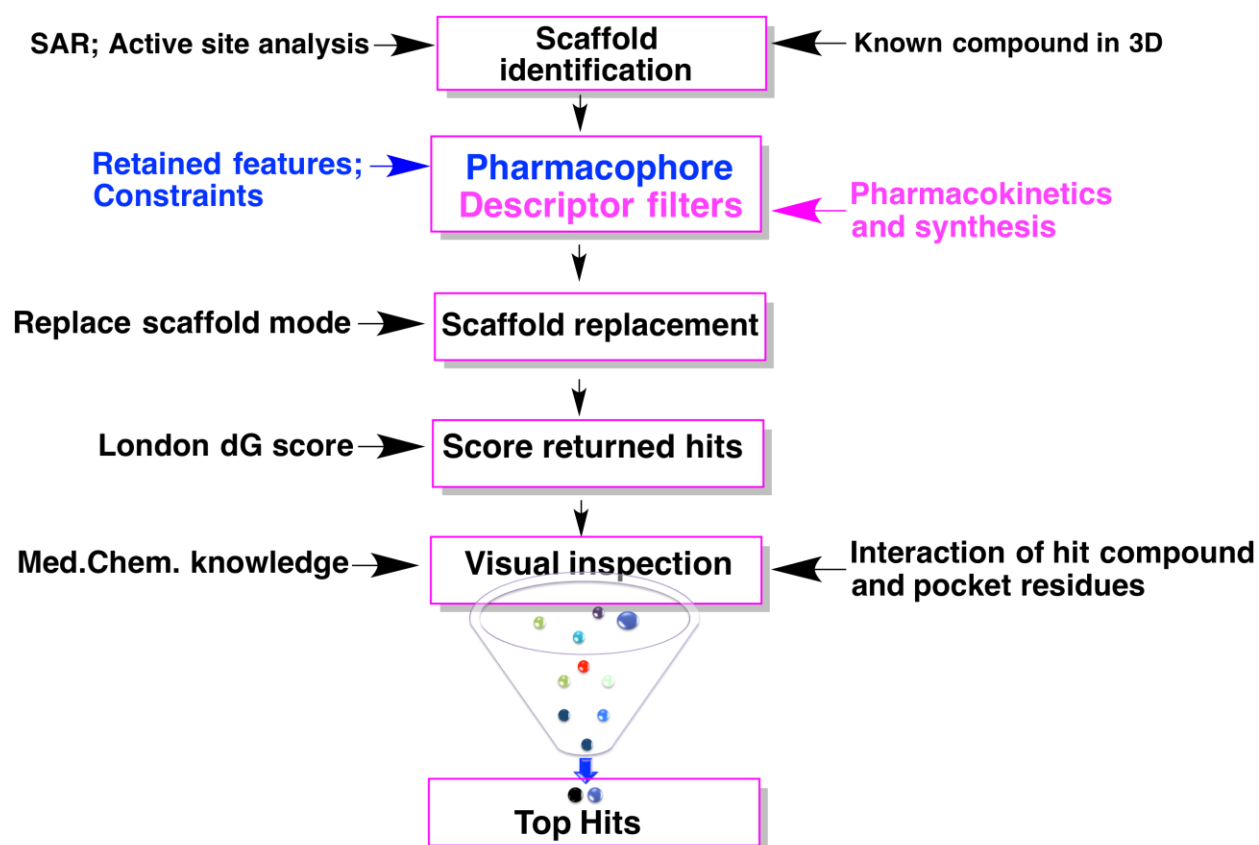
Fig 2. 2: Schematic representation of scaffold replacement and selection of hit compounds.

In the present study, the D3R bound to the high affinity D2/D3 antagonist eticlopride was employed as a computational template. The model was built based on the recent 3.15 Å-resolution D3R-eticlopride cocrystal (Chien et al., 2010) (Figure 3). The eticlopride conformation within the receptor pocket was used as a starting point, and scaffold replacement was carried out using MOE (MOE 2013.08). The D3R computational model was used to evaluate and refine DFDD methodologies: scaffold replacement, MedChem transformations, and ligand building. This proof of concept exercise was undertaken first with a structurally well-defined drug-receptor template to understand, evaluate, and refine the novel methods before applying them to proteins of interest that are implicated in depression.
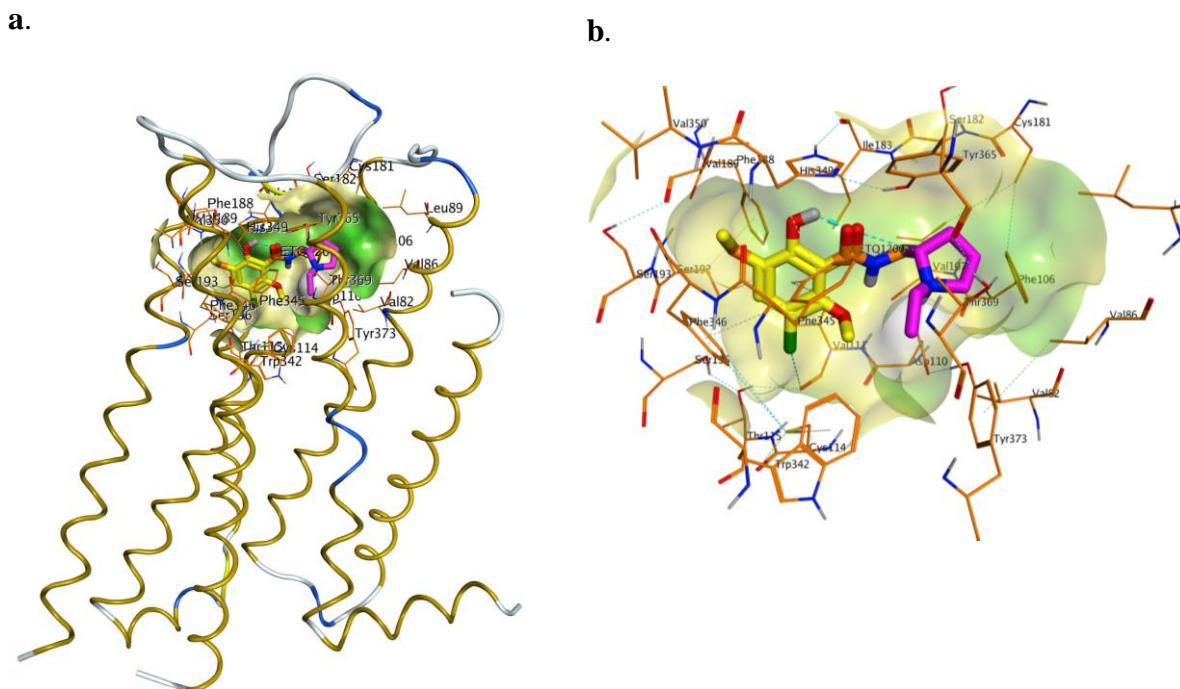
Fig 2.3: D3R receptor and its antagonist-binding pocket occupied by eticlopride. Panel **a** represents eticlopride in the D3R binding pocket. Eticlopride (aryl group in yellow, amide linker in orange, and ethyl pyrrolidine group in pink) is shown within the antagonist-binding pocket (cloud) of the D3R. Hydrophilic (green), charge-neutral (yellow) and hydrophobic (white) regions of the pocket are indicated, as are receptor side chains (annotated orange sticks) in the vicinity of the pocket. The seven D3R transmembrane α-helices (gold coils), helix-breaking turns (blue) and intervening loops (gray) are indicated. Panel **b** represents zoom view of the binding pocket region.

A pharmacophore feature ("Don2|Cat&Don", of 1.5Å) was used to preserve the biologically important receptor interaction with the tertiary amine of the ethylpyrrolidine ring of eticlopride. "Don 2" denotes a projected location of potential H-bond acceptors, "Don" denotes an H-bond donor heavy atom, and "Cat" denotes a cationic heavy atom like nitrogen (**Figure 2.**

4). This pharmacophore feature depicts the tertiary amine that forms a salt bridge with the amine-recognizing aspartic acid 110 in TM3. Macromolecular X-ray crystal structures may have defects due to poor resolution that includes missing and misplaced residues, loops that are altogether absent, and flexible regions that have positional misplacement. Such defects should be corrected before performing any computational analysis. Due to relatively modest resolution that resulted in some defects, the D3R crystal structure was corrected. Missing and misplaced residues and loops were corrected using the protein preparation mode protocol available in MOE. Ligx mode was also used to add hydrogen atoms, set protonation states, energy-minimize the complex, and immobilize atoms 4 angstroms away from the ligand-binding site.

The scaffold of eticlopride was identified based on structure-activity relationships of eticlopride analogs and active site analysis of the D3R pocket with ligand interaction and electrostatic maps. The SAR of eticlopride suggests that heteroaromatic substitution of the extended aryl amide increases affinity, while the amide linker is important for synthesis (Heidbreder and Newman, 2010). The tertiary amine in ethyl pyrrolidine is reported to be highly crucial for the high affinity and pKa of eticlopride (Chien et al., 2010). Active site analysis showed which residues of the pocket interact with eticlopride's features and revealed the sites of hydrophobic, hydrogen donor and hydrogen acceptor residues. Scaffold replacement was performed using the "select scaffold" mode in MOE. The aryl and ethylpyrrolidine moieties were replaced using a database of 800,000 fragments. First, the ethyl pyrrolidine portion was replaced without altering the remainder of the molecule. The "hit" compounds returned from the search were ranked based on London dG score and visual inspection. The top hits were further modified by replacing the previously retained ethyl pyrrolidine moiety, resulting in new potential scaffolds.
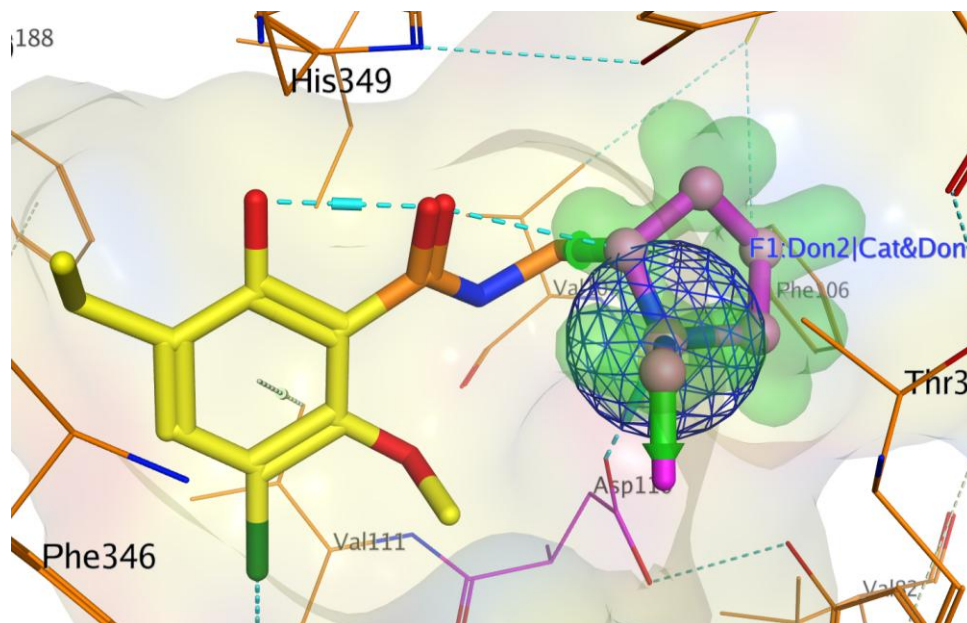
Fig 2.4: Scaffold replacement of eticlopride within the D3R antagonist pocket. A pharmacophore feature, Don2|Cat&Don of 1.5 Å radius (blue sphere), was created to preserve the biologically important interaction (cyan) with the tertiary amine in the ethylpyrrolidine ring (purple) of eticlopride. The green clouds around the ethyl pyrrolidine group show the scaffold to be replaced and vectors that specify the scaffold. Key receptor residues are indicated (orange sticks).

In a second trial, the order of replacing the parts of eticlopride was reversed, starting with the aryl portion and followed by replacement of the ethyl pyrrolidine ring. In order to generate drug-like substances capable of crossing the BBB through lipophilicity, compounds were filtered by molecular weight, surface area, chiral centers, hydrogen bond acceptors and donors, number of rotatable bonds, number of double bonds, and synthesis plausibility. Specifically, the following descriptor filters were used: Weight < 500, Slog [2.14-5.62], TPSA [40,140], rsynth [0.5-1], a_don [0, 5], mutagenic [0,0] b_rotN [2,8], b_double [0,2], chiral [0,1], a_acc [0,10]

(Ertl et al., 2000; Kaziu et al., 2005; Oprea, 2000; Wildman et al., 2001). Generated drug-like compounds were minimized using Merck Molecular Force Field 94X (MMFF94X) (Halgren, 1996; Halgren, 1998) and ranked using London dG score. Excluded volumes were automatically generated to prevent candidate fragments from clashing with the receptor and the R-groups, and those that clashed were eliminated.

From the two rounds of scaffold replacement, the resulting compounds were analyzed for their binding mode in the D3R binding pocket. Based on the binding mode, the London dG score, and further visual inspection, the top 60 hit compounds were selected and searched using SciFinder Scholar (SciFinder, Chemical Abstracts Service, Columbus, OH) for their commercial availability. None of the 60 hits were commercially available; however, closely related commercially available analogs were purchased.

2.2.1.1.1 Identifying the scaffold of eticlopride

Before starting the scaffold replacement, the scaffold and the R-groups must be identified. To identify these features, structure activity relationships and the binding mode of the known ligand should be analyzed and determined. To determine the binding mode and interaction of the known ligand with the receptor, active site analysis tools such as ligand interaction diagram, contact statics and electronic maps can be used.

2.2.1.1.1.1 SAR of eticlopride

1) An extended aryl amide is necessary for a relatively modest increase in affinity.

2) Addition of heteroatoms to the extended aryl amide increases affinity.

3) The amide linker is important for synthesis but not for D3R affinity or selectivity.

4) The linker between the aryl amide and the amino terminus must be of a 4-carbon atom

length for optimal D3R affinity and selectivity over the dopamine D2 receptor D2R

(Boeckler and Gmeiner, 2006; Chien et al., 2010; Feng et al., 2012; Shi and Javitch, 2002; Strader et al., 1991).

2.2.1.1.1.2 Active site analysis

Active site analysis is a process of assessing the characteristics of a ligand within a receptor-binding pocket. It defines and analyzes the interaction, electron distribution, and binding mode of the ligand. Generally, it helps to comprehend how the features of a ligand contribute to its binding strength.
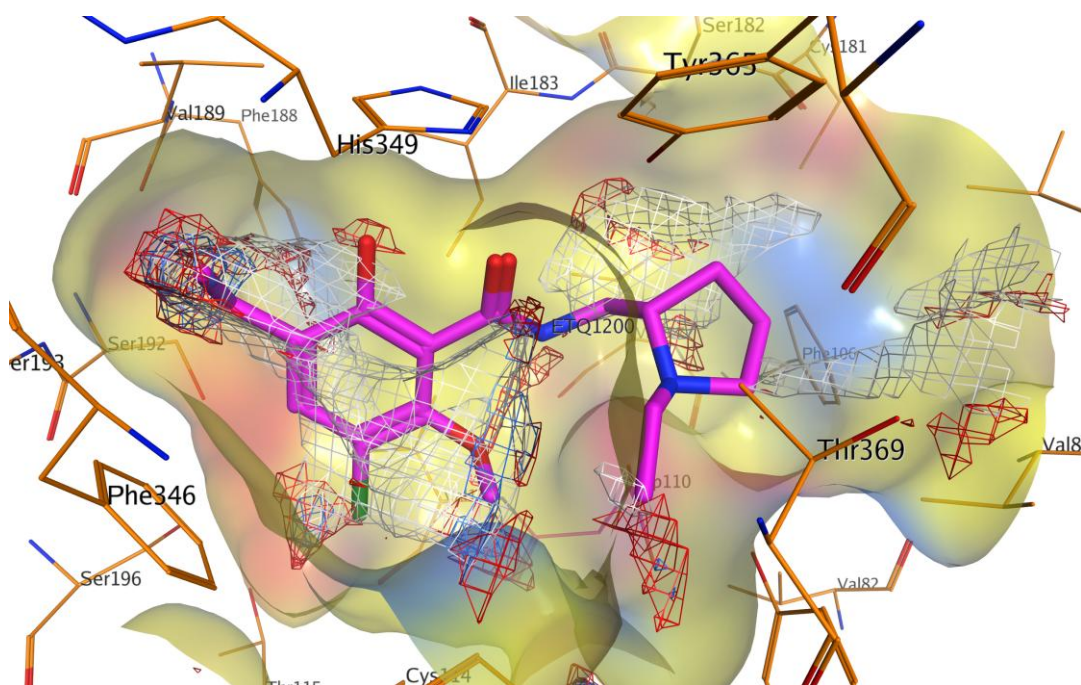
Electrostatic Map

Fig 2. 5: Electrostatic map of eticlopride in D3R binding pocket. The wire mesh indicates favorable interactions between the ligand (pink) and the antagonist pocket (yellow). Isocontours of interaction energy may be hydrophobic (white), acceptor (red) or donor (blue). The electrostatic field was calculated using MOE's "surfaces and maps" mode. The surface of the receptor was calculated at a distance of 4.5 **Å** from the ligand.

Electrostatics, one of the active site analysis tools, help to understand the pocket electric field. This is the distribution of the electrons across the pocket, in the form of charged groups, donors, acceptors and hydrophobic groups. Understanding such a distribution can help to identify important features of a ligand to be retained and those that are to be replaced. The electrostatics tool also affects the chemical nature of the returned compounds by creating a pharmacophore feature that directs the scaffold replacement process to generate a donor, acceptor or hydrophobic feature at a particular space of the active binding site (**Figure 2. 5**).

2.2.1.2 Visual inspection

Visual inspection is a process of subjectively selecting hit compounds after performing a computational process that created or filtered compounds. As a final and critical process, visual inspection is done manually to select hit compounds with desired structures, interactions and binding poses within a receptor binding pocket. Visual inspection requires medicinal chemistry knowledge that includes the structural nature of compounds known to bind to a particular protein, synthesis plausibility, drug-likeness of created structures, and the nature of ligand-receptor interactions. Visual inspection employs ligand interaction diagrams, active site analysis tools, and orientation of the ligand in comparison to known ligands. It is based on the following measures: the number and type of interactions between the ligand and pocket residues (ionic or electrostatic interactions, ion-dipole and dipole-dipole interactions, hydrogen bonds, charge – transfer complexes (π-π stacking), hydrophobic interactions and van der Waals forces, in order of strength), the binding pose (orientation and conformation of the ligand), structural novelty of the ligand that is created or filtered, and steric clashes, if any (Immadisetty et al., 2013). One may ask why manual inspection is employed in a computational process. The reason is that the currently used scoring functions often cannot accurately predict the *in vitro* binding affinity of

compounds. A combination of scoring function values and visual inspection can be used to select virtual hit compounds that are subsequently confirmed as ligands. Visual inspection includes inspecting ligand interactions with the binding pocket residues using "active site view", and visualizing pocket residue exposure to a ligand using a ligand interaction diagram (**Figure 2.6**).
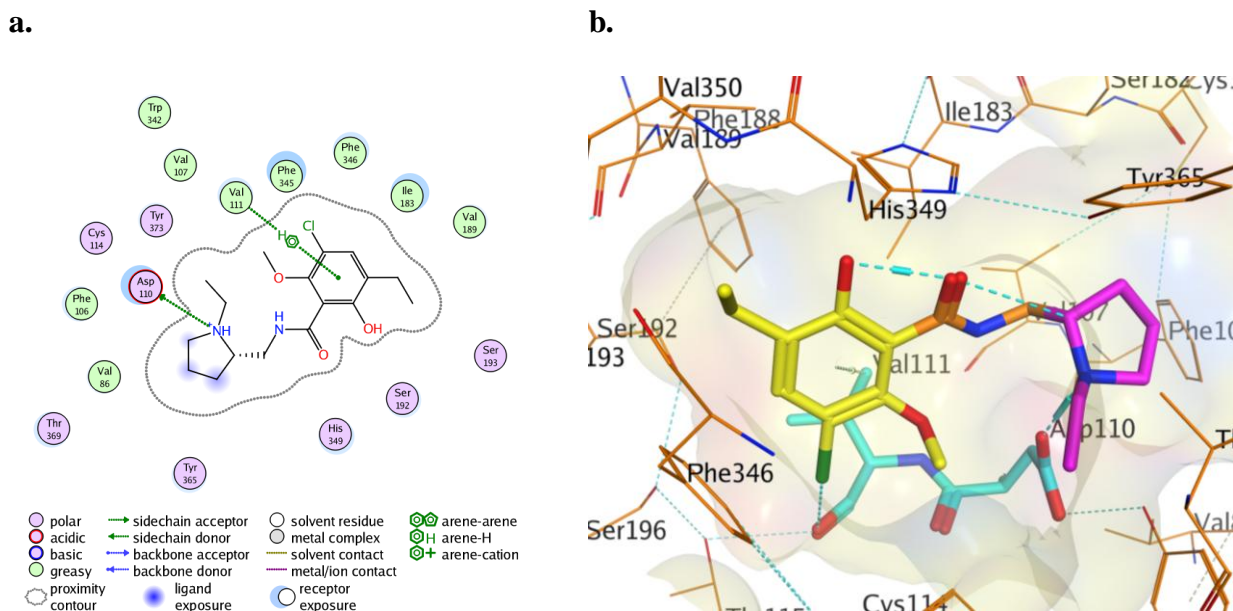
a.   **b.**

Figure 2.6: Ligand interaction diagram and binding mode of eticlopride within its D3R binding pocket. (a) The 17 residues shown are in the vicinity of the D3R antagonist pocket. Green arrows show intermolecular interactions. (**b**) Eticlopride-D3R binding pose. TM 3 side chains (cyan) interacting with eticlopride include Asp110 (ionic), Val111 (arene-H and ionic-dipole interactions). Comparison of the panels involves a 180-degree rotation of the ligand.

Eticlopride is shown to have two major intermolecular interactions: an ionic interaction between the ligand tertiary amine and Asp110, and an arene-H interaction between the ligand aryl group and Val111 (**Figure 2.6**). The strength of binding of a ligand can be estimated in part by counting the number and type of interactions, the number of residues present in binding pocket at close contact with the ligand, and halo sizes (representing degree of interaction)(Clark and Labute, 2007). For example, eticlopride has one ionic interaction, one hydrophobic interaction, three "large halo" residues and five small halo residues.

2.2.1.3 Scoring functions

Scoring functions are integral parts of structure-based drug design and are used to predict the *in vitro* (experimental) binding affinity of compounds that are generated using computational methods (Huang et al., 2010). The currently used scoring functions have challenges in that they fail to accurately predict the *in vitro* affinity but can provide important information in ligand ranking in virtual screening and fragment building methods (Immadisetty et al., 2013; Li, et al., 2014; Perola et al., 2004; Warren et al., 2006). There are many different scoring functions that are developed for specific computational programs. Different scoring functions use different algorithms and set of proteins to calibrate the precise prediction of experimental affinity. However, the success of computational methods has been undermined due to lack of an energy scoring function that precisely and quickly characterizes the interaction between protein and ligand (Huang et al., 2010).
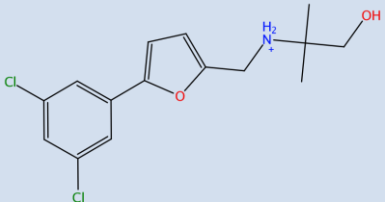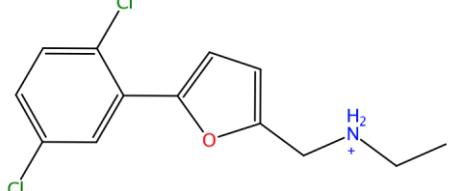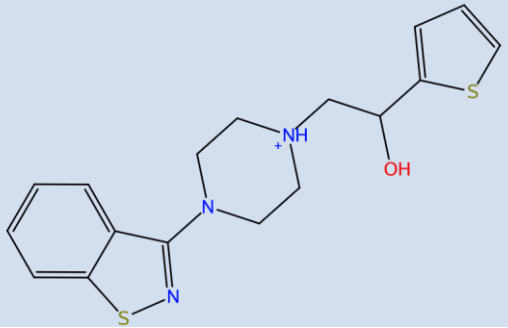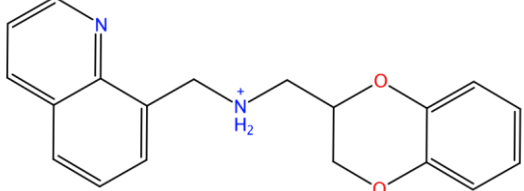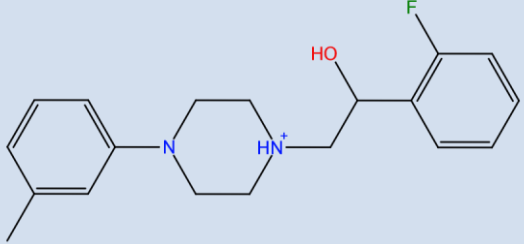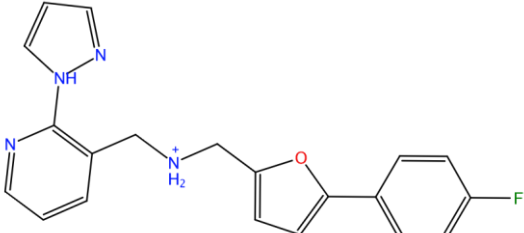
Scoring functions are essential for ranking hit compounds in fragment building and virtual screening methods because these methods dock the generated structures or database to be filtered in the binding pockets of proteins. Hence, a scoring function can provide information regarding the binding mode and site of the ligand binding, binding affinity of the ligand and

protein, and hit compounds that are potential lead compounds for drug discovery (Joseph-McCarthy et al., 2007; Rajamani and Good, 2007; Seifert et al., 2007; Shoichet et al., 2002). An accurate scoring function should be able to rank known ligands according to their experimental binding affinities. Therefore, in the present study, a procedure was set to evaluate the accuracy of the scoring functions that are used for DFDD. Because MOE was used for performing DFDD, the scoring functions that are available in the software were evaluated. These included ASE, Affinity dG, Alpha HB, London dG, and GBVI/WSA dG scoring. London dG score, however, was used to rank the resulting hit compounds in our experiments because it was previously used to predict BIRGB 796, a P^{38} kinase inhibitor, from its initial hit compound using scaffold replacement with MOE (Grimshaw, 2010). MOE scaffold replacement nearly predicted the lead optimization of BIRGB 796 from its initial hit compound.

Sets of three different groups of D3R ligands were used to evaluate the five scoring functions used in MOE to examine if there is a linear relationship between the experimental affinity and virtual affinity. The first group of compounds was comprised of 11 D3R ligands (**Table 2.1**) that were filtered via virtual screening of a 3.1 million molecules database at the D3R crystal structure and homology model, and *in vitro* affinity of the filtered compounds were determined (Carlsson et al., 2011). The second group of test set compounds was made of nine D3R ligands (**Table 2.2**) that were used in predicting the effectiveness and calibration of D3R homology model, and identification of binding sites. The *in vitro* affinity of the nine ligands was determined. (Bocker et al., 2007). The third test set group was comprised of seven known D3R antagonists (**Table 2.3**) that have high affinity; these compounds were previously used to determine the effect of D3 antagonist on the thermostability of a purified D3R wild type receptor (Chien et al., 2010). The structure of the compounds were drawn in 3D in MOE and were

docked in the D3R binding pocket using Triangle Matcher placement method and force field refinement. The docking poses were scored using the different scoring functions. The docking was performed three times and the average values were used to evaluate the relationship between experimental affinities and virtual affinities. The three trials were used to generate R^2 values using linear regression with Graph Pad prism (GraphPad Prism version 6.00 for Mac OS X).

Table 2.1: Eleven compounds for scoring function evaluation (Carlsson et al. 2011)

No.	Compound	Ki (uM)	Compound No. in the original paper
1		0.080	56
2		0.100	61
3		0.20	4
4		0.30	28
5		0.50	7
6		1.300	6
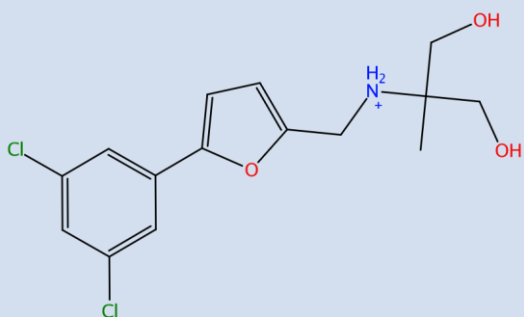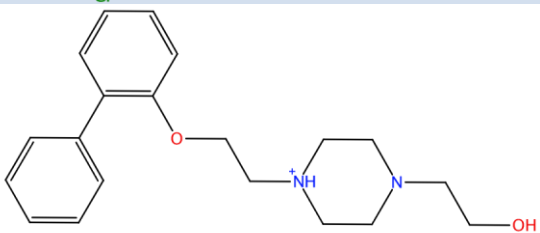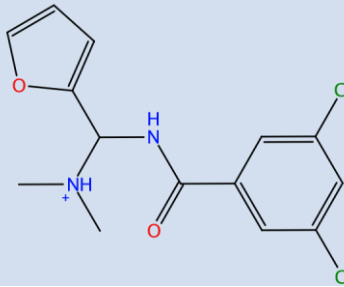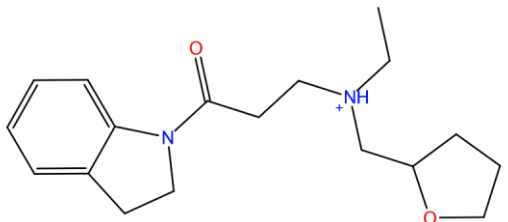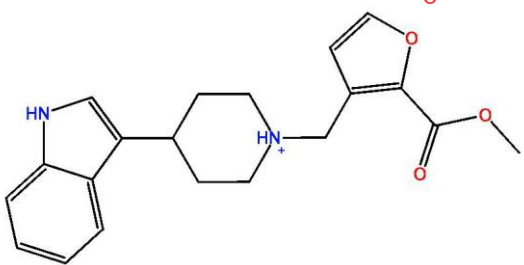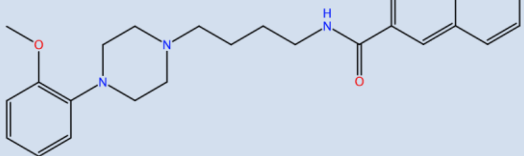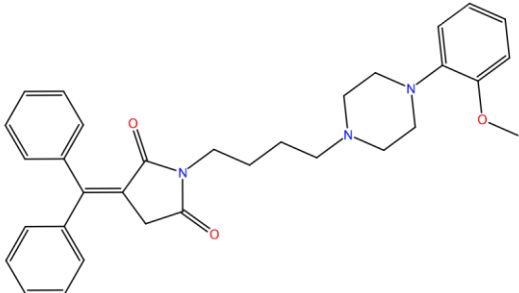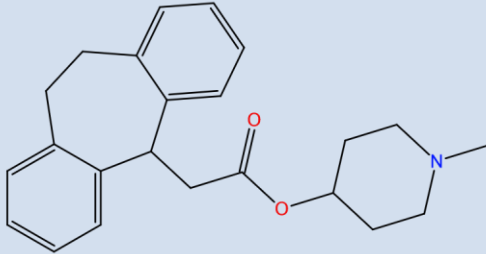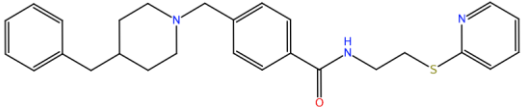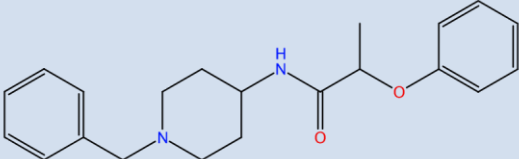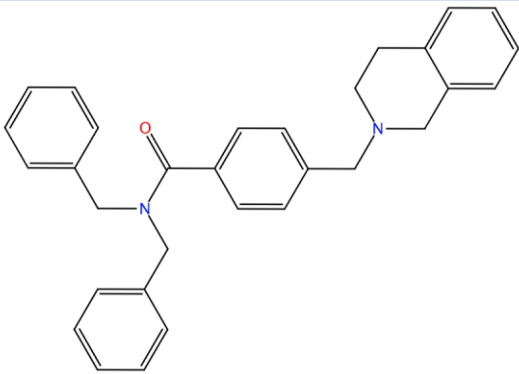
7		1.600	3
8		1.800	5
9		2.200	29
10		3.00	32
11		3.100	2

Table 2. 2: Nine compounds for scoring function evaluation (Bocker et al. 2007)

No.	Compound	KI (nM)	Cmp No. in the original paper
1		0.91	BP 879
2		65	18
3		190	14
4		214	5
5		984	7
6		1000	20
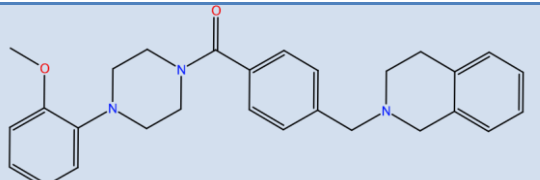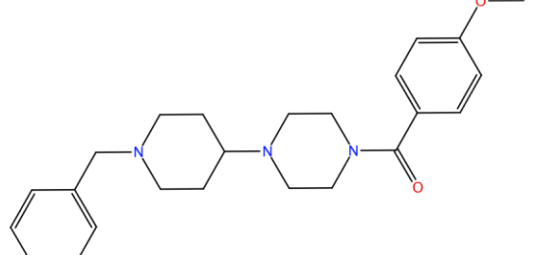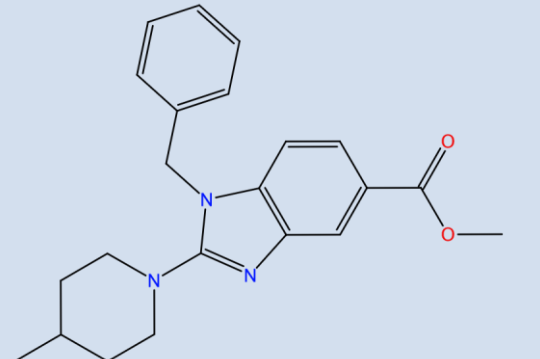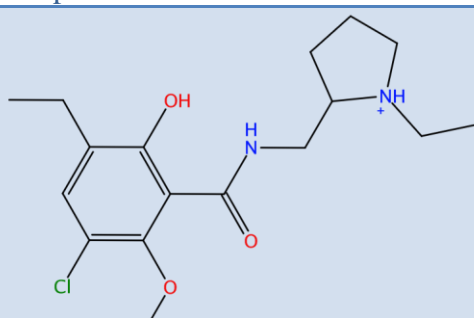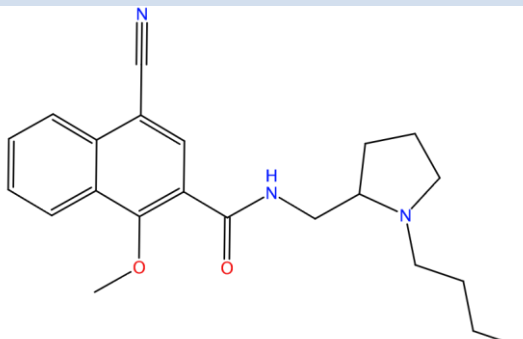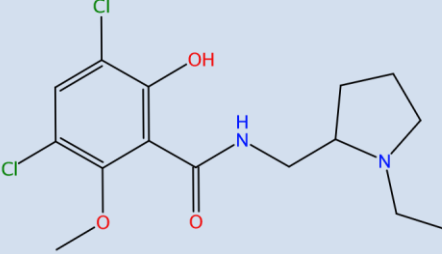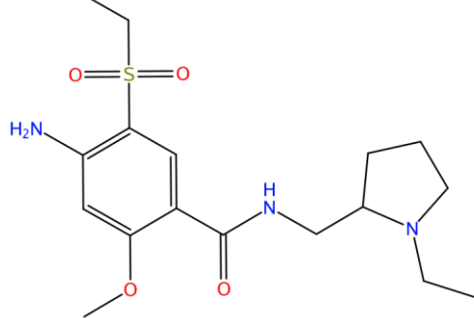
7		1368	3
8		4526	8
9		5000	13

Table 2. 3: Seven known D3R compounds for scoring function evaluation

No.	Compound	Ki (nM)	Original Compound's Name
1		0.16	**Eticlopride**
2		0.52	**Nafadotride**
3		3.50	**Raclopride**
4		3.80	**Amisulpride**
5		9.80	**Haloperidol**

6		25.0	**(-) Sulpride**

7		100.0	**Tiapride**

2.2.1.4 MedChem transformations

MedChem transformation is a method employed to search new hit compound by using a set of transformation rules to existing known ligands. Classic MedChem transformation can be used to exchange functional groups, atoms, or change all or part of an individual rings at the same time preserving the remaining part of the ligand. Transformations can be performed iteratively to giv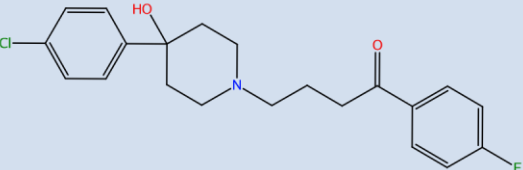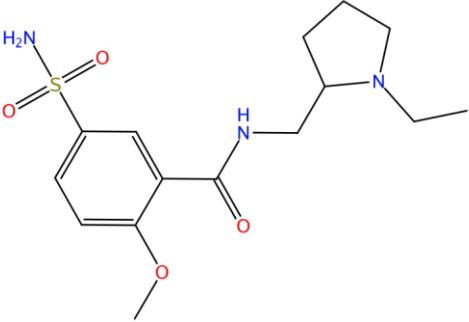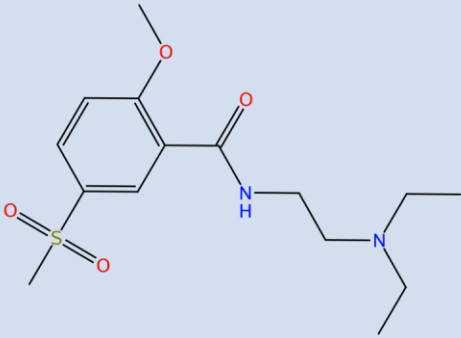e a new structure after collective changes. This repeated transformation enhances the diversity and novelty of the generated structures. When the ligand to be transformed is within a receptor, forcefield refinement can be utilized to dock the resulting structures with different docking poses that can be scored with scoring functions. MedChem transformation is based on Stewart's work with Drug Guru software (Stewart et al., 2006) that uses a set of transformations to encrypt medicinal chemistry knowledge from a historical experience of drug discovery programs. The results of such transformations of a known compound are analogs of plausible synthesis. There are two types of MedChem transformations:

bioisosteric transformation, which retains properties of the parent compound (**Figure 2.8**) and ring substitution or cyclization that generate structures with different properties (**Figure 2.9**). The same receptor after protein preparation, the same method to identify the scaffold, and the same pharmacophore features, descriptor filters, and scoring functions used for scaffold replacement were also used for MedChem transformation. However, MedChem transformation provides flexibility in that any parts of a known ligand can be selected and transformed. This can allow performing many different sets of transformations or replacements of eticlopride. Six experiments of replacement of eticlopride were performed (**Figure 2.7**):

1. Replace ethyl pyrrolidine while retaining aryl amide and then the retained aryl amide

2. Replace amide ethyl pyrrolidine while retaining the aryl and then replace the retained aryl

3. Replace aryl while retaining the amide ethyl pyrrolidine and then replace the retained amide ethyl pyrrolidine.

4. Replace aryl amide while retaining ethyl pyrrolidine and replace the retained ethyl pyrrolidine.

5. Replace both aryl and ethyl pyrrolidine while retaining the linker (methyl amide)

6. Replace the whole eticlopride structure.

MedChem Transformations of Eticlopride
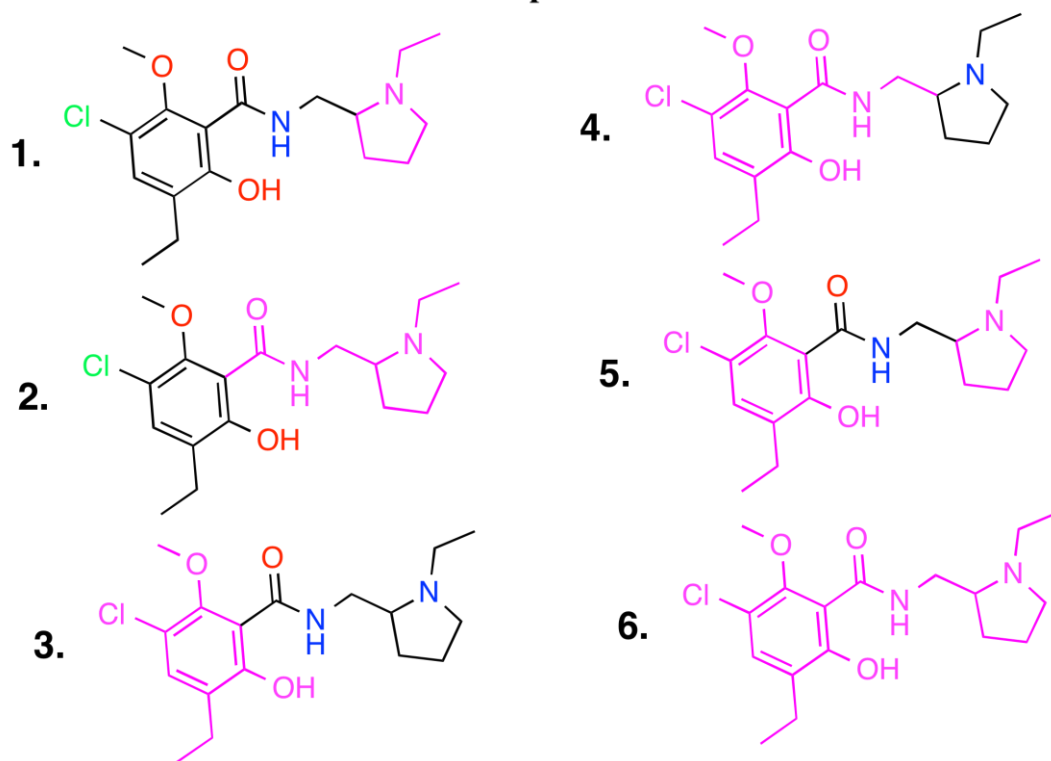
Figure 2.7: MedChem transformations of eticlopride parts. The six numbers show the different experiments of eticlopride transformations. In each experiment, in the first round, the pink colored parts of eticlopride were transformed while the black colored were retained. The retained (black) were then replaced in the second transformation. However, in experiments five and six, eticlopride parts (pink) were replaced at once.

A total of 451,549 new structures were generated from the different sets of eticlopride MedChem transformation, and 187 structures were selected based on London dG score and visual inspection. The commercial availability of the selected compounds was searched in SciFinder Scholar for purchase and then for experimental affinity determination. However, none of these compounds were commercially available. After critical analysis of synthetic plausibility

of the selected compounds, six compounds were selected for synthesis in industry or academic lab.

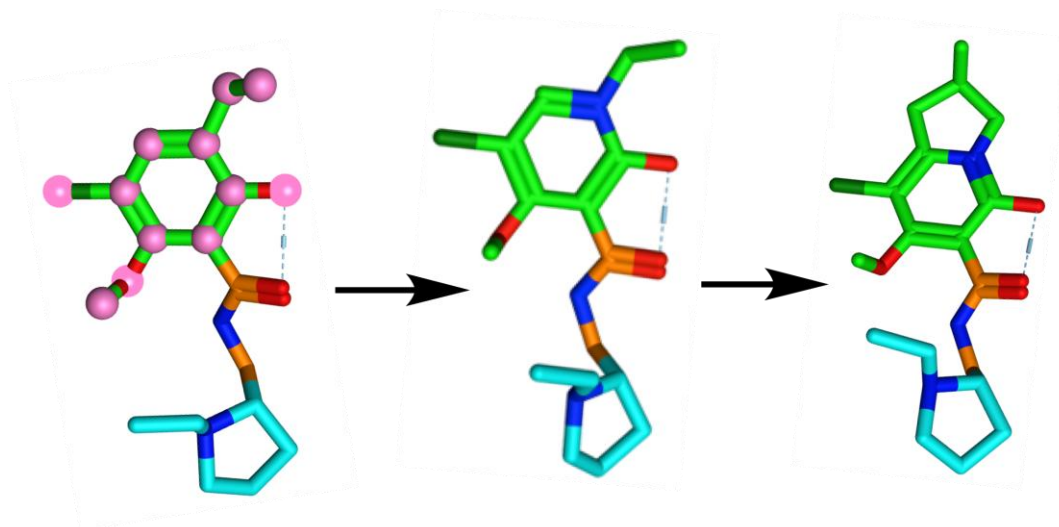**Figure 2.8: Bioisosteric MedChem transformations.** The individual atoms of the aryl part of eticlopride (green) were selected for transformation. A new structure was formed after the methyl group was transformed into an amine functional group. Finally, a new structure with a different aryl part was generated.
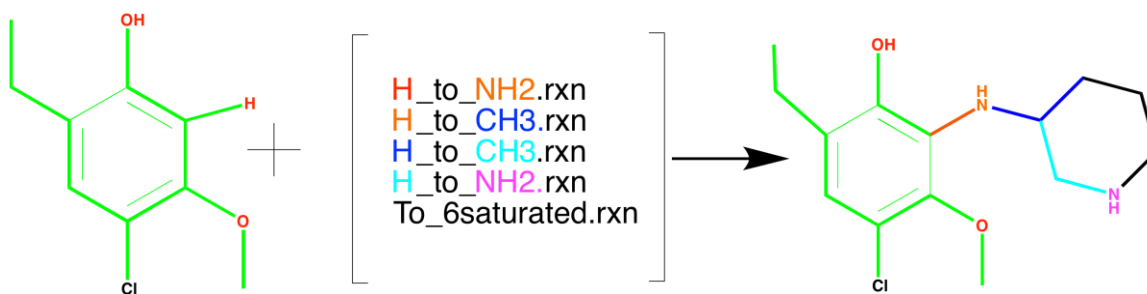
Figure 2.9: Ring substitution or cyclization MedChem transformations. MedChem transformation starting from aryl part of eticlopride generated an aminopyridine after transformation and cyclization of atoms. The colors show individual atoms transformations that started from the hydrogen (red) in the aryl starting structure.

2.2.1.5 Ligand building

The ligand building method uses the molecule builder module in MOE(MOE 2013.08). The builder can be used to construct or edit ligands as 3D structures by changing elemental properties, bond types and ionization states. The stereochemistry, ionization and tautomerization of ligands within a receptor crystal structure or homology model can be altered. For creating ligands, the terminal hydrogen atom from where functional groups are added is used; however, more than one terminal atom can be used to generate structures. The "molecule builder" mode has a fragment database containing commonly used functional groups and atoms, and considers general medicinal chemistry properties when creating compounds.

Before employing ligand-building method to generate useful drug-like compounds, it was necessary to evaluate the efficiency of the method. The prepared D3R receptor was used as described above for scaffold replacement and MedChem transformations. Ligand building was used to predict the parts of eticlopride by deleting them one at a time. First the ethyl pyrrolidine

part of eticlopride was deleted, and regenerated by constructing it from the retained aryl group at the selected hydrogen atom (**Figure 2.10**). In the same manner, the aryl part was predicted by its deletion and construction from the retained ethyl pyrrolidine group. Ligand building was able to predict both parts except the tertiary amine at the ethyl pyrrolidine part and the 2-methoxy at the aryl part.
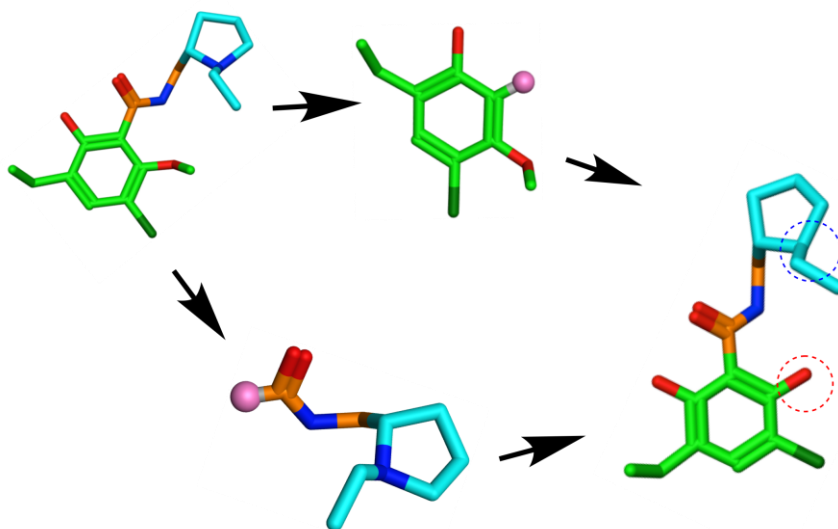

Figure 2.10: Prediction of eticlopride parts using ligand-building mode. Eticlopride parts were deleted and predicted using the remaining parts. Ligand building predicted parts of eticlopride except the tertiary amine and 2-methoxy groups. The selected hydrogens represent points of ligand construction.

2.2.2 Pharmacological

2.2.2.1 Cell culture

Human embryonic kidney (HEK-293) cell lines stably expressing D3R were used (courtesy Dr. Robert Luedtke from the UNTHSC). The cells were grown in complete DMEM media (high glucose, Na-pyruvate, L-glutamine) that is supplemented with 10% fetal bovine serum (FBS), 1% Pen/Strep (100 units of penicillin, 100 ug of streptomycin per ml of medial final volume), and 400 μg/ml of G-418. Cells were grown as monolayers in 75 cm^2 flasks at 37˚C and 5% CO_2 and subcultured twice a week (every 3 days). For subculturing, the exhausted media in the flask was aspirated and the confluent adherent cells were washed with 10 ml of Hanks buffered salt solution (HBSS). To detach the cells from the flask, 2 ml of trypsin-EDTA was added and swirled to cover the cell monolayers. When the cells were detached from the flask, 10 ml of complete DMEM media was added to inactivate the trypsin-EDTA. Eight ml of the cell suspension was discarded, and then 18 ml of complete fresh DMEM media was added. The flask was tightly capped and then gently swirled to evenly suspend the cells. After loosening the cap, the flask was placed in the incubator and the cells were allowed to grow until the next subculturing.

2.2.2.2 D3R HEK293 membrane preparation

Stably D3R expressing HEK293 cells grown at 37°C in a 5% CO_2 incubator on 150 x 20 mm plates were used to prepare membranes. Cells were washed twice with 12 ml of cold phosphate–buffered saline (DPBS) after reaching 85% confluence (3-4 days growth). After adding another 12 ml of DPBS, cells were scraped, harvested, and transferred to 15 ml cold centrifuge tube. The supernatant was discarded after cells were centrifuged at low speed (700 x g), and the cell pellet was resuspended in 500 μL of cold buffer (50 mM Tris, 1 mM EDTA, pH

7.5). After cells were centrifuged for 30 min at 100000 x g at 4°C and the supernatant was discarded, the pellet formed was frozen at -20°C for later membrane binding assays.

2.2.2.3 Preliminary *in vitro* screening of "hit" compounds

SciFinder-identified analogs of scaffold replacement generated hit compounds were obtained and dissolved in 100% DMSO to make a stock concentration of 10 mM. A 10 μM final concentration preliminary one-point competitive binding assay was performed. Competitive binding assays were conducted employing membranes of D3R stably expressing HEK293 cells with [^{3}H]-spiperone as a tracer radioligand. One hundred μL of [^{3}H]-spiperone and 10 μl of 10 mM nonradioactive hit compound or eticlopride were added to 240-μL membrane preparation (about 30-40 μg protein) in 12x75 mm borosilicate glass tubes. After gentle shaking for 15 min, binding was terminated. Screening results were analyzed with one-way ANOVA, nonparametric ($P < 0.05$).

2.2.2.4 D3R membrane binding assay

Cell pellets were first dissolved in 6 ml of D3R binding buffer (1M Tris base, 0.5 M KCl, 0.5 M CaCl$_2$, 0.5 M MgCl$_2$, pH 7.4). To determine competitive binding constants, the membrane preparation aliquots of 30 – 40 μg total protein were combined with 0.1 nM final concentration of [^{3}H]-spiperone and a range of final concentrations (1 fM – 10 μM) of either nonradioactive hit compound or eticlopride and incubated with gentle shaking at 25°C for 1 h in 12x75 mm borosilicate glass tubes. Binding was terminated using a Brandel Model 24 harvester via rapid filtration through Whatman GF/B filters (Schleicher and Schuell, Keene, NH) presoaked in 0.5% polyethylenimine (v/v). Filters were washed rapidly twice with 3 – 4 ml of wash buffer (0.1 M of Tris buffer, pH 7.4) and filter discs from each well of the harvester were transferred using tweezers to scintillation vials. After adding 5 mL scintillation fluid to the vials, the radioactivity

trapped in the filter was quantified using a liquid scintillation analyzer (TRI-CARB 2100TR). Three independent competitive binding assays were performed (with points in duplicate), and data were analyzed (GraphPad Prism version 6.00 for Mac OS X). IC50 values were determined and converted to Ki values using the Cheng-Prusoff equation ($K_i = IC_{50}/(1+[^3H]$-spiperone]/(Kd $[^3H]$-spiperone).

CHAPTER THREE

3   RESULTS AND DICUSSION

3.1   Results

3.1.1   Computational studies

3.1.1.1 Scaffold replacement of eticlopride at the dopamine D3 receptor

As proof of concept, the current study was undertaken to evaluate scaffold replacement for the design of chemically novel ligands for GPCRs using MOE software. We used the recently co-crystallized D3R – eticlopride complex to build D3R antagonists of novel scaffold (Chien et al., 2010). Two experiments were performed to replace portions of eticlopride. In the first experiment, the ethylpyrrolidine portion of eticlopride was replaced while retaining the aryl part, resulting in 29,405 initial hits. These hits share benzene or other ring structures that form hydrophobic interactions with residues of the receptor pocket. A tertiary amine important for salt bridge formation between eticlopride and Asp 110 in TM 3 was an essential feature of the returned hits. Based on visual inspection, structural novelty, and London dG score, 24 of the initial hits were chosen for further modification. Next, the retained aryl portion of the 24 hit compounds was replaced, resulting in 17,744 returned hits, many of which possessed undesirable double bonds or chiral centers that reduced synthetic plausibility. More robust descriptor filters (described in Methods) were introduced, requiring synthetic scores in the range of 0.8 to 1 and chiral center scores in the range 0 to 1. To avoid terminal double bonds, this "range" was initially set from 0 to 0. Few hits were returned, however, so compounds were allowed to have at most one double bond. This filtering search resulted in 10,206 returned hits. The amide linker portion of eticlopride was also replaced; however, many of the resulting hits were excluded due

to poor London dG scores, poor synthetic plausibility, or unfavorable interactions in the D3 receptor pocket.

In the second experiment, the order of replacing the parts of eticlopride was reversed, starting with the aryl and followed by replacement of the ethyl pyrrolidine ring portion. The replacement of the aryl portion resulted in 30,091 hits. Based on visual inspection, structural novelty and London dG score, 11 top ranked hits were selected from the aryl replacement. The ethyl pyrrolidine portion of these 11 hits was subsequently replaced resulting in 22,140 hit compounds. Descriptor filters were introduced at the start of Experiment 2 to eliminate compounds with undesirable double bonds, chiral centers and poor synthetic scores. Reversing the order of replacing parts of eticlopride generated more hits (**Table 3.1**). This could be due to better overlay of the bonds between the part of eticlopride that are conserved (R-groups) and the fragments that replace the scaffold. Despite the use of stringent descriptors for synthetic plausibility, most of the returned hits shared complex structures with many aromatic rings, making their synthesis difficult. This could be due to the fragment database used or inefficient synthesis descriptor filters to predict synthetic plausibility.

The final returned hits from both trials (22,140 + 10,206 = 32,346) were further analyzed based on visual inspection, structural novelty and London dG score, and 60 hits were selected. These top 60 compounds had a better fit within the D3 receptor-binding pocket and involve more interactions than the parent compound. Eticlopride has a -13.45 kcal/mol London dG score and all the top 60 compounds have scores ranging from -13.99 kcal/mol to -18.114 kcal/mol. Therefore, the 60 hit compounds have better London dG scores than eticlopride. Compounds with lower London dG scores (better virtual affinity) are predicted to better interact and fit in the binding pocket. Compound 22 (**Figure 3.1**), one of the top hits with -16.13 kcal/mol London dG

score, has shown more hydrogen bond interactions and a better fit within the pocket than the lead compound eticlopride. Specifically, the nitrile group of Compound 22 formed hydrogen bonds with Ser182, Ile183 and His349, and the sulfur carbon double bond terminus formed weak hydrogen bonds with Ala167 and Thr 369.

In order to test the affinity of these top 60 hit compounds *in vitro*, their commercial availability was determined using SciFinder Scholar. While none of these exact compounds was commercially available, 39 similar structures were identified (**Table 3.2**). These 39 compounds were redocked into the D3 receptor pocket, and six compounds were selected and purchased from the database of the 39 analogs based on visual inspection, structural novelty, and London dG score for initial hD3R –HEK293 pharmacological evaluation (**Figure 3.2**).

Table 3.1: Eticlopride scaffold replacement

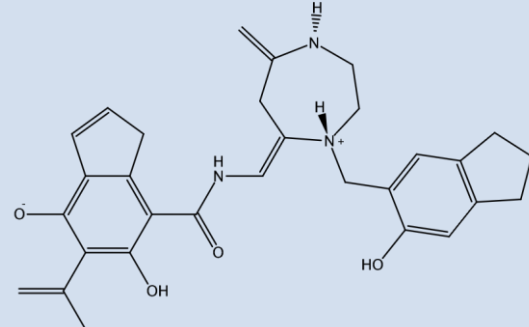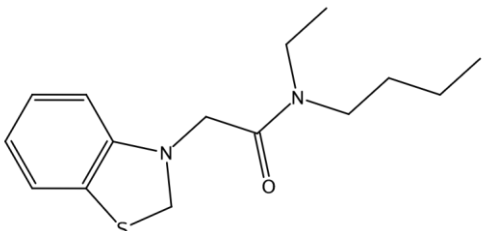| Experiment No.	First Part Replaced	Returned hits	Selected hits	Second Part Replaced	Returned Hits	Refined
1.	Ethyl Pyrrolidine	29,405	24	Aryl	17,744	10,206
2.	Aryl	30,091	11	Ethyl Pyrrolidine	22,140	22,140
Total Returned hits	-	-	-	-	39,884	32,346
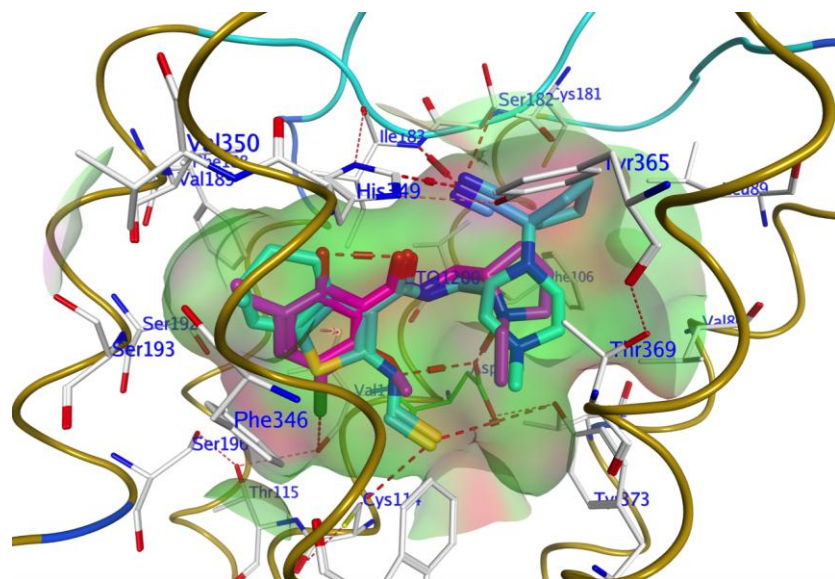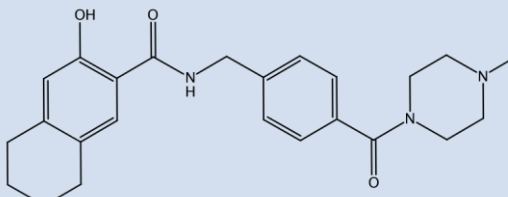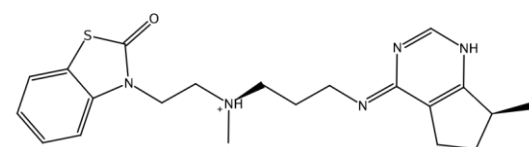
Fig 3.1:   The superposition of Compound 22, one of the 60 original compounds, with eticlopride in the D3R antagonistic binding pocket. The pink (eticlopride) and cyan (Compound 22) structure were superposed on the D3R binding pocket. The Compound 22-nitrile group interacted with pocket residues Ser 182, Ile 183, Val, and Val 350 (white sticks, annotated). The sulfur atoms of Compound 22 is shown interacting with Cys 114 and Tyr 373. Compound 22 fit better in the binding pocket than eticlopride.

Table 3. 2: Thirty-nine analogs and their original precursors

Analog Number	Analog Structures	London dG Score	Original Compound	Original Compound Numbers	London dG Score	% Similarity (T.C)
1		-13.22		16	-16.52	60
2		-9.72		60	-12.667	60
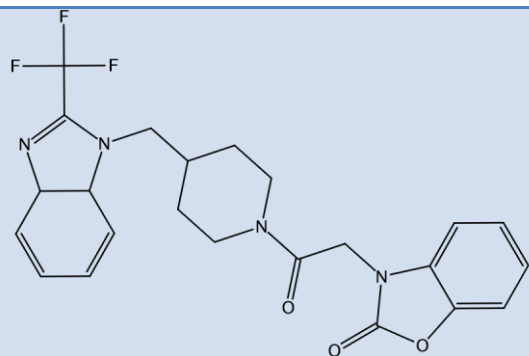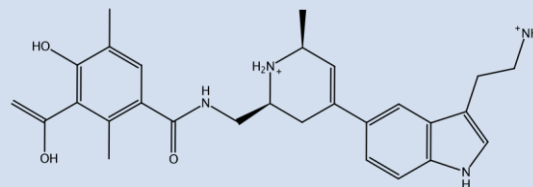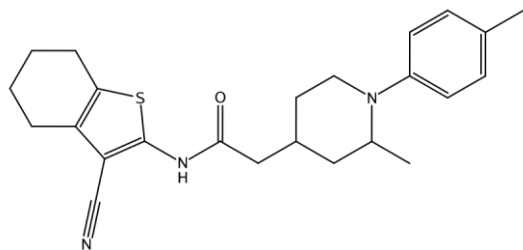
3		-10.60		19	-16.41 69
4		-11.03		22	-16.12 62
5		-10.81		24	
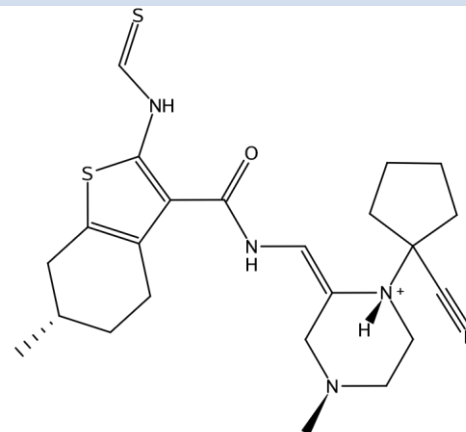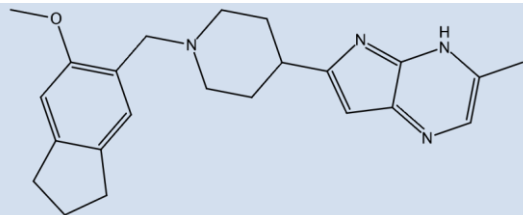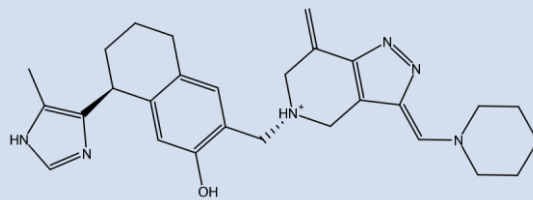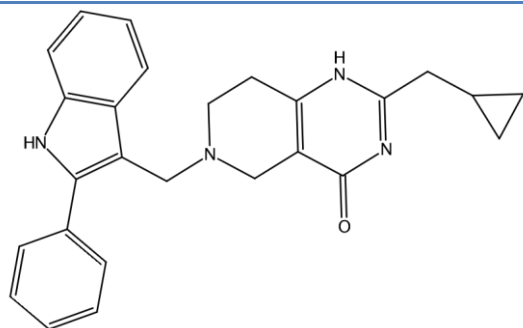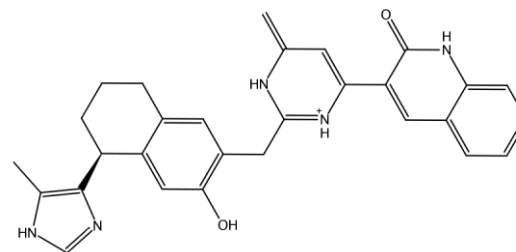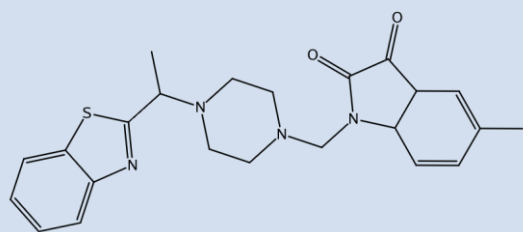
6		-12.77		27	-15.75	62
7		-11.83		29	-15.60	64
8		-12.27		29	-15.60	64
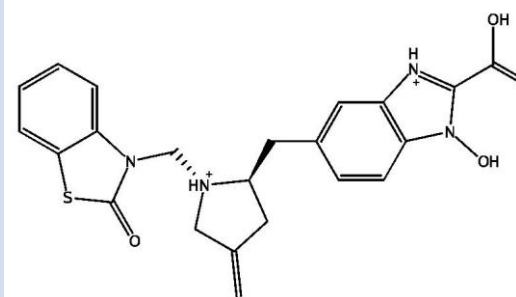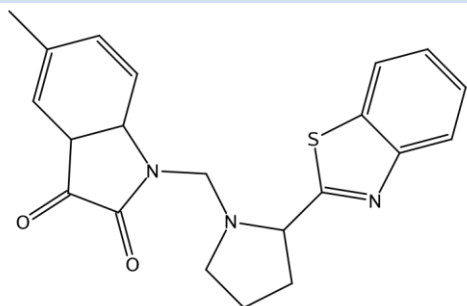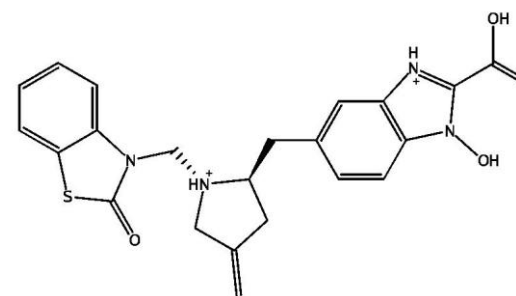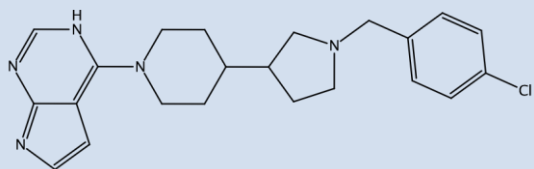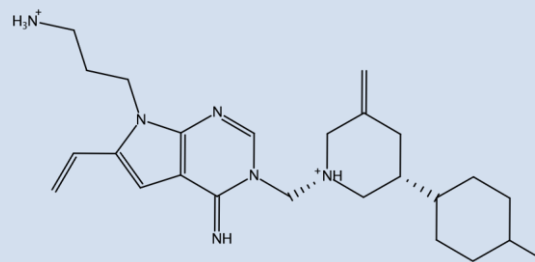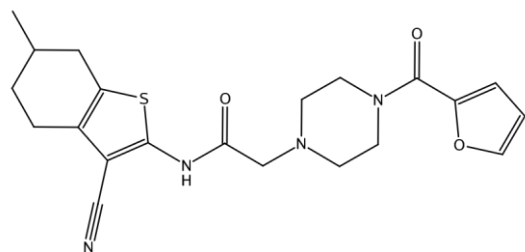
9		-11.30		30	-15.53	62
10		-11.81		31	-16.86	67
11		-10.72		31	-16.86	67
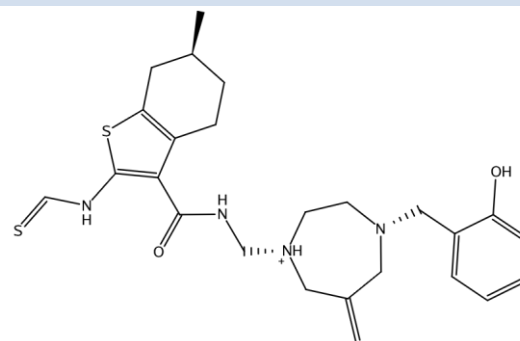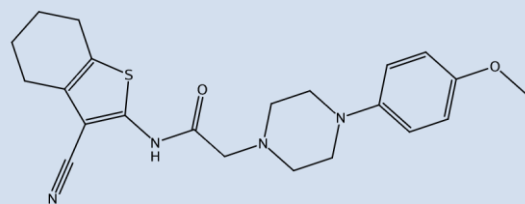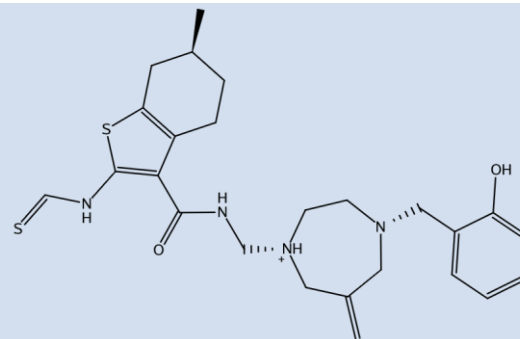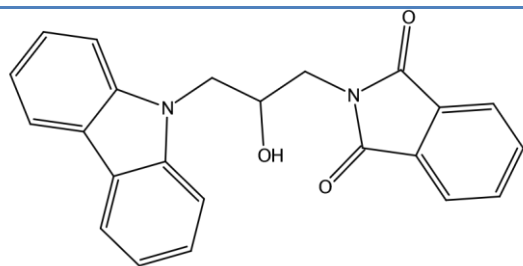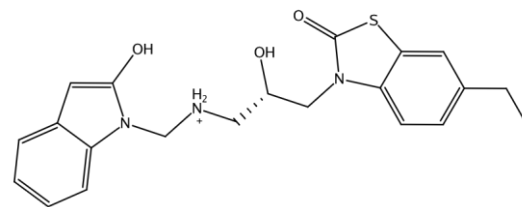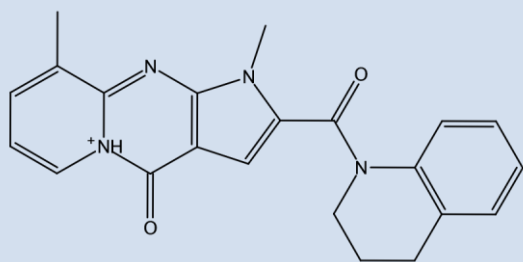
12		-10.08		33	-15.43	68
13		-11.69		**12**	**-16.70**	63
14		-9.65		33	-15.43	68
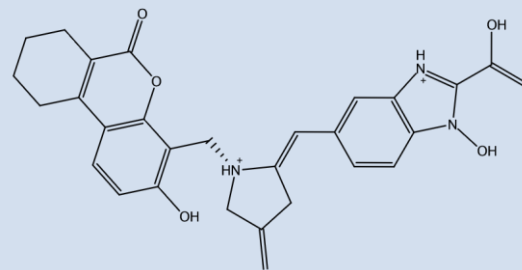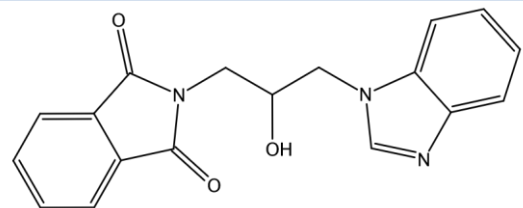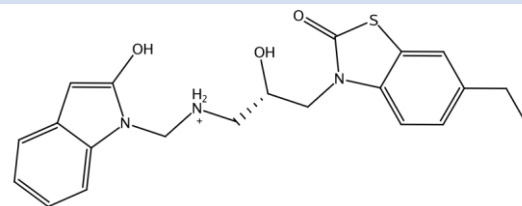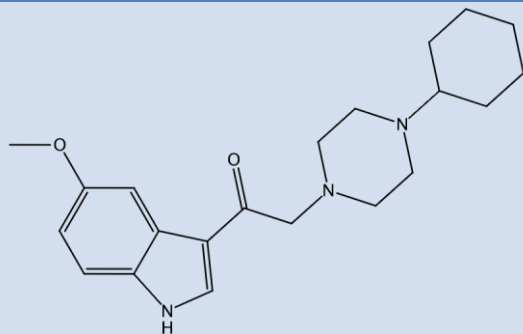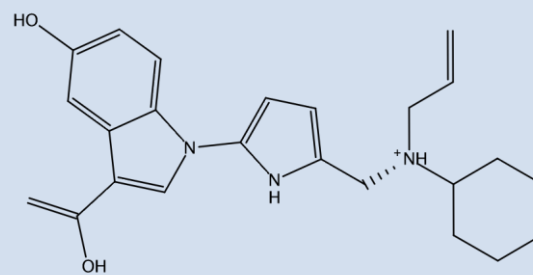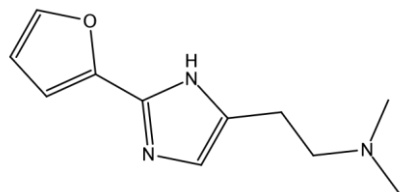
15	-9.95	35	-15.35	60
16	-7.73	36	-15.30	63
17	-10.81	37	-15.21	66
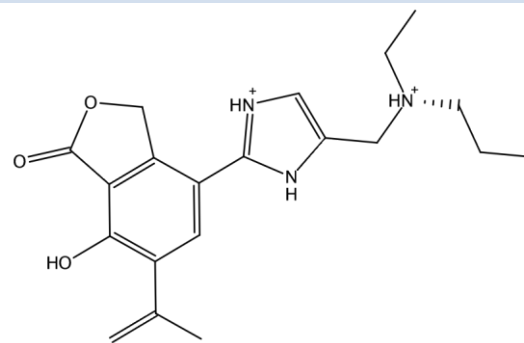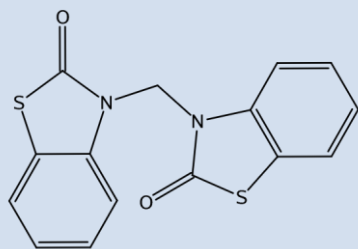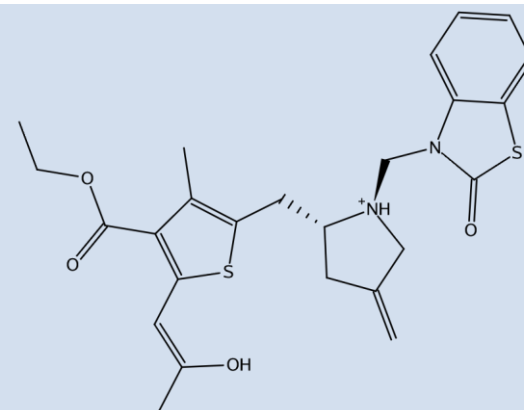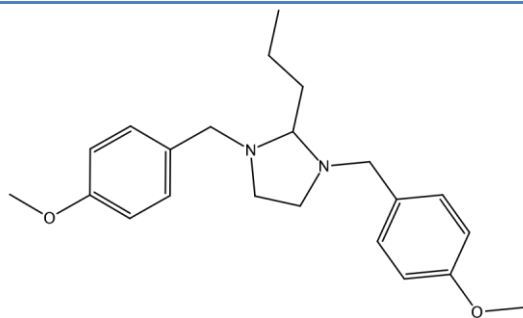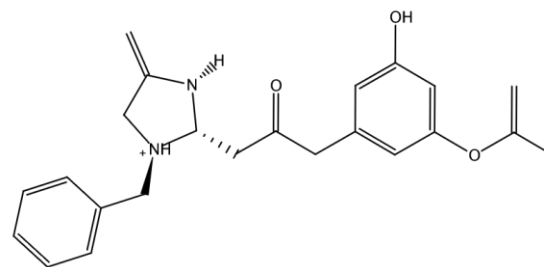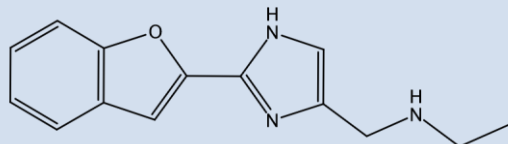
18		-11.28		38	-15.02	67
19		-7.20		39	-14.83	74
20		-13.20		40	-14.73	70
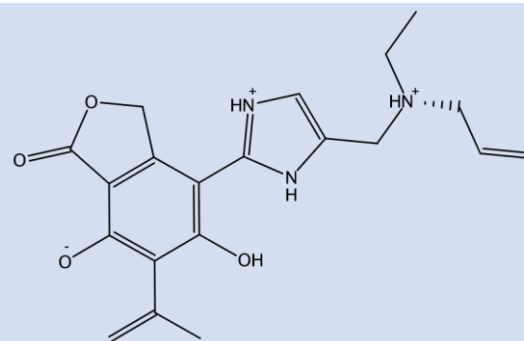
21		-11.03		40	-14.73	60
22		-8.77		44	-14.51	60
23		-10.00		46	-14.35	61
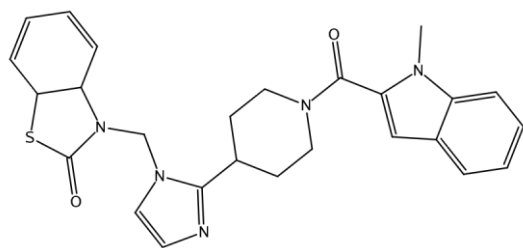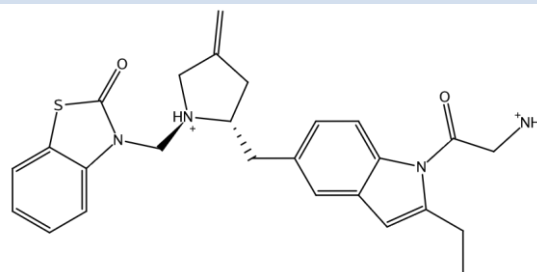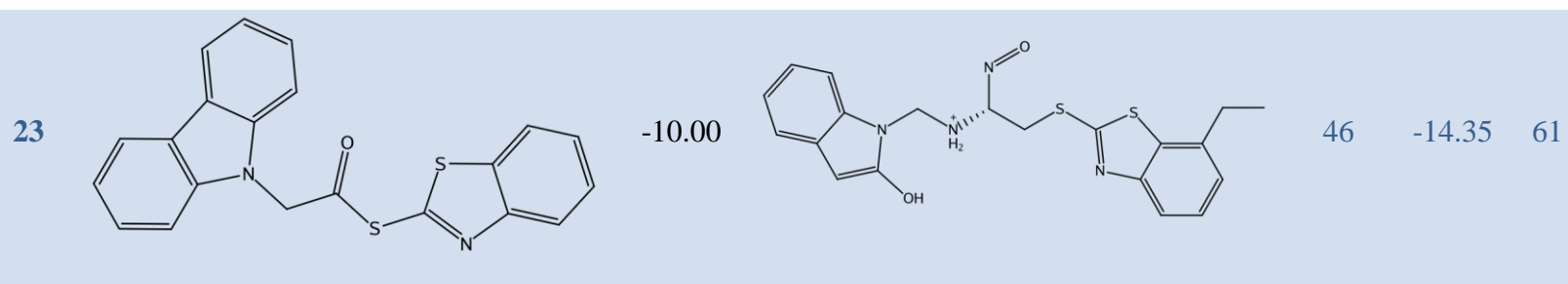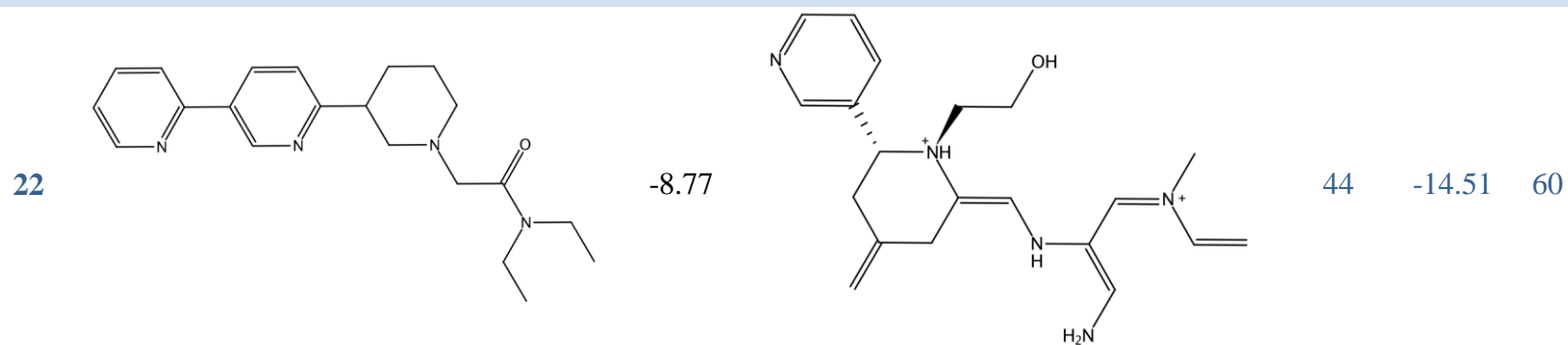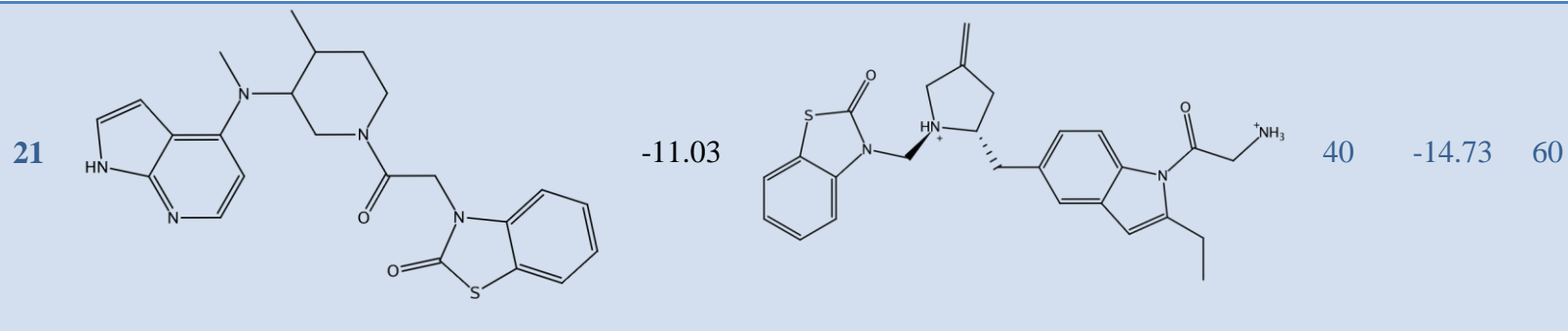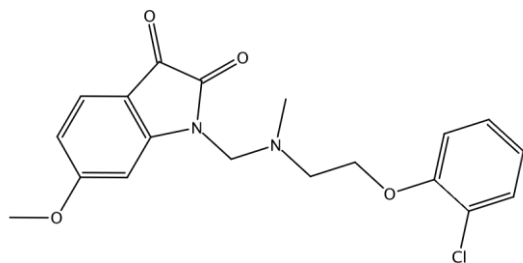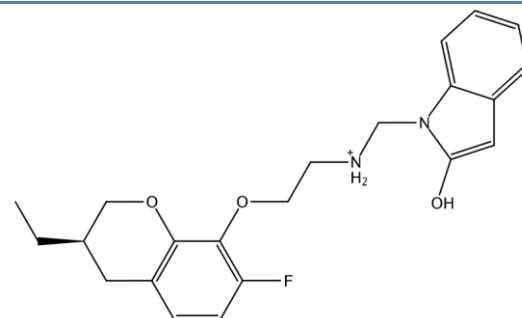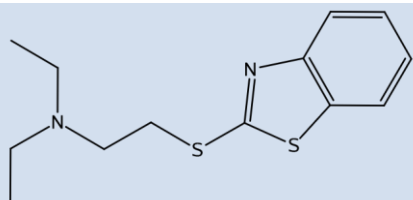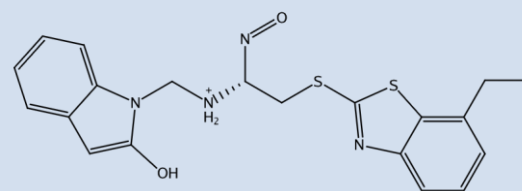
24		-11.43		45	-14.45	62
25		-8.18		46	-14.35	71
26		-10.29		48	-14.10	65
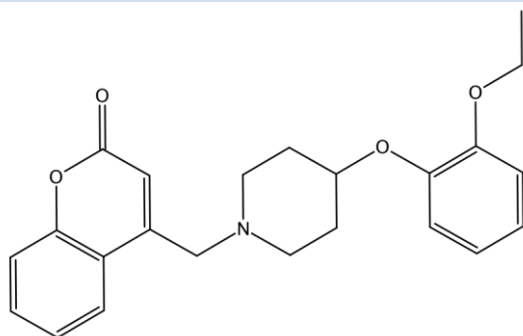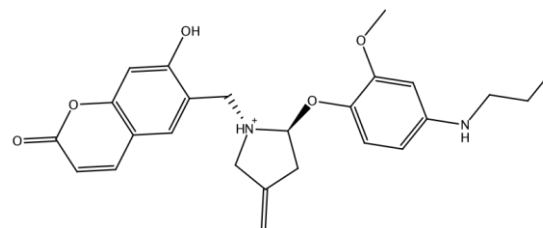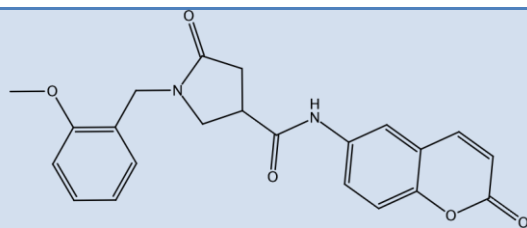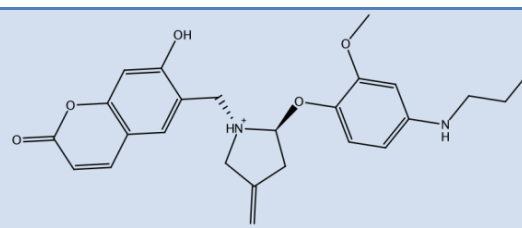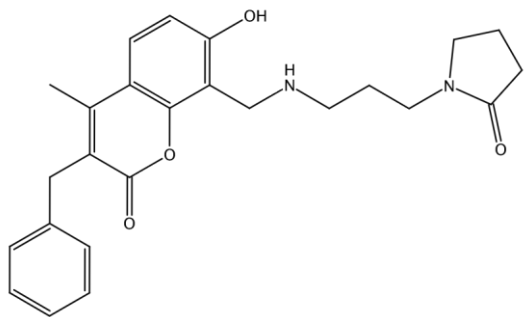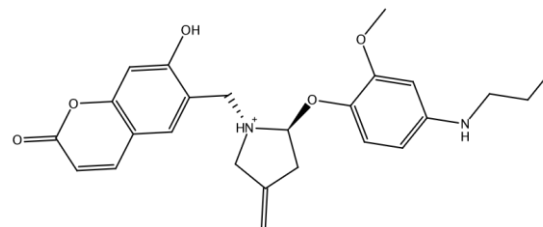
	Structure	Value	Structure			
27		-7.54		48	-14.10	66
28		-10.54		48	-14.10	65
29		-14.47		48	-14.10	65
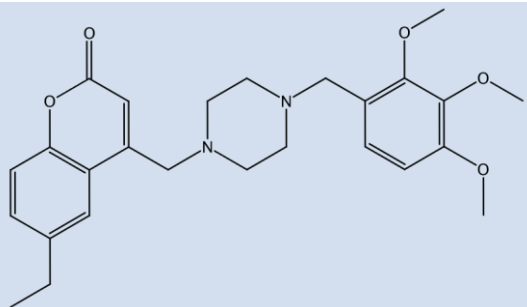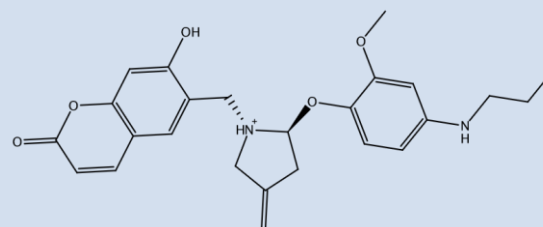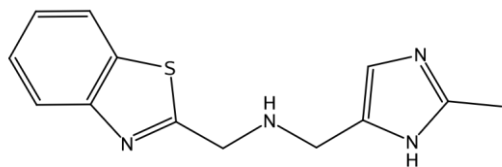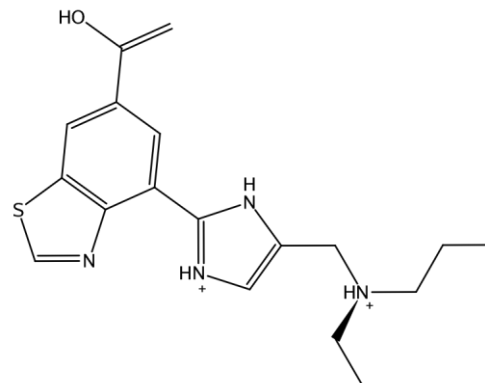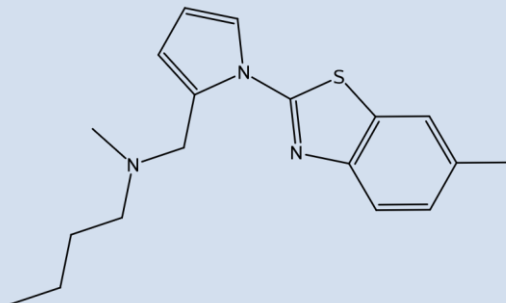
30		-8.97		49	-13.99	65
31		-10.93		49	-13.99	63
32		-12.04		49	-13.99	63
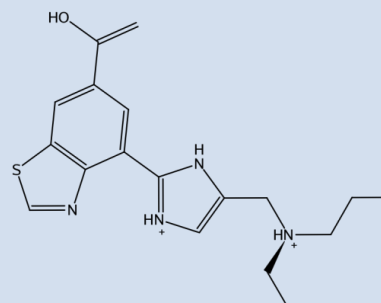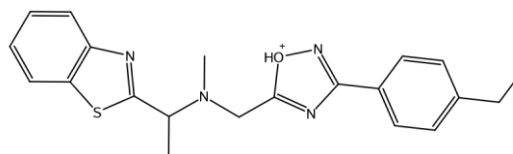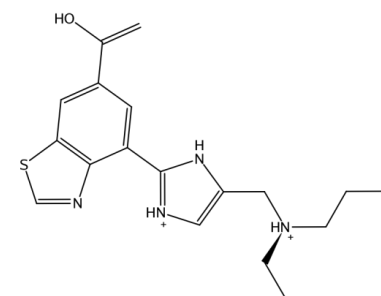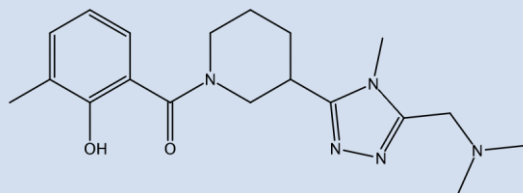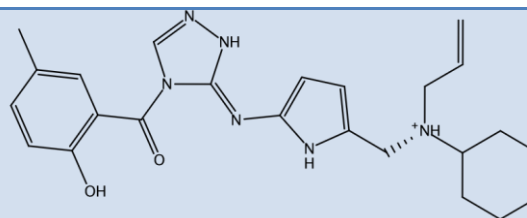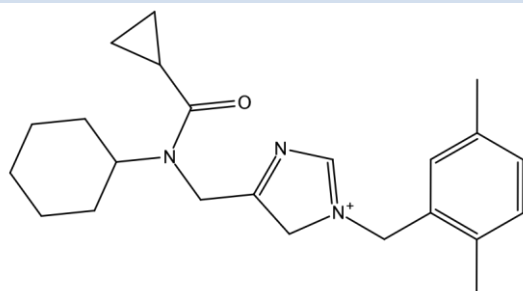
33		-13.25		51	-13.95	60
34		-12.46		51	-13.95	60
35		-10.32		33	-15.438	69
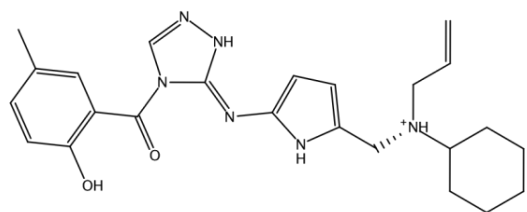
36 -12.77 57 -13.65 61

37 -10.93 28 -15.71 62

38 -9.68 47 -14.21 63

39

-10.60

58   -13.47   63

Figure 3.2: The six analogs purchased for pharmacological assay. The analogs were given numbers according to their rank in the analog database. Analogs were coded DH1 to DH6 for convenience. The analogs were scored and ranked using London dG score. Percent similarity to one of the 60 hit compounds (in parentheses) is given. For example, analog 10 is coded "DH2", has a London dG score of -11.81, and is 67% similar to hit compound 31.

3.1.1.2 Evaluation of scoring functions

Scoring functions are essential in computational experiments, especially when docking of a ligand in a protein's binding pocket is involved. They enable computational chemists to rate and rank hit compounds generated after a computational process. Many scoring functions have been used for different software programs according to the preference of developers. MOE software employs five scoring functions that differ in the algorithm used to predict the interaction of the ligand and protein as a change of free energy of binding. Scoring functions have different success rates depending on the ligand-protein complexes used; therefore, it is important to use different sets of protein-ligand complexes to evaluate their *in vitro* affinity prediction power. However, in this study in order to choose and apply the best out of five MOE scoring functions at D3R, we have used one set of protein-ligand (D3R-ligand) complex to evaluate the scoring function used in MOE software.

Three sets of D3R ligands from different published sources were imported into MOE 2013.08 and docked into the D3R binding pocket using three trials (**Tables 3.3 – 3.5**). The first set was comprised of 11 D3R ligands with range of nanomolar to micromolar affinities, the second set was made up of nine different D3R ligands with a range of nanomolar to micromolar affinities, and the third set was comprised of seven known high range of nanomolar affinity D3R ligands. To assess scoring function predictive power for actual ligand affinities, Graph Pad Prism 6.0 was employed to assess the linear relationship between the average virtual affinity values and the experimental *in vitro* affinities of the test set ligands. The R^2 values for each scoring function and test set ligand ranged from 0.00029 (no linearity) in the evaluation of Alpha HB score to 0.46 in ASE score evaluation. Generally, the prediction was better for the seven known ligands that have high affinities, as R^2 values were the highest among the three test sets.

This suggested that compounds with higher affinities are good test sets, and scoring functions with rigorous criteria can only partially provide important ranking information. London dG scoring was used to rate the DFDD generated hit compounds; however, ASE scoring may be the better predictor (**Table 3.6**).

Superposed GBVI/WSA and Affinity dG score linear regressions lines indicated similar values (**Figure 3.3**). Such superimposed lines could be due to the similarity of algorithm used to generate the virtual affinity; basically, ASE score uses the summation of pairs of atoms of the ligand and the pairs of atoms of the receptor that come in contact at specific distance that favors interaction. Affinity dG score measures the enthalpic impact to the free energy of binding of most interactions that includes hydrogen bonding, ionic interaction, metal ligation, hydrophobic interaction, interaction between a hydrophobic and polar groups, and an interaction between any two atoms. These criteria that are used to measure ASE and Affinity dG scores have a good degree of similarity in measuring the free energy of ligand-receptor interactions.

Table 3. 3: MOE scoring function evaluation of 11 compounds

Ki(nM)	London dG Score			ASE Score			Alpha HB Score			GBVI/WSA Score			Affinity dG Score		
80	-13.87	-13.87	-13.87	-21.80	-21.6	-21.92	-94.80	-94.97	-94.80	-6.400	-6.50	-6.73	-7.63	-7.6	-7.6
100	-14.58	-14.35	-14.24	-20.30	-20.6	-20.60	-83.40	-91.54	-82.98	-6.340	-6.12	-6.70	-6.90	-6.9	-6.9
200	-12.24	-12.16	-12.25	-23.30	-23.2	-22.80	-93.70	-96.10	-97.40	-7.140	-7.11	-6.80	-7.80	-7.8	-7.8
300	-14.12	-13.54	-13.54	-25.50	-23.8	-24.70	-106.32	-104.98	-102.50	-7.300	-7.12	-7.30	-7.40	-7.4	-7.4
500	-13.69	-13.70	-13.70	-25.05	-24.4	-24.20	-102.80	-101.70	-97.70	-7.100	-6.80	-7.13	-8.50	-8.5	-8.5
1300	-15.22	-15.22	-15.22	-25.90	-25.1	-25.60	-127.10	-117.20	-113.10	-8.012	-7.97	-6.90	-8.70	-8.7	-8.7
1600	-13.00	-13.73	-13.73	-20.10	-21.8	-20.70	-101.43	-93.70	-100.42	-6.700	-6.50	-6.30	-7.80	-7.8	-7.8
1800	-14.43	-12.65	-12.65	-26.00	-27.3	-27.70	-106.34	-104.30	-103.21	-7.230	-7.23	-7.23	-7.60	-7.7	-7.7
2200	-13.45	-13.45	-13.45	-19.60	-20.1	-21.20	-83.80	-84.40	-95.65	-6.300	-6.90	-6.30	-6.80	-6.8	-6.8
3000	-16.27	-16.27	-16.46	-28.30	-28.2	-28.50	-99.10	-113.30	-98.98	-7.300	-7.24	-7.30	-7.70	-7.6	-7.6
3100	-12.92	-12.91	-12.92	-27.11	-26.4	-25.10	-106.42	-106.40	102.70	-7.200	-7.20	-7.20	8.20	-8.2	-8.2

Table 3.4: MOE scoring function evaluation of 9 compounds

Ki(nM)	London dG Score			ASE Score			Alpha HB Score			GBVI/WSA Score			Affinity dG Score		
0.91	-13.9	-13.4	-13.4	-31.9	-29.8	-30.1	-107.4	-97.2	-97.2	-7.1	-7.1	-7.2	-8.7	-8.7	-8.4
65	-18.8	-15.6	-15.1	-32.9	-30.4	-32.8	-111.7	-107.5	107.5	-8.1	-8.1	-7.3	-11.2	-11.1	-11.9
190	-12.3	-12.3	-12.3	-28.7	-28.3	-28.7	-117.5	-115.2	-115.1	-6.0	-5.9	-5.8	-9.2	-9.0	-9.2
214	-13.5	-13.5	-13.3	-31.6	-30.1	-30.1	-106.3	-100.4	-100.5	-7.6	-7.9	-7.8	-9.7	-10.1	-9.8
984	-13.6	-13.6	-13.6	-27.3	-28.9	-27.8	-103.4	-87.5	-87.5	-7.1	-7.1	-6.9	-7.2	-7.8	-7.2
1000	-14.1	-14.0	-14.0	-28.5	-29.3	-27.9	-90.1	-98.1	-98.1	-7.1	-7.4	-7.3	-9.7	-9.3	-9.7
1368	-13.9	-13.9	-13.6	-28.6	-28.4	-29.1	-98.9	-98.1	-98.9	-7.1	-7.2	-7.2	-9.0	-9.0	-9.0
4526	-13.7	-10.9	-10.9	-30.8	-31.5	-30.1	-112.5	-112.5	-112.5	-6.9	-6.9	-6.3	-11.2	-11.1	-11.1
5000	-12.8	-12.8	-12.8	-28.8	-28.8	-28.8	-103.8	-105.4	-105.5	-6.1	-6.1	-6.2	-8.4	-8.0	-8.5

Table 3.5: Scoring function evaluation using 7 known D3R ligand

Ki (nM)	London dG Score			ASE Score			Alpha HB Score			GBVI/WSA Score			Affinity dG Score		
0.16	-13.70	-13.72	-14.36	-27.30	-27.30	-27.30	-98.3	-98.3	-98.3	-8.10	-8.10	-8.03	-7.30	-7.30	-7.3
0.52	-14.09	-14.09	-14.02	-32.80	-32.80	-32.80	-118.2	-118.2	-118.2	-7.30	-7.30	-7.30	-8.12	-8.20	-8.2
3.5	-12.16	-12.16	-12.16	-22.70	-22.70	-22.70	-100.8	-100.8	-100.8	-7.45	-7.45	-7.30	-7.30	-7.30	-7.3
3.8	-14.36	-14.36	-14.36	-27.60	-27.60	-27.50	-126.4	-126.4	-126.4	-7.50	-7.10	-7.80	-7.30	-7.30	-7.3
9.8	-12.29	-12.28	-12.29	-26.97	-26.97	-26.97	-104.4	-104.3	-104.3	-7.12	-7.10	-7.12	-8.70	-8.70	-8.7
25	-13.16	-13.16	-13.16	-24.80	-24.80	-24.80	-111.1	-111.1	-111.1	-7.30	-7.20	-7.28	-5.90	-5.90	-5.9
100	-12.82	-12.82	-11.78	-25.14	-15.14	-25.14	-104.9	-104.9	-104.9	-7.40	-7.30	-7.40	-5.80	-5.80	-5.8

a

MOE Scoring function Evaluation of 11 (Carlsson et al., 2011) D3R Compounds
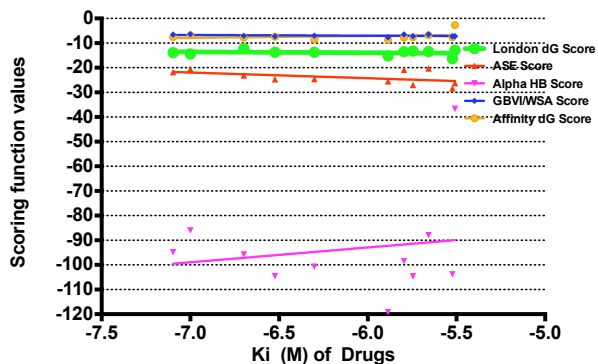
	London dG Score	ASE Score	Alpha HB Score	GBVI/WSA Score	Affinity dG Score
R square	0.03498	0.2412	0.02861	0.1663	0.08350

b

MOE Scoring Function Evaluation of 9 (Bocker A et al., 2007) D3R Compounds
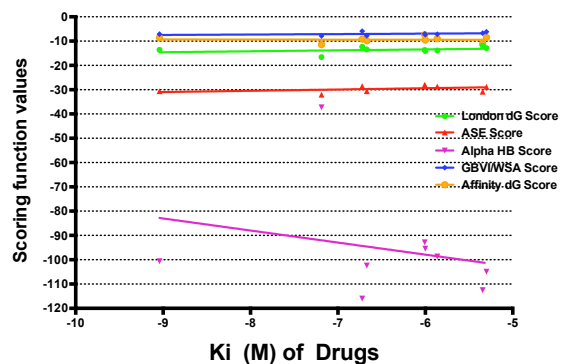
	London dG Score	ASE Score	Alpha HB Score	GBVI/WSA Score	Affinity dG Score
R square	0.1132	0.1916	0.06122	0.1002	0.001111

c

MOE Scoring Function Evaluation of 7 Known D3R Compounds
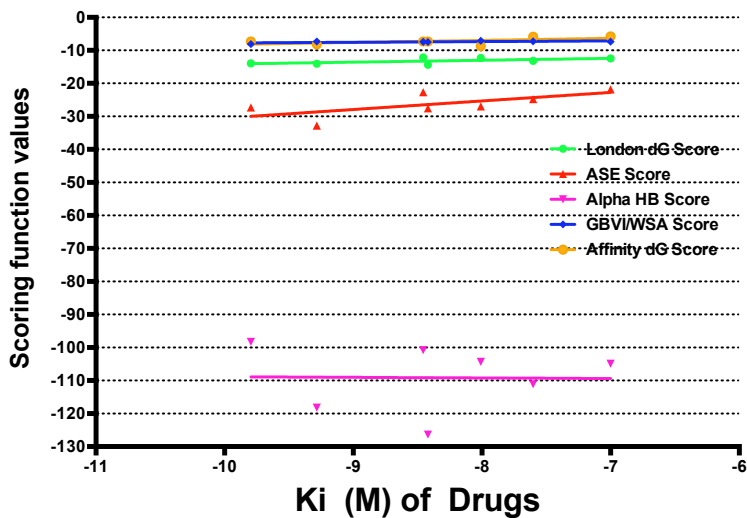
	London dG Score	ASE Score	Alpha HB Score	GBVI/WSA Score	Affinity dG Score
R square	0.3591	0.4555	0.0002899	0.4118	0.3107

81

Figure 3.3: Linear regression of VS experimental affinities of three test sets. The five scoring functions, London dG score (green), ASE score (red), Alpha HB score (pink), GBVI/WSA score (blue) and Affinity dG score (orange) are shown as linear colored lines. Panel **a** is a linear regression graph of virtual and experimental affinities of test set one (11 compounds), panel **b** represents test set two (9 compounds) and panel **c** test set three (7 compounds). Evaluation shows that there is no linear relationship between the virtual and experimental affinities (highest R^2 values of 0.45 or less). GBVI/WSA (blue line) and Affinity dG score (orange line) superposed showing similar virtual affinity values. The R^2 values are shown in tables under each graph test set. Data were derived via docking the test set compounds in the D3R binding pocket and linear regression of the experimental and virtual affinity values of each test set was graphed. Data represents an average of three independent experiments.

Table 3.6: Evaluation of scoring functions in terms of R^2

Test set	London dG Score (R^2)	ASE Score (R^2)	Alpha HB Score (R^2)	GBVI/WSA Score (R^2)	Affinity dG Score (R^2)
First (11 ligands)	0.03498	0.2412	0.02861	0.1663	0.08350
Second (9 ligands)	0.1132	0.1916	0.06122	0.1002	0.00111
Third (7 known ligands)	0.3591	0.455	0.0002899	0.4118	0.3107

3.1.1.3 MedChem transformations

The D3R receptor that was previously prepared and used for scaffold replacement was also employed for MedChem transformations. Bioisosteric and ring substitution/cyclization options were used to generate hit compounds from the transformation of eticlopride. MedChem transformations could be performed on multiple parts or even the entire structure of a known compound. This flexibility enables sequential transformation of all parts of eticlopride. Six experiments (six transformation options) were conducted. Because MedChem transformation allows up to 50 iterations in one transformation batch, a huge number of hit compounds may be generated. Transformation iteration number ranges from five to 50, depending on the number of hits returned and if their chemical nature supports further transformation. London dG score, structural novelty, and visual inspection were used to select hit compounds. One complete transformation of eticlopride was typically comprised of two events: transforming one part of the molecule while retaining the remainder, then transforming the remainder using hits from the first transformation. There were exceptions to this process in that experiments five and six were

transformed at once. In Experiment 5 almost all parts of eticlopride were transformed except the linker (methyl amide); in six, the entire molecule was transformed (**Table 3.7**).

In Experiment 1, the ethyl pyrrolidine part of eticlopride transformation yielded 53 hits. Based on the selection criteria described above, two hits were selected and their aryl amide part was further transformed, generating 50,193 hits. Nine hits were selected for final commercial availability search. In Experiment 2, amide ethyl pyrrolidine transformation produced 17,904 hits, two of which were selected for aryl transformation to generate 44,567 hits, and 47 of these selected for commercial availability search. In Experiment 3, aryl transformation yielded 12,564 hits, three of which were selected for subsequent amide ethyl pyrrolidine transformation. This produced 207,380 hits, 57 of which were searched for commercial availability. In Experiment 4, aryl amide transformation yielded 15,756 hits; however, none of these hits were selected for further transformation because visual inspection revealed that they lacked promising drug-like features. In Experiment 5, the aryl and ethyl pyrrolidine portions were transformed at the same time resulting in 48,716 hits, and 23 hits were selected for commercial availability. In Experiment 6, 84,937 hits were generated, and 51 hits were selected for commercial availability. In total, 187 hit compounds were selected for pharmacological characterization; surprisingly, none of these hits were commercially available. Most drug-like hits with synthetic plausibility were identified based on medicinal chemistry knowledge, and six top-ranked compounds were selected for synthesis (**Figure 3.4**).
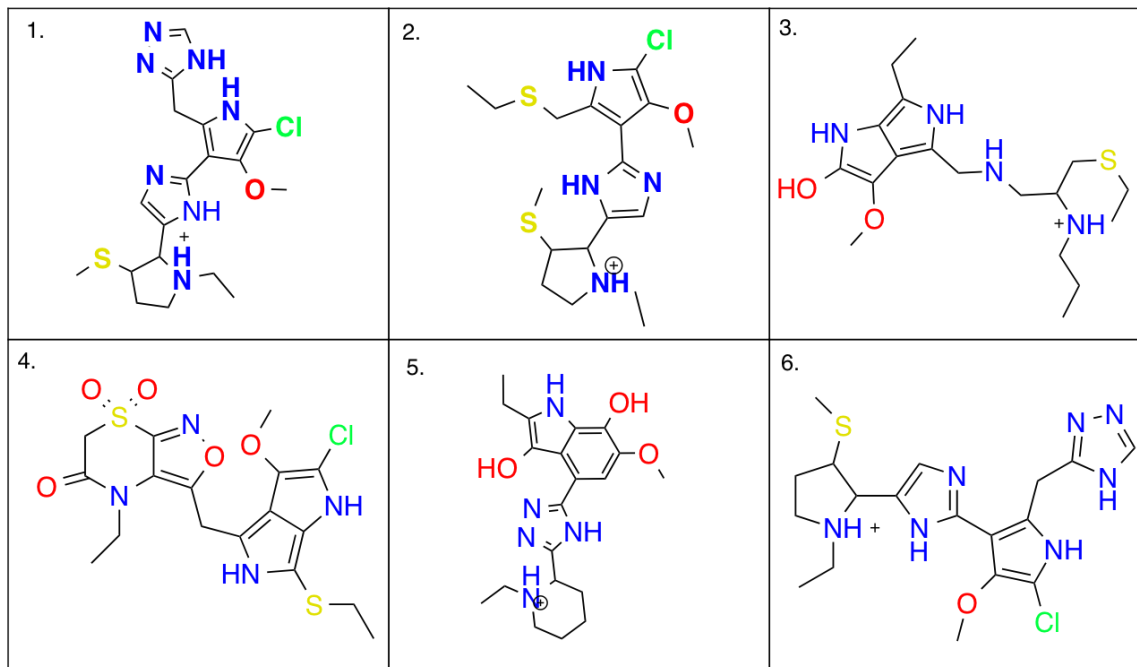
Figure 3. 4: Six MedChem transformation-generated compounds that have synthetic plausibility.

Table 3. 7: MedChem transformation of eticlopride

Exp. No.	Part transformed	Part Retained	Hits of the transformed part	Retained part transformed hits	Hits Selected	Commercial availability
1	Ethyl pyrrolidine	Aryl amide	53	50,140	9	0
2	Amide ethyl pyrrolidine	Aryl	17,904	26,663	47	0
3	Aryl	Amide ethyl pyrrolidine	12,564	194,816	57	0
4	Aryl Amide	Ethyl Pyrrolidine	15,756	0	0	0
5	Aryl and ethyl pyrrolidine	Linker (methyl amide)	48,716	Untransformed	23	0
6	Whole eticlopride	-	84, 937	0	51	0
Total	-	-	179,930	271,619	187	0

3.1.2 Pharmacology

D3R stably transfected HEK293 cells were used to prepare membranes. HEK293 cells are a popular choice because of their fast and easy reproduction and maintenance, amenability to transfection with high efficacy and protein production, and small cell size (Thomas and Smart, 2005). It was reported that stably expressing D2R in the human neuronal cell line SH-SY5Y produced stronger functional signals than when D3R was expressed at HEK293 cells (Alberts et al., 2000). However, because this study involved binding assays, choice of cell line is expected to have limited effects.

Before pharmacological characterization of the purchased compounds, it was necessary to determine the concentration of membrane preparation to be used for membrane binding assays. Serial dilution of a membrane pellet (30 - 40 µg) was prepared using a D3R membrane-binding buffer (1 M Tris base, 0.5 M KCl, 0.5 M $CaCl_2$, and 0.5 M $MgCl_2$ pH 7.4). Extensive radioligand displacement by the high affinity D2/3R antagonist eticlopride was observed when the membrane pellet of 30 - 40 µg was dissolved in 6.5 ml of the D3R membrane-binding buffer. It was also necessary to optimize the D3R membrane-binding assay, adapted from the Luedke laboratory and improved for the present work. Nonradioactive eticlopride was used in a competitive membrane-binding assay with the D3R antagonist radioligand [^{3}H]-spiperone. A Ki value of 0.5 nM was obtained (**Figure 3.5a**), comparable to the previously reported 0.16 nM affinity (Chien et al. 2010). This confirmed the functionality of the membrane-binding assay.

The six purchased hit compounds were initially tested in a one-point membrane binding assay at 10 µM concentration using membranes prepared from hD3R-HEK293 cells, measuring percentage displacement of [^{3}H]-spiperone. Compound DH3 showed statistically significant inhibition (55%) of radioligand binding (**Figure 3.5b**). Compared to the positive control,

eticlopride, the radioligand inhibition shown by DH3 was low. A multipoint competitive membrane-binding assay indicated a DH3 binding Ki value of 1.97 ± 0.36 μM (**Figure 3.6a**). Because DH3 and DH5 were similar in their linker and pyrrolidone groups, the binding affinity of DH5 was determined, at 10.16 ± 3.00 μM (**Figure 3.6b**). Both hit compounds showed modest affinities towards D3R, and low affinities compared with eticlopride. DH3 and DH5 were generated from Experiment 1 of scaffold replacement of eticlopride, in which first the ethyl pyrrolidine and then the aryl group was replaced, resulting in hit compounds that were not commercially available. The search for commercially available analogs generated DH3 and DH5 that are 65-70% similar to their original precursors, and both have structural similarity only differing at their aryl region (**Figure 3.7**).

a
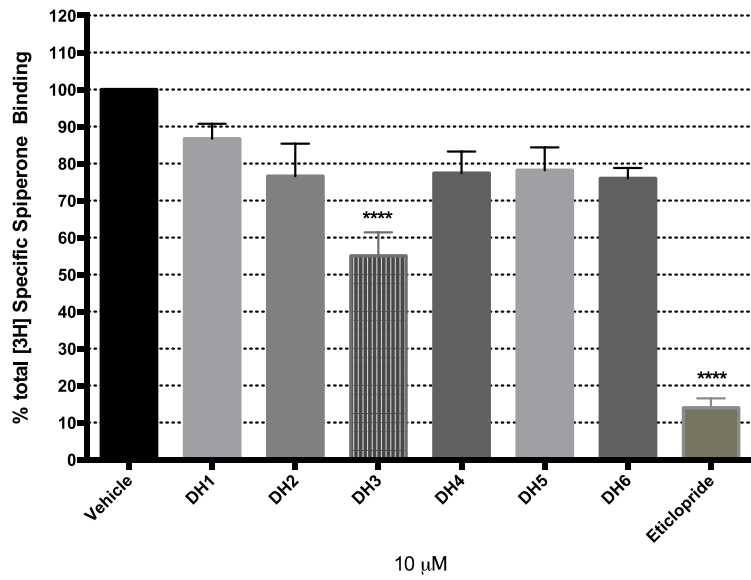
$Ki_{ave} = 0.496 \pm 0.112$ nM

b

****P < 0.0001 Vs Vehicle in that assay. Data represent N= 3 independent experiments. Ordinary One-way ANOVA followed by Dunnett's multiple comparisons test.

Figure 3.5: Eticlopride competitive membrane binding assay and initial one-point membrane binding assay of the six initial hit compounds (DH1-DH6). Panel **a** represents affinity of eticlopride at HEK293 cells stably expressing hD3R. Ki value was derived from experiments incubating D3R stably transfected cell membranes with eticlopride in the presence of [^{3}H] spiperone (0.5nM) at room temperature in D3R binding buffer. Panel **b** represents an initial 10μM membrane binding assay of DH1, DH2, DH3, DH4, DH5 and DH6. One-point binding affinities were assessed via [^{3}H] spiperone (0.5nM) displacement when DH1 –DH6 were incubated at hD3R-HEK293 cell membranes. The data represents mean ± SEM of at least 3 separate experiments.

a

(Panel a: % total [3H] Specific Spiperone Binding vs Log [DH3])

Ki $_{ave}$ = 1.97± 0.36 μM

b

(Panel b: % total [3H] Specific Spiperone Binding vs Log [DH5])

Ki $_{ave}$ = 10.16 ± 3 μM
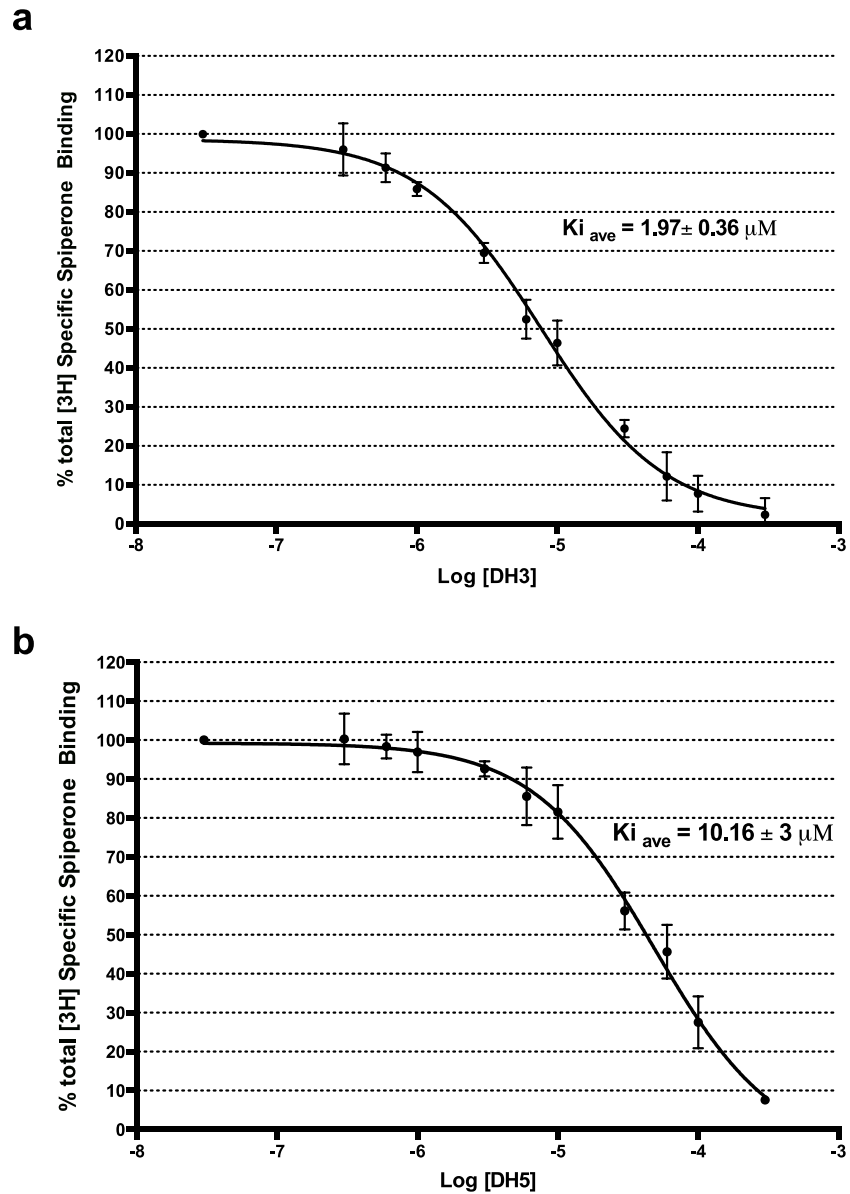
Figure 3.6: Affinity of DH3 and DH5 at hD3R stably expressing HEK293 cell membranes. Panel **a** represents affinity of DH3 and panel **b** represents affinity of DH5. Ki values were determined via incubating membranes from hD3R-HEK293 cell with DH3 and DH5 in the presence of [^{3}H] spiperone (0.5nM) at room temperature in D3R binding buffer. Values represent the mean $\pm$ SEM from three independent experiments, each conducted in duplicate determinations.

a

Eticlopride

Cmp252 ethyl
Pyrrolidine R. of Eti

Cmp 25 (Aryl amide
R. of Cmp 252)

Analog 35 (DH3) (SciFinder
Scholar)

b

Eticlopride

Cmp138 of ethyl Pyrrolidine R of Eti.

Cmp 39 (Aryl R. of Cmp 138)

Analog 28 (DH5) (SciFinder Scholar)

92
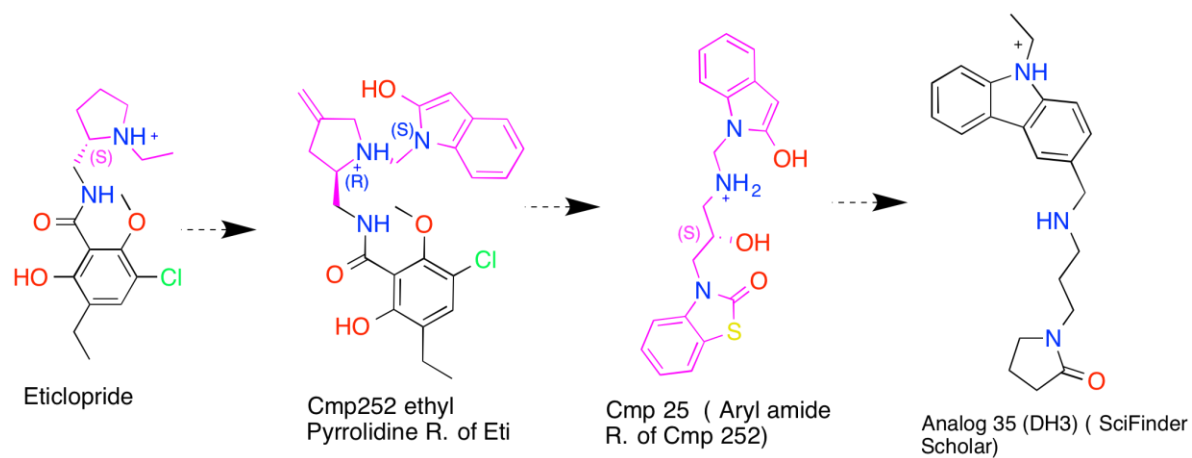
Figure 3.7: Development of DH3 and DH5. Panel **a** is showing scaffold replacement of eticlopride that lead to generation of DH3. Eticlopride pyrrolidine part (pink) was replaced resulting in Compound 252 (number in the returned database in the replacement of ethyl pyrrolidine). The aryl and the linker part of Compound 252 were replaced further generating Compound 25 (ranked 12 in the 60 selected compounds). Commercial unavailability of Compound 25 lead to selection of a 69% structural similar analog, DH3 (Analog 35). (R.) Represents replacement; compound's number represents ranking of returned hits within the database resulting from scaffold replacement of a part of eticlopride. Panel **b** is showing scaffold replacement of eticlopride that lead to generation of DH5. Eticlopride ethyl pyrrolidine part (pink) was replaced resulting in Compound 138. The aryl part of Compound 138 was further replaced generating Compound 39. Commercial unavailability of Compound 39 led to selection of 65% similar analog, DH5 (Analog 28).

Eticlopride has a tertiary amine in its ethyl pyrrolidine group that is ionized at physiological pH, forming an ionic interaction with Asp110 that is important for the drug's affinity. A pharmacophore feature was created to retain this tertiary amine in the resulting hit compounds; however, DH3 and DH5 lack this feature, as they are analogs of the original hit compounds. Rather, these analogs have an amide feature in their pyrrolidone group (**Figure 3.8a**). Analogs were sought that have a tertiary amine in this site to determine if a tertiary amine in the pyrrolidone portion of DH3 is critical for high D3R affinity. Four analogs, coded DH3A1, DH3A2, DH3A3 and DH3A4, were identified from SciFinder Scholar (**Figure 3.8b**), and were purchased. These DH3 analogs have a tricyclic hydrophobic group and a linker of four to five atoms that link the tricyclic rings to a six membered ring group, with the exception of DH3A4 that has a methyl amide linker connected to the amine group. DH3A1, DH3A2, and DH3A4 have an amide group in their linker comprising four atoms including the amide, while DH3A3 has a secondary amine group in its linker of five atoms including the secondary amine (**Figure 3.8b**). In their six membered rings, the analogs differ in that DH3A1 has a cyclohexane group, DH3A2 has a benzene ring, and DH3A3 has a morpholine group and a tertiary amine that can be ionized at physiological pH.
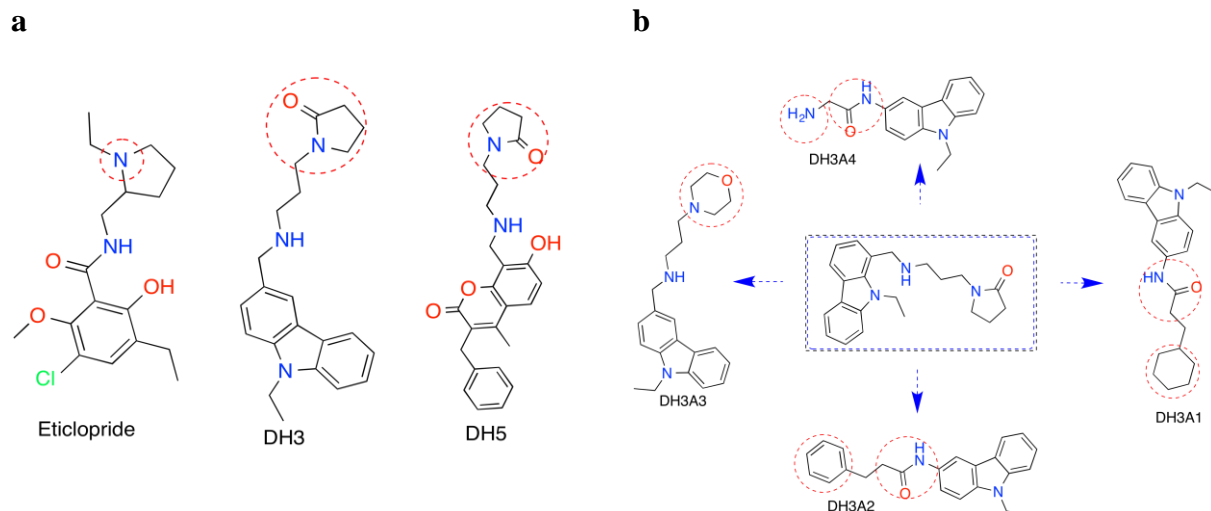
Figure 3.8: Structural similarities and differences between eticlopride, DH3 and its analogs, and DH5. (**a**) Eticlopride, DH3, and DH5 structural differences are shown at the eticlopride tertiary amine. (**b**) Structural differences of DH3 derivatives are shown at the six membered ring and the linker.

The one-point binding assay revealed that DH3A1, DH3A3, and DH3A4 showed statistically significant inhibition of the radioligand compared to the positive control, eticlopride (**Figure 3.9a**). The concentration-response full curve assay showed that only DH3A3 has modest affinity (1.56 ± 0.53 μM) (**Figure 3.9b**). This was apparently a sensitivity issue, as the low passage cell lines (Passage 17-19) used to prepare membranes may have had low expression of the D3R protein. DH3A3 was expected to have higher affinity at D3R due its ionizable tertiary amine in its morpholine ring that could potentially interact with Asp110 to form an ionic interaction; nevertheless, its affinity was modest.

a
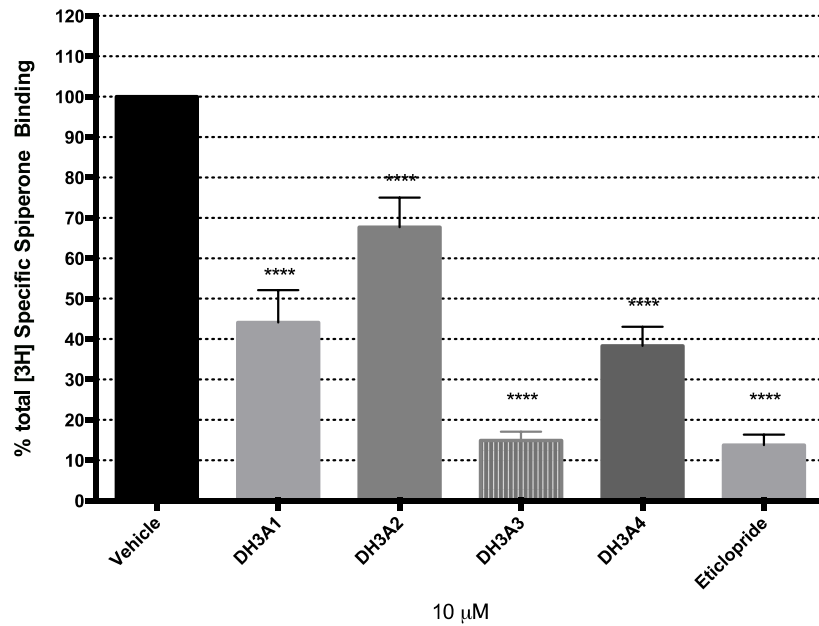
y-axis: % total [3H] Specific Spiperone Binding

x-axis categories: Vehicle, DH3A1, DH3A2, DH3A3, DH3A4, Eticlopride

10 μM

****P < 0.0001 Vs vehicle in that assay. Data represent N= 3 independent experiments. Ordinary one-way ANOVA followed by Dunnett's multiple comparisons test.

b

y-axis: % total [3H] Specific Spiperone Binding

x-axis: Log [DH3A3]

$Ki_{ave} = 1.56 \pm 0.53\ \mu M$
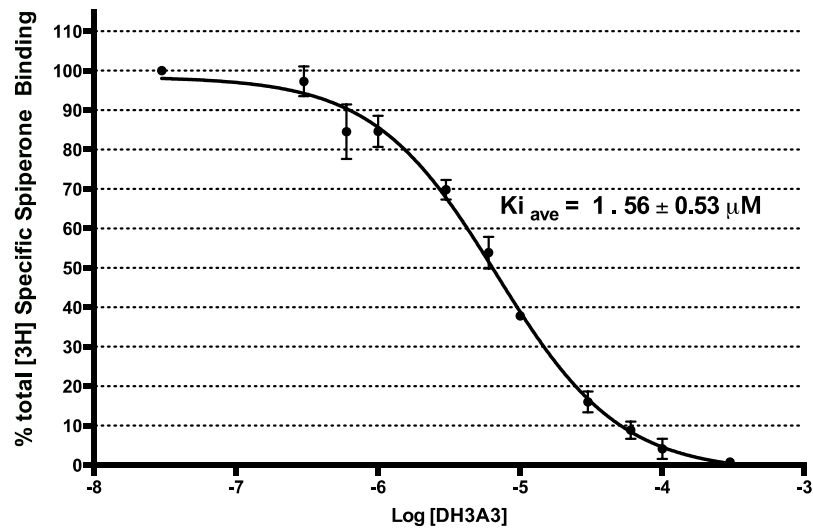
Figure 3.9: Initial one-point membrane binding assay of four DH3 derivatives (DH3A1-DH3A4) and DH3A3 competitive membrane binding assay. Panel **a** represents one-point membrane binding affinities at 10μM assed via [³H] spiperone (0.5nM) displacement when DH3A1 –DH3A3 were incubated at hD3R-HEK293 cell membranes at room temperature. Panel **b** represents affinity of DH3A3 at HEK293 cells stably expressing hD3R. DH3A3 Ki value was derived from experiments incubating D3R stably transfected cell membranes with DH3A3 in the presence of [³H] spiperone (0.5nM) at room temperature in D3R binding buffer. Data values represent the mean $\pm$ SEM from three independent experiments, each conducted in duplicate determinations.

London dG score, structural novelty, and visual inspection were used to select top hits from the 39 analogs for pharmacological characterization, giving more emphasis to the structural features that are predicted to bind well in the D3R binding pocket and on the docking and binding interaction of the hits within the pocket. However, the fragment building method generated too many hit compounds for all to be visually inspected. Thus, scoring functions ranked the top 1000 to 2000 hits in every DFDD process for prioritizing visual inspection. The *in vitro* affinity prediction power of London dG score was also assessed by using the scoring value of eticlopride (-13.45 kcal/mol) as a standard to select hits with high and low scoring values from the 39 analogs (**Figure 3.10**). Analogs 29 (-14.472) and 33 (-13.253) had scores comparable to eticlopride; Analogs 16 (-7.73) and 19 (-7.2042) with poor scores were also selected for control purposes. Analogs 29 and 33 were purchased for pharmacological characterization; however, analogs 16 and 19 were prohibitively expensive. Although the initial

binding screen indicated significant D3R affinity, full characterization of Analog 29 revealed a

modest binding affinity (3.47± 2.4 μM) (**Figure 3.11b**).
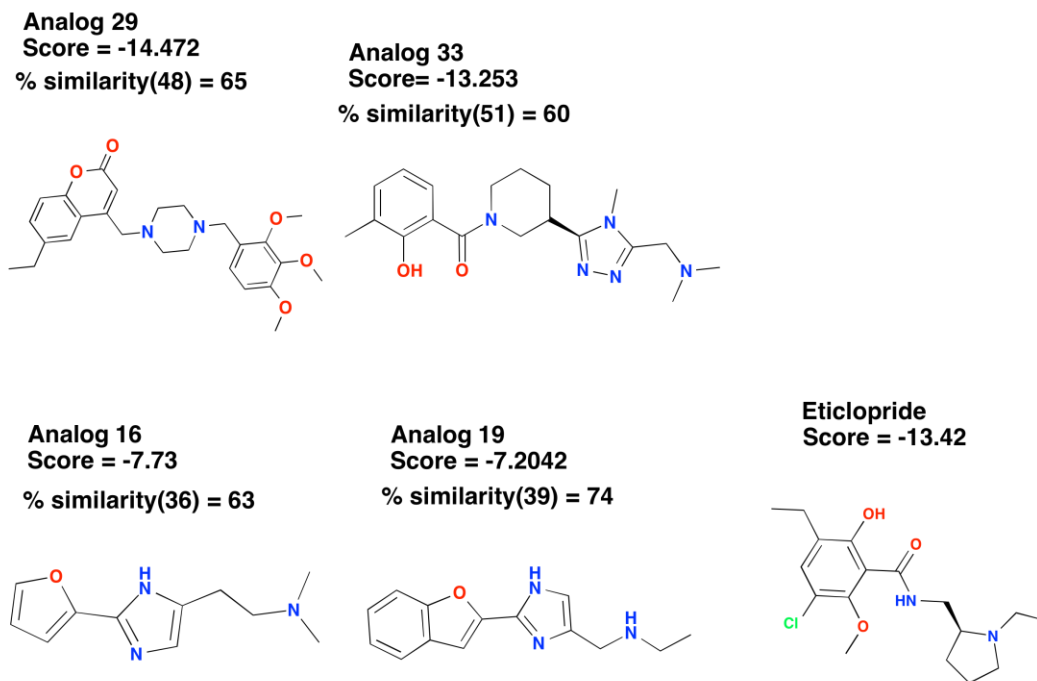
Figure 3.10: Scaffold replacement hit analogs of high and low London dG score.

The numbers in parentheses represent the rank of the hits within the database of the 60

selected hits.
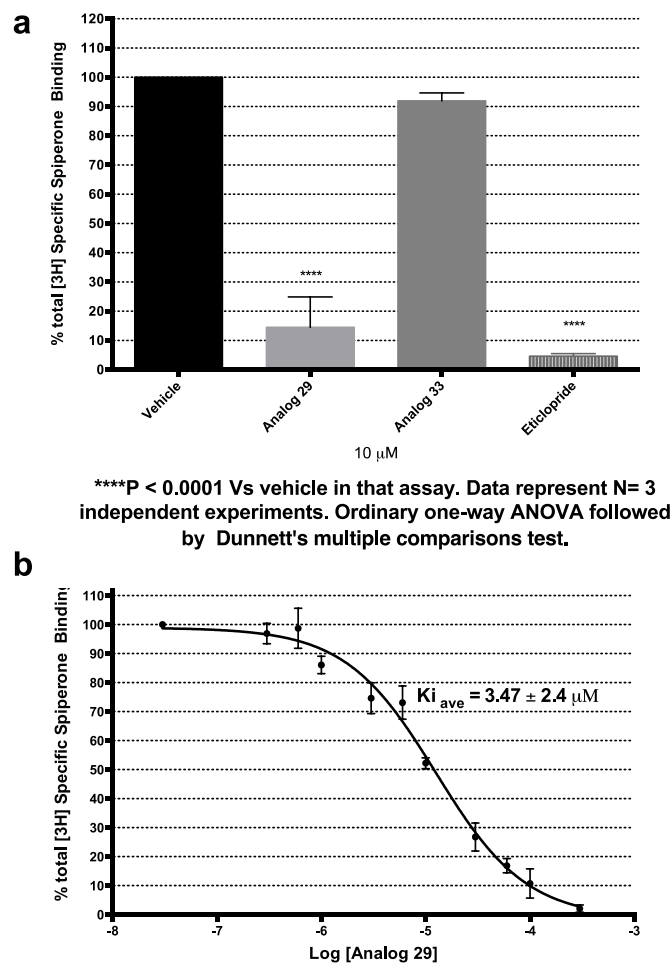
Figure 3.11: Initial one-point membrane binding assay of Analogs 29 and 33; Analog 29 competitive membrane binding assay. (**a**) One-point binding affinities at 10μM assessed via [^{3}H] spiperone (0.5nM) displacement when Analog 29 or 33 was incubated at hD3R-HEK293 cell membranes at room temperature. (**b**) Affinity of Analog 29 at HEK293 cells stably expressing hD3R. The Analog 29 Ki value was derived from experiments incubating D3R stably transfected cell membranes with Analog 29 in the presence of [^{3}H] spiperone (0.5nM) at room temperature in D3R binding buffer. Data values represent the mean ± SEM from three independent experiments, each conducted in duplicate determinations.
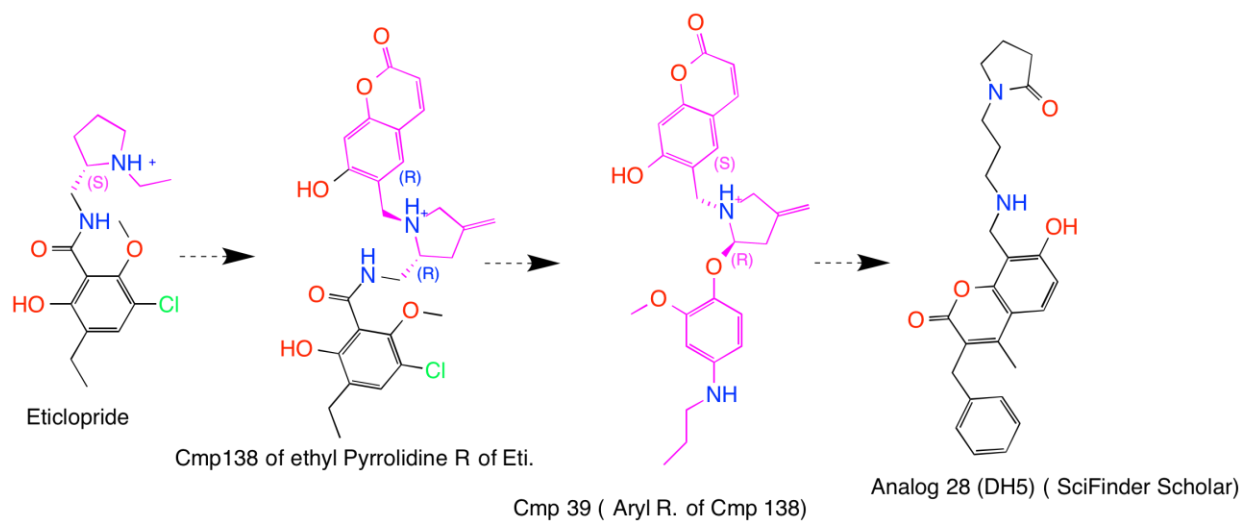
The passage number for a cell line is important to membrane binding assays because it may affect the degree of cell surface expression of the target protein encoded by the transfection. In the one-point membrane-binding assay of DH3 derivatives (**Figure 3.9a**) and Analogs 29 and 33 (**Figure 3.11a**), it was observed that the sensitivity of the assay was very low. This insensitivity was confirmed by full curve competitive membrane binding assay of individual compounds, as only DH3A3 and Analog 29 showed detectable binding affinity. The result may have been due to the cell passage used (Passage 17-19); optimal results are typically achieved when the passage lines are between 20 and 30. In order to test this notion, cell passage lines between 20 and 30 were used in the one-point membrane-binding assay for all purchased hit compounds (**Figure 3.12**). Consistent results were shown with the previous full curve competitive membrane-binding assays of DH3A3 and Analog 29, and with the previous one-point membrane binding assays of the first six hit compounds (DH1-DH6) (**Figure 3.5**). As shown in **Figure 3.12**, only DH3, DH3A3, Analog 29, and DH3A1 showed significant radioligand inhibition compared to eticlopride, consistent with their full curve competitive membrane binding assays. Interestingly, DH3A1 showed significant radioligand inhibition at one-point membrane binding but did not show appreciable binding affinity when its radioligand inhibition ability was tested at different concentrations in competitive membrane binding assays. This could be due to solubility problems.
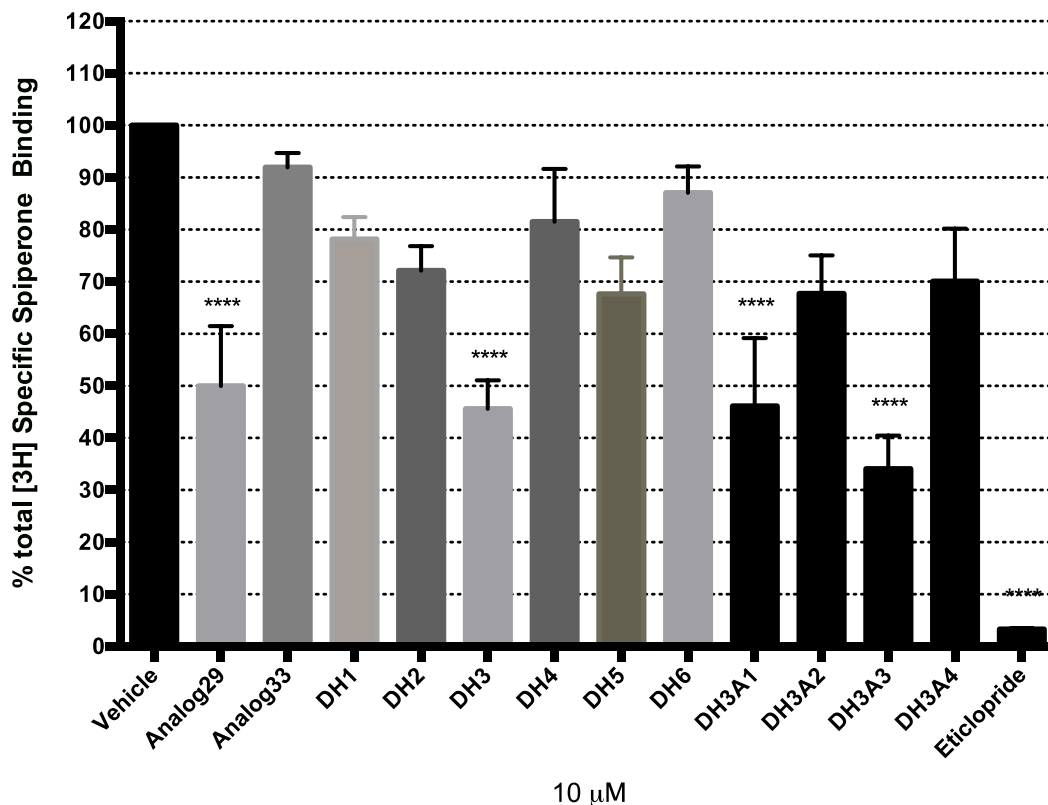
Figure 3.12: One-point D3R membrane binding affinities of all purchased hit compounds.

Ten μM final concentration of each hit compound was assessed for ability to displace [^{3}H]

spiperone (0.5nM) at hD3R-HEK293 cell membranes in D3R binding buffer solution at room

temperature. Data values represent the mean $\pm$ SEM from three independent experiments, each

conducted in duplicate determinations.

The D3R hit compounds purchased were derivatives of the 60 top selected hits that were generated from scaffold replacement of eticlopride, a D2/D3 receptor-selective antagonist. Though efficacy assays would be needed to determine the status of the hit compounds as agonist, antagonist or partial agonist, it was logical to compare hit compound binding affinities with the natural D3R agonist, dopamine. Compounds with either no (DH6), modest (Analog 29) or high (eticlopride) D3R affinity were chosen for direct comparison. In order to prevent its oxidization, dopamine was dissolved in 50 mM (1% w/v) ascorbic acid in D3R binding buffer solution. The one-point (10 µM) binding assay suggested that dopamine significantly inhibited radioligand binding; DH6 and Analog 29 showed radioligand inhibition consistent with previous results (**Figure 3.13a**). Surprisingly, 1% ascorbic acid in D3R binding buffer solution was found to significantly inhibit radioligand binding comparable to the positive control eticlopride. Moreover, when dopamine was dissolved in the 1% ascorbic acid buffer solution, a slight synergistic effect was shown compared to dopamine dissolved in normal D3R binding buffer. Consequently, it was logical to test ascorbic acid's effect on each compound (DH6, Analog 29 and eticlopride). It was found out that all hit compounds that were tested by dissolving in 1% ascorbic acid D3R binding buffer solution showed similar radioligand inhibition effects (**Figure 3.13b**). It would appear that ascorbic acid could displace the radioligand at the D3R or denature the 3D structure of the receptor protein. Dopamine binding affinity was also determined to compare it with the affinity of hit compounds that were tested and was found to be 25.88 ± 0.12 nM (**Figure 3.14**) comparable to the literature value of 25 ± 2 nM (Robinson et al., 1994).

a

10 μM

****P < 0.0001 Vs vehicle in that assay. Data represent N= 3
independent experiments. Ordinary one-way ANOVA followed
by Dunnett's multiple comparisons test

b

10 μM

****P < 0.0001 Vs vehicle in that assay. Data represent N= 3
independent experiments. Ordinary one-way ANOVA
followed by Dunnett's multiple comparisons test
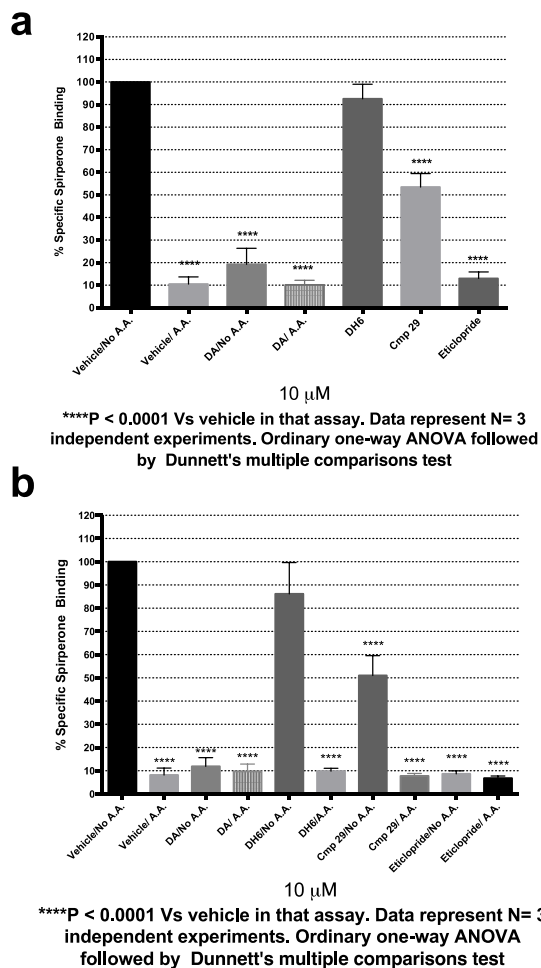
Figure 3.13: One-point D3R membrane binding affinities of dopamine, DH6, Analog 29 and eticlopride. (**a**) One point D3R membrane binding affinities of dopamine with and without 1% ascorbic acid (A.A.) binding buffer, DH6, Analog 29 and eticlopride. (**b**) One point D3R membrane affinities of dopamine, DH6, Analog 29 and eticlopride with or without 1% AA D3R binding buffer. Inhibitor concentrations were 10μM; affinity was assessed by measuring [^{3}H] spiperone (0.5nM) displacement at hD3R-HEK293 membranes. Data values represent the mean ± SEM from three independent experiments, each conducted in duplicate determinations.
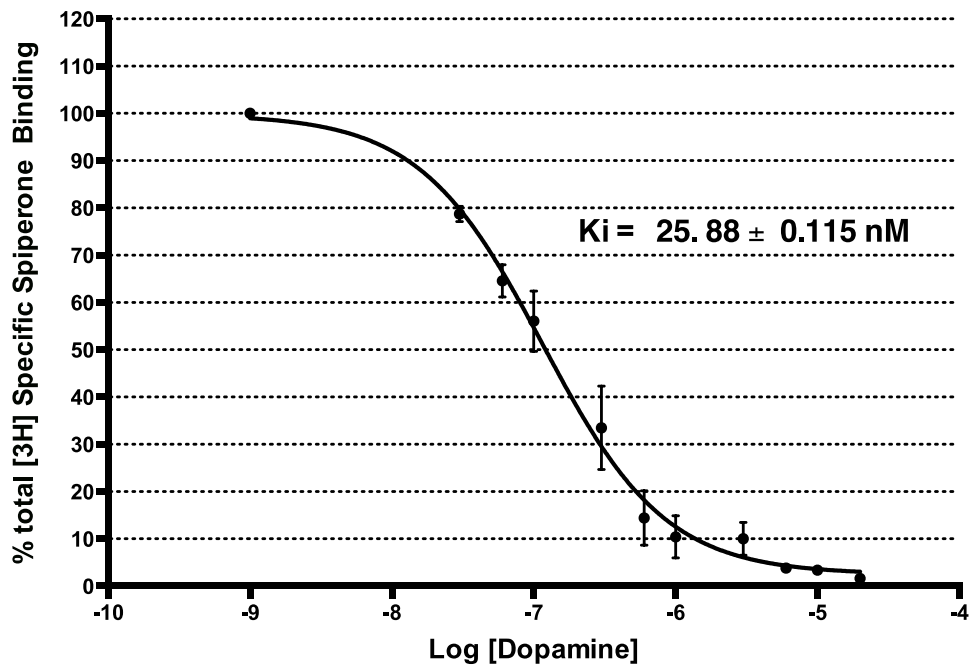
Figure 3.14: Competitive membrane binding assay of dopamine. Ki value was derived from experiments incubating D3R stably transfected cell membranes with dopamine in the presence of [³H] spiperone (0.5nM) at room temperature in D3R binding buffer. Data values represent the mean ± SEM from three independent experiments, each conducted in duplicate determinations.

Table 3.8: Scaffold replacement hit compounds and their D3R binding affinities
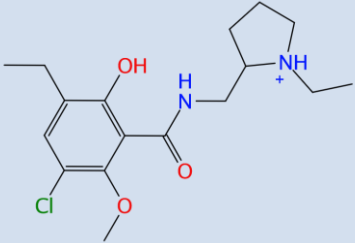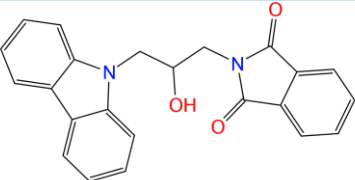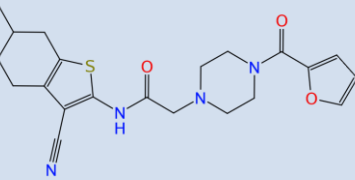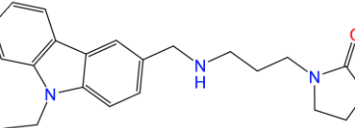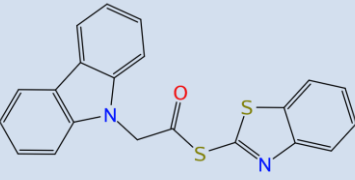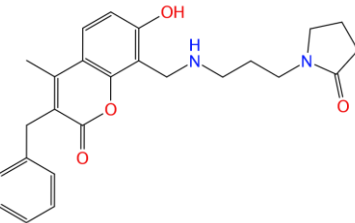
No.	Compound	D3R binding affinity (nM)
1	Eticlopride	0.49 ± 0.11
2	DH3	1970 ± 360
3	DH3A3	1560 ± 530
4	DH5	$10,160 \pm 3000$
5	Analog 29	3470 ± 2400
6	Dopamine	25.88 ± 0.12
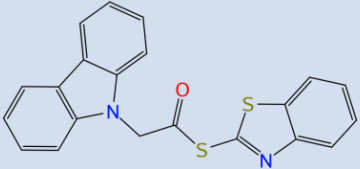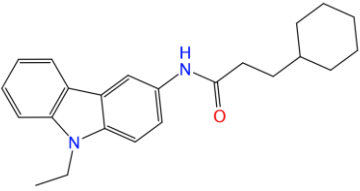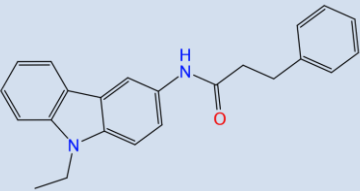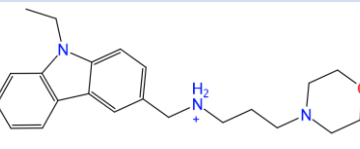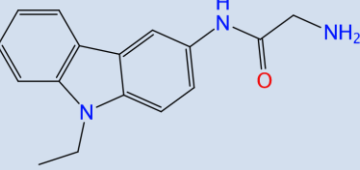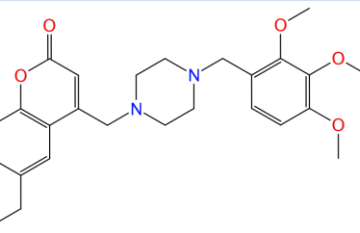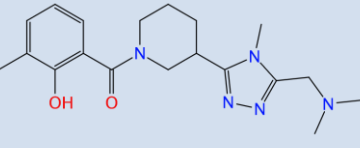
3.1.2.1 Structural novelty of the pharmacologically characterized compounds

Hit compound analogs that were purchased and pharmacologically characterized were assessed for similarity to eticlopride, the parent compound, using the Tanimoto coefficient (Tc). This coefficient is based on 2D molecular fingerprints that compare structural similarities between two compounds, and it is the method of choice for *in silico*-guided, fingerprint-related similarity calculations (Willett, 2006). Tc measures structural similarity between two samples as defined by the number of common features divided by the total available features. In order to determine the novelty of the pharmacologically characterized analogs, a MOE database was created that included eticlopride, the parent compound, and all purchased analogs. The database was converted to SDF file format from MDB and was used to calculate similarities between the analogs and eticlopride using OpenBabel software (O'Boyle et al., 2011). Including eticlopride, 13 molecules were analyzed for their similarity percentage; almost all were structurally dissimilar to the parent compound. The highest level of uniqueness is observed when Tc is less than 0.35 (Carlsson et al., 2011). Only Analogs 29 and 33 have Tc values above this threshold;

however, they are dissimilar to eticlopride because they have Tc values of less than or equal to 0.4. The compounds least similar to eticlopride were DH3 (0.14) and DH3A4 (0.17), while the compounds most similar to eticlopride in the database were Analog 33 (0.4) and Analog 29 (0.39) (**Table 3. 9**). Hit compound analogs that were pharmacologically characterized had low affinities compared to the parent compound, eticlopride. This could be due to limitations in DFDD ability to generate high affinity ligands, and the analogs being derivatives of the originally selected hit compounds. DFDD methods are reported to generate low micromolar affinity hit compounds (Hajduk and Greer, 2007; Hoffer et al., 2011; Schneider and Fechner 2005).

Table 3. 9: Structural novelty of pharmacologically characterized compound

Purchased analogs	Structure of purchased analogs	London dG Score	Experimental affinity (Ki nM)	Analog similarity to eticlopride (T.C.)
Eticlopride		-13.45	0.49 ± 0.112nM	1.00
DH1 (Analog 12)		-10.0848	N/A	0.192308
DH2 (Analog 10)		-11.8131	N/A	0.294872
DH3 (Analog 35)		-10.3205	1970 ± 360 nM	0.142857
DH4 (Analog 23)		-10.0034	N/A	0.348571
DH5 (Analog 28)		-10.5444	10,160nM ± 3000nM	0.336957

DH6 (Analog 26)		-10.2952	N/A	0.307143
DH3A1		-12.1818	N/A	0.181208
DH3A2		-11.1381	N/A	0.225166
DH3A3		-15.0789	1560 ± 530 nM	0.248276
DH3A4		-11.2277	N/A	0.170213
Analog 29		-14.4721	3470 ± 2400nM	0.391304
Analog 33		-13.2530	N/A	0.402299

N/A = analog does not have D3R affinity.

3.2   Discussion

As expected, scaffold replacement SR generated a huge number of hit compounds ("hits") even when somewhat strict descriptor filters were used to ensure drug-like compounds. Scaffold replacement of certain eticlopride portions, however, returned few hits, especially when stricter descriptor filters were used. This is due to the chemical nature of the R-groups used to generate new structures. For a new structure to be created, the bond length, hybridization, orientation and bond angle of the fragment and the R-group should match. In such situations, the descriptor filters were slightly relaxed to generate enough hits.

Surprisingly, the 60 hits selected for pharmacological characterization were not commercially available in vendor databases. This could be due to the relatively complex hit structures attributed to the fragment database used, and synthesis plausibility scores that had weak predicting power. The commercial unavailability also reflects the structural novelty of the hits. Clearly, there is room for improvement regarding the available MOE fragment database and the predicting power of the synthetic plausibility score.

The aim of this study was to evaluate and refine DFDD methodologies (scaffold replacement, MedChem transformation, and ligand building) via generating novel structures that may have D3R binding activity. For such evaluation, either commercially available hits should be generated or analogs of such hits should be identified. Because the 60 selected top hits were not commercially available, 39 commercially available analogs were identified from the SciFinder Scholar database. Three of these analogs (DH3, DH5, and analog 29) and one analog of DH3 (DH3A3) were found to have modest D3R binding affinity, supporting the hypothesis that DFDD can be used to generate D3R ligands. Most lead compounds generated via DFDD have micromolar affinities for the target receptor (Hajduk and Greer, 2007; Hoffer et al., 2011;

Schneider and Fechner 2005). Consistent with this observation, the pharmacologically characterized hits have low range micromolar binding affinities (**Table 3.8**).

Any part of a known bioactive ligand can be replaced using MOE scaffold replacement when the scaffold is not essential for biological activity and has two exit vectors defined (**Figure 1.4**). The core portion of a known active ligand can also be used to achieve scaffold hopping (SH) using other computational programs (Langdon, 2010). There are many programs and approaches that can perform SH; however, the "scaffold" definition and the SH approach vary among programs (Krueger et al., 2009; Mauser and Guba, 2008; Tsunoyama et al., 2008; Zhao, 2007). Each has advantages, disadvantages and limitations depending on the codes, algorithms, scoring functions, and fragment databases used.

In the present work, scaffold replacement was performed using MOE software (Grimshaw, 2010; Sourial, 2007); other programs refer to the scaffold replacement approach as SH (Brown and Jacoby, 2006; Fontaine et al., 2009; Quintus et al., 2009; Vaino, 2013). Scaffolds have been replaced by SH to improve bioavailability via increased lipophilicity (Beaulieu et al., 2006), enhance solubility by introducing polar groups (Bovens et al., 2009), increase binding affinity by increasing rigidity of compounds (Koltun et al., 2009), and avoid formation of toxic metabolites (Roy, 1997). Such projects were medicinal chemist controlled and relied mainly on medicinal chemistry knowledge; these ligand based drug discovery approaches resulted in few hit compounds. Selected hits were then synthesized and pharmacologically characterized. The disadvantages of such projects were that they did not explore a larger chemical space within protein binding pockets with the possibility of generating novel structures, and were expensive and time-consuming. However, in MOE scaffold replacement, scaffolds were replaced using wider "chemical space" of an 800,000-fragment

database generated from 4.3 million molecules in vendor databases. The molecules were first subjected to "washing" and filtering to render a pool of drug-like compounds. The washed compounds were then exposed to retrosynthetic methods that break bonds using RECAP rules (Lewell et al., 1998) and Schuffenhauer decomposition (Schuffenhauer et al., 2007). Such methods may not generate exclusively synthesizable structures even if further scored for synthetic plausibility, as such scores can be of questionable accuracy (Grimshaw, 2010). Avoiding huge numbers of hits that are either not synthesizable or less druggable are the major challenges of DFDD.

In the present study, selection of hits for further computational processes or for pharmacological characterization was based on three important factors: scoring function values (London dG score), novelty of generated structures, and visual inspection. Commercial availability and cost of the hit compound were also considered. Scoring functions are important in rating and ranking of hits in computational experiments even though their success rate is limited (Li et al., 2013; Moal et al., 2013). To improve the current functions, algorithms that can precisely predict ligand protein interactions should be developed (Halperin et al., 2002; Warren et al., 2006). In order to choose the best of the five MOE scoring functions, each was assessed using a D3R-eticlopride complex data test set. Results showed that these functions failed to predict the experimental affinity of known ligands; however, as in many previously performed evaluation experiments (Cheng et al. 2009; Kontoyianni et al., 2004; Li et al., 2014; Warren et al. 2006; Wang et al., 2003), many protein–ligand complex data test sets should be included for more precise consensus assessments. In this study, London dG score was used for rating and ranking of hits because of its previous use in a similar scaffold replacement evaluation experiment using a different protein-ligand complex (Grimshaw, 2010). In this evaluation of

scoring function, ASE score ranked higher than London dG score, but neither reached the threshold R^2 value that depicts a linear relationship between two variables (R^2 =0.81). While the currently used scoring functions lack *in vitro* affinity prediction power, they are essential to alleviating the manual assessment of each hit, and providing easy, rapid hit rankings.

Structural similarity affects pharmacological activity (yera et al., 2011), and the field of chemical informatics operates under the notion that similar chemical structures show similar pharmacological activity (Nettles et al., 2006). Structurally similar drugs may also have similar adverse effects (Vilar et al., 2012; Vilar et al., 2012). Many antipsychotics and antidepressants have severe adverse effects that challenge their usability and competency (Ferguson, 2001; Goldstein and Goodnick, 1998; Muench and Hamer, 2010). In such scenarios, lead compounds that are structurally dissimilar to known therapeutics could reduce the likelihood of adverse effects (Nolan et al., 2011). The D3R hits generated via scaffold replacement of eticlopride were found to be structurally dissimilar to the parent compound. The degree of similarity was quantified by calculation of Tanimoto coefficients(Tversky, 1977). The structural novelty of the D3R hits was an important successful outcome of DFDD.

Because of the limited precision of the currently used scoring functions and problems with accurate determination of free energy of ligand binding, manual assessment of hits generated from computational experiments was essential. This type of *in silico* assessment of individual hit compounds within the receptor binding pocket is called visual inspection, which increases the success rate of *in silico* experiments when performed by medicinal and computational chemistry experts (Cosconati et al., 2010). In visual inspection, the virtual interaction of a hit compound with key residues of the receptor binding pocket is analyzed, as is the chemical nature of the hit compound (Immadisetty et al., 2013). However, a crystal

structure-based pose of the virtual interaction between the receptor binding pocket and a ligand reveals only one scenario; due to the overall dynamics of the protein-ligand interaction, hundreds of conformations, orientations, and positions of the ligand within the pocket are generated. Such shortcomings hinder the accuracy of visual inspection. Even though automated scoring functions alone may not reveal the actual interaction of a ligand and protein, success rates increase with the addition of visual inspection. The drawback of using either criterion alone or combination of both is that selection could be biased in a way that eliminates promising hits. Employing the dynamics of a protein-ligand complex using powerful computer processors could enhance the efficiency of visual inspection, even if it is demanding.

In order to understand, refine and evaluate novel drug design computational methodologies before applying them to target proteins that are implicated in disease, a proof of concept is essential to avoid wastage of time and resources. In this study, the D3R was used as a tool for evaluating DFDD; antagonists identified and developed in this manner should be useful agents against pathologies involving the D3R. Antagonists of this receptor can be used in the treatment of substance abuse (Heidbreder et al. 2005; Newman et al., 2012; Newman et al., 2005), in schizophrenia (Crider and Scheideler, 2001; Gurevich et al., 1997; Jardemark et al., 2002; Semba, 2004), in alcohol consumption (Harrison and Nobrega, 2005; Jeanblanc et al., 2006; Leggio et al., 2014; Thanos et al., 2005), and in appetite disorders (obesity) (Dodds et al., 2012; Mogg et al., 2012). D3R partial agonists can be used for effective treatment of schizophrenia. In schizophrenia, dopamine release is excessive in the subcortical regions of the brain but low in the cortical regions. This phenomena demands ligands that stabilize the concentration of dopamine throughout these regions; partial agonists are "stabilizers" that behave as antagonists at subcortical regions and agonists at the cortical regions creating uniform

dopamine concentrations (Bolonna and Kerwin, 2005; Crismon et al., 2003; Cousins and Young, 2005). The pharmacologically characterized analogs of hit compounds generated in this study could have potential D3R partial agonistic effects, but this was not assessed. According to the evaluation in the current study, DFDD in MOE may be a powerful tool for drug design after further refinement and improvement.

Ligand building is a method that was added to MOE software for lead optimization and building of new structures either from a free space in a binding pocket or from a smaller structure. It employs medicinal chemistry rules for generating novel structures, especially when a protein is used. The prediction of one half of the eticlopride molecule, by its deletion and reconstruction by growing from the remaining half, was only partially successful. The computational ligand building method did not rebuild exactly the starting structure of eticlopride, regardless of which molecule half (aryl or ethyl pyrrolidine) was used to seed growth. Specifically, the tertiary amine from the ethyl pyrrolidine moiety and the 2-methoxy group from the aryl moiety could not be generated (**Figure 2.10**). The failure to generate these regions of eticlopride could be due to the limited number of building fragments that were available in the MOE database at that time. The availability of fewer fragments and the software following strict medicinal chemistry rules to build structures within a protein-binding pocket yielded very few structures. In the course of evaluating the ligand building method, much was learned toward understanding and applying DFDD approaches; nevertheless, for the reasons provided above the ligand-building method was not used to generate new structures from eticlopride or other parent compounds.

Previously, MedChem transformation has been described and evaluated for generating drug-like compounds (Ekins et al., 2010; Kirchmair et al., 2008; Segall et al., 2011; Stewart et

al., 2006). Segall and colleagues identified 206 MedChem transformation rules relevant to drug design. Most of the compounds generated via such rules were drug-like molecules that were familiar to skilled medicinal chemists (Segall et al., 2011). Applying this method to the present work yielded a huge pool of hits that were commercially unavailable, indicating structural novelty but also undesirable synthetic plausibility. After selection of top hits based on structure novelty, scoring function and visual inspection, the compounds were analyzed by experienced medicinal chemists. Based on synthetic plausibility and drug-likeness, many of the hits were eliminated, and few passed the filtering process for synthesis.

The flood of information related to drug-like properties, synthesis, and physical and chemical properties, combined with shortcomings in the *in silico* descriptor filters, scoring functions, and medicinal chemistry rules to predict drug feasibility and characteristics, renders the computational methods described here suboptimal. Therefore, further fine-tuning of DFDD is necessary for making such methods more effective and an integral part of drug design projects.

In conclusion, although computational techniques are yet to be full-fledged, they are assuming a pivotal role in the drug discovery process and have shown some success in the identification of new lead compounds for drug design. DFDD methods are faster, cheaper, and generate higher hit rates than their virtual screening and traditional high throughput screening counterparts; however, it could be time-consuming also if such methods are not well understood, performed and managed. DFDD can generate novel structures that are dissimilar to the parent compound, providing a new avenue for lead optimization and reduction of adverse effects related to known ligands. Virtual screening filters compounds that already synthesized and collected in a library, potentially reducing innovation. Proof of concept is essential to evaluate novel *in silico* methods before being employed to target proteins. Such evaluation is essential especially when

115

the 3D structure of the target receptor has yet to be resolved at the lab bench. Virtual methods for such cases could save time and resources in drug discovery. DFDD may not provide the expected and desired outcome, but could still give very important results toward reaching lead compounds that could be optimized. The challenging part of such methods is that it is difficult to determine at which intermediate step one has achieved "success" or "failure". Moreover, even though lead compounds may be identified, the unverified native-binding mode of the lead compound within the protein pocket could be challenging to rapid, successful lead optimization. In this study, DFDD was successful in generating hit compounds with modest binding affinity that could be used as lead compounds. This success arguably provides confidence in applying DFDD to other target proteins.

CHAPTER FOUR

4   SUMMARY

The results achieved in this study are significant to the ongoing efforts in the development of novel antidepressants with fast onset of action, improved efficacy and reduced adverse effects.   The evaluation of DFDD (MOE scaffold replacement, MedChem transformation and ligand building) as tools for drug design was successful, especially scaffold replacement.   Scaffold replacement of eticlopride generated novel structures that have low micromolar D3R affinities.   Hit compounds generated by the above methods were not commercially available, but the scaffold replacement method generated analogs of hit compounds that could be purchased and pharmacologically characterized for their binding affinity at D3R.   Six analogs of 60 selected hit compounds were pharmacologically tested, and only the compound coded "DH3" was found to have low micromolar affinity (1970 ± 360 nM).   To improve the affinity of DH3, four analogs of DH3 were purchased.   Only "DH3A3" was found to have low micromolar affinity (1560 ± 530nM); there was no significant affinity improvement over that of DH3.   In the process of evaluating the ability of scoring function to predict experimental affinity, Analog 29 was found to also have micromolar affinity (3470 ± 2400nM).   From evaluating the MOE London dG score alone, it is apparent that further evaluation processes are needed, and currently available scoring functions are in need of improvement.   Although pharmacological characterization of MedChem transformation generated hit compound analogs were not performed, the method generated a huge pool of hit compounds, confirming its ability to generate novel structures.   Novelty of generated structures was part of the evaluation process of the computational methods, and all of the pharmacologically characterized analogs were structurally novel to the parent compound,

eticlopride. This specific quality suggests that novel structures could be generated from established antidepressant drugs in a way that might isolate and remove any undesirable properties. The discovered compounds with modest D3R affinity reported within may also be valuable lead compounds for combating diseases in which D3R is implicated.

The present study suggests the successful use of combined approaches that include computational chemistry (DFDD), medicinal chemistry (visual inspection), and pharmacology (membrane binding assay) to evaluate *de novo* fragment-based drug design methods of scaffold replacement, MedChem transformation and ligand building. The identification of the DH3, DH5, DH3A3 and Analog 29 compounds confirms the ability of scaffold replacement to generate novel structures that may be useful as lead compounds for combating many neurological and psychiatric diseases such as depression, addiction, Parkinson's disease, and schizophrenia.

5   BIBLIOGRAPHY

Acharya, C., A. Coop, J. E. Polli, and A. D. Mackerell, Jr. (2011). Recent advances in ligand-based drug design: relevance and utility of the conformationally sampled pharmacophore approach. *Curr Comput Aided Drug Des*, *7* (1), 10-22.

Adams, C. P., and V. V. Brantner. (2006). Estimating the cost of new drug development: is it really 802 million dollars? *Health Aff (Millwood)*, *25* (2), 420-8.

Al-Harbi, K. S. (2012). Treatment-resistant depression: therapeutic trends, challenges, and future directions. *Patient Prefer Adherence*, *6*, 369-88.

Aparoy, P., K. K. Reddy, and P. Reddanna. (2012). Structure and ligand based drug design strategies in the development of novel 5- LOX inhibitors. *Curr Med Chem*, *19* (22), 3763-78.

Artigas, F. (2013). Future directions for serotonin and antidepressants. *ACS Chem Neurosci*, *4* (1), 5-8.

Baldessarini, R. J. (1989). Current status of antidepressants: clinical pharmacology and therapy. *J Clin Psychiatry*, *50* (4), 117-26.

Beaulieu, P. L., J. Gillard, D. Bykowski, C. Brochu, N. Dansereau, J. S. Duceppe, B. Hache, A. Jakalian, L. Lagace, S. LaPlante, G. McKercher, E. Moreau, S. Perreault, T. Stammers, L. Thauvette, J. Warrington, and G. Kukolj. (2006). Improved replicon cellular activity of non-nucleoside allosteric inhibitors of HCV NS5B polymerase: from benzimidazole to indole scaffolds. *Bioorg Med Chem Lett*, *16* (19), 4987-93.

Berton, O., and E. J. Nestler. (2006). New approaches to antidepressant drug discovery: beyond monoamines. *Nat Rev Neurosci*, *7* (2), 137-51.

Bocker, A., B. C. Sasse, M. Nietert, H. Stark, and G. Schneider. (2007). GPCR targeted library design: novel dopamine D3 receptor ligands. *ChemMedChem*, *2* (7), 1000-5.

Boeckler, F., and P. Gmeiner. (2006). The structural evolution of dopamine D3 receptor ligands: structure-activity relationships and selected neuropharmacological aspects. *Pharmacol Ther*, *112* (1), 281-333.

Bosker, F. J., B. H. Westerink, T. I. Cremers, M. Gerrits, M. G. van der Hart, S. D. Kuipers, G. van der Pompe, G. J. ter Horst, J. A. den Boer, and J. Korf. (2004). Future antidepressants: what is in the pipeline and what is missing? *CNS Drugs*, *18* (11), 705-32.

Bourin, M., D. J. David, P. Jolliet, and A. Gardier. (2002). Mechanism of action of antidepressants and therapeutic perspectives. *Therapie*, *57* (4), 385-96.

Bovens, S., M. Kaptur, A. S. Elfringhoff, and M. Lehr. (2009). 1-(5-Carboxyindol-1-yl)propan-2-ones as inhibitors of human cytosolic phospholipase A2alpha: synthesis and properties of bioisosteric benzimidazole, benzotriazole and indazole analogues. *Bioorg Med Chem Lett*, *19* (8), 2107-11.

Brown, N., and E. Jacoby. (2006). On scaffolds and hopping in medicinal chemistry. *Mini Rev Med Chem*, *6* (11), 1217-29.

Carlsson, J., R. G. Coleman, V. Setola, J. J. Irwin, H. Fan, A. Schlessinger, A. Sali, B. L. Roth, and B. K. Shoichet. (2011). Ligand discovery from a dopamine D3 receptor homology model and crystal structure. *Nat Chem Biol*, *7* (11), 769-78.

Chaki, S., T. Okubo, and Y. Sekiguchi. 2006. Non-monoamine-based approach for the treatment of depression and anxiety disorders. *Recent Pat CNS Drug Discov*, *1* (1), 1-27.

Cheng, T., X. Li, Y. Li, Z. Liu, and R. Wang. (2009). Comparative assessment of scoring functions on a diverse test set. *J Chem Inf Model*, *49* (4), 1079-93.

Chien, E. Y., W. Liu, Q. Zhao, V. Katritch, G. W. Han, M. A. Hanson, L. Shi, A. H. Newman, J. A. Javitch, V. Cherezov, and R. C. Stevens. (2010). Structure of the human dopamine D3 receptor in complex with a D2/D3 selective antagonist. *Science*, *330* (6007), 1091-5.

Clark, A. M., and P. Labute. (2007). 2D depiction of protein-ligand complexes. *J Chem Inf Model*, *47* (5), 1933-44.

Connolly, K. R., and M. E. Thase. (2011). If at first you don't succeed: a review of the evidence for antidepressant augmentation, combination and switching strategies. *Drugs*, *71* (1), 43-64.

Cosconati, S., S. Forli, A. L. Perryman, R. Harris, D. S. Goodsell, and A. J. Olson. (2010). Virtual Screening with AutoDock: Theory and Practice. *Expert Opin Drug Discov*, *5* (6), 597-607.

Cramer, R. D., R. J. Jilek, S. Guessregen, S. J. Clark, B. Wendt, and R. D. Clark. (2004). Lead hopping. Validation of topomer similarity as a superior predictor of similar biological activities. *J Med Chem*, *47* (27), 6777-91.

CRC. (1994). *CRC Handbook of Chemistry and Physics*, CRC Press.

Crider, A. M., and M. A. Scheideler. (2001). Recent advances in the development of dopamine D(3) receptor agonists and antagonists. *Mini Rev Med Chem*, *1* (1):89-99.

Dickson, M., and J. P. Gagnon. (2004). The cost of new drug discovery and development. *Discov Med*, *4* (22), 172-9.

Dodds, C. M., B. O'Neill, J. Beaver, A. Makwana, M. Bani, E. Merlo-Pich, P. C. Fletcher, A. Koch, E. T. Bullmore, and P. J. Nathan. (2012). Effect of the dopamine D3 receptor antagonist GSK598809 on brain responses to rewarding food images in overweight and obese binge eaters. *Appetite*, *59* (1), 27-33.

Drevets, W. C., and M. L. Furey. (2010). Replication of scopolamine's antidepressant efficacy in major depressive disorder: a randomized, placebo-controlled clinical trial. *Biol Psychiatry*, *67* (5), 432-8.

Drozak, J., and J. Bryla. (2005). Dopamine: not just a neurotransmitter. *Postepy Hig Med Dosw*, *59*, 405-20.

Ekins, S., J. D. Honeycutt, and J. T. Metz. (2010). Evolving molecules using multi-objective optimization: applying to ADME/Tox. *Drug Discov Today*, *15* (11-12), 451-60.

Environment(MOE), Molecular Operating. 2013.08. Chemical Computing group Inc., 1010 Sherbooke St. West, Suite #910, Montreal, QC, Canada, H3A 2R7, 2013.

Erlanson, D. A. 2012. Introduction to fragment-based drug discovery." *Top Curr Chem* no. 317:1-32.

Ertl, P., B. Rohde, and P. Selzer. (2000). Fast calculation of molecular polar surface area as a sum of fragment-based contributions and its application to the prediction of drug transport properties. *J Med Chem*, *43* (20), 3714-7.

Feighner, J. P. (1999). Mechanism of action of antidepressant medications. *J Clin Psychiatry*, *60* Suppl 4, 4-11, discussion 12-3.

Feng, Z., T. Hou, and Y. Li. (2012). Selectivity and activation of dopamine D3R from molecular dynamics. *J Mol Model*, *18* (12), 5051-63.

Ferguson, J. M. (2001). SSRI Antidepressant Medications: Adverse Effects and Tolerability. *Prim Care Companion J Clin Psychiatry*, *3* (1), 22-27.

Fontaine, F., S. Cross, G. Plasencia, M. Pastor, and I. Zamora. (2009). SHOP: a method for structure-based fragment and scaffold hopping. *ChemMedChem*, *4* (3), 427-39.

Furey, M. L., and W. C. Drevets. (2006). Antidepressant efficacy of the antimuscarinic drug scopolamine: a randomized, placebo-controlled clinical trial. *Arch Gen Psychiatry*, *63* (10), 1121-9.

Geldenhuys, W. J., K. E. Gaasch, M. Watson, D. D. Allen, and C. J. Van der Schyf. (2006). Optimizing the use of open-source software applications in drug discovery. *Drug Discov Today*, *11* (3-4), 127-32.

Giuliani, D., and F. Ferrari. (1997). Involvement of dopamine receptors in the antipsychotic profile of (-) eticlopride. *Physiol Behav*, *61* (4), 563-7.

Goldstein, B. J., and P. J. Goodnick. (1998). Selective serotonin reuptake inhibitors in the treatment of affective disorders--III. Tolerability, safety and pharmacoeconomics. *J Psychopharmacol*, *12* (3 Suppl B), S55-87.

GraphPad Prism version 6.00 for Mac OS X, GraphPad Software, San Diego California USA, http://www.graphpad.com.

Grimshaw, Simon. (2010). Scaffold Replacement in MOE. *Chemical Computing Group*, 1010 Sherbrooke Street West, Suite 910 Montreal, Canada H3A 2R7

Gumnick, J. F., and C. B. Nemeroff. (2000). Problems with currently available antidepressants. *J Clin Psychiatry*, *61* Suppl 10, 5-15.

Gurevich, E. V., Y. Bordelon, R. M. Shapiro, S. E. Arnold, R. E. Gur, and J. N. Joyce. (1997). Mesolimbic dopamine D3 receptors and use of antipsychotics in patients with schizophrenia. A postmortem study. *Arch Gen Psychiatry*, *54* (3), 225-32.

Hackling, A. E., and H. Stark. (2002). Dopamine D3 receptor ligands with antagonist properties. *Chembiochem*, *3* (10), 946-61.

Hajduk, P. J., and J. Greer. (2007). A decade of fragment-based drug design: strategic advances and lessons learned. *Nat Rev Drug Discov*, *6* (3), 211-9.

Halgren, TA. (1998). Force fields: MMFF94. *Encyclopedia of computational chemistry*, *2*, 1033-1035.

Halgren, Thomas A. (1996). Merck molecular force field. I. Basis, form, scope, parameterization, and performance of MMFF94. *Journal of Computational Chemistry*, *17* (5-6), 490-519.

Halperin, I., B. Ma, H. Wolfson, and R. Nussinov. (2002). Principles of docking: An overview of search algorithms and a guide to scoring functions. *Proteins*, *47* (4), 409-43.

Han, C., S. M. Wang, H. J. Seo, B. C. Lee, H. J. Jeon, W. Kim, K. P. Kwak, and C. U. Pae. (2014). Aripiprazole augmentation, antidepressant combination or switching therapy in patients with major depressive disorder who are partial- or non-responsive to current antidepressants: a multi-center, naturalistic study. *J Psychiatr Res*, *49*, 75-82.

Harrison, S. J., and J. N. Nobrega. (2009). A functional role for the dopamine D3 receptor in the induction and expression of behavioural sensitization to ethanol in mice. *Psychopharmacology (Berl)*, *207* (1), 47-56.

Hartenfeller, M., and G. Schneider. (2011). De novo drug design. *Methods Mol Biol*, *672*, 299-323.

Hartenfeller, M., H. Zettl, M. Walter, M. Rupp, F. Reisen, E. Proschak, S. Weggen, H. Stark, and G. Schneider. (2012). DOGS: reaction-driven de novo design of bioactive compounds. *PLoS Comput Biol*, *8* (2), e1002380.

Hartman, G. D., M. S. Egbertson, W. Halczenko, W. L. Laswell, M. E. Duggan, R. L. Smith, A. M. Naylor, P. D. Manno, R. J. Lynch, G. Zhang, and et al. (1992). Non-peptide

fibrinogen receptor antagonists. 1. Discovery and design of exosite inhibitors. *J Med Chem*, *35* (24), 4640-2.

Heidbreder, C. A., E. L. Gardner, Z. X. Xi, P. K. Thanos, M. Mugnaini, J. J. Hagan, and C. R. Ashby, Jr. (2005). The role of central dopamine D3 receptors in drug addiction: a review of pharmacological evidence. *Brain Res Brain Res Rev*, *49* (1), 77-105.

Heidbreder, C. A., and A. H. Newman. (2010). Current perspectives on selective dopamine D(3) receptor antagonists as pharmacotherapeutics for addictions and related disorders. *Ann N Y Acad Sci*, *1187*, 4-34.

Hoffer, L., J. P. Renaud, and D. Horvath. (2011). Fragment-based drug design: computational & experimental state of the art. *Comb Chem High Throughput Screen*, *14* (6), 500-20.

Honma, T. (2003). Recent advances in de novo design strategy for practical lead identification. *Med Res Rev*, *23* (5), 606-32.

Hopkins, A. L., and C. R. Groom. (2002). The druggable genome. *Nat Rev Drug Discov*, *1* (9), 727-30.

Howland, R. H. (2010). Serendipity and psychopharmacology. *J Psychosoc Nurs Ment Health Serv*, *48* (10), 9-12.

Huang, S. Y., S. Z. Grinter, and X. Zou. (2010). Scoring functions and their evaluation methods for protein-ligand docking: recent advances and future directions. *Phys Chem Chem Phy*, *12* (40), 12899-908.

Immadisetty, K., L. M. Geffert, C. K. Surratt, and J. D. Madura. (2013). New design strategies for antidepressant drugs. *Expert Opin Drug Discov*, *8* (11), 1399-414.

Jaccard, P. (1901) Distribution de la flore alpine dans le bassin des Dranses et dans quelques régions voisines. Bulletin de la Société Vaudoise des Sciences Naturelles *37*, 241-272.

Jain, A. N. (2004). Virtual screening in lead discovery and optimization. *Curr Opin Drug Discov Devel*, *7* (4), 396-403.

Janero, D. R. (2012). Productive university, industry, and government relationships in preclinical drug discovery and development: considerations toward a synergistic lingua franca. *Expert Opin Drug Discov*, *7* (6), 449-56.

Jardemark, K., M. L. Wadenberg, P. Grillner, and T. H. Svensson. (2002). Dopamine D3 and D4 receptor antagonists in the treatment of schizophrenia. *Curr Opin Investig Drugs*, *3* (1), 101-5.

Jeanblanc, J., D. Y. He, N. N. McGough, M. L. Logrip, K. Phamluong, P. H. Janak, and D. Ron. (2006). The dopamine D3 receptor is part of a homeostatic pathway regulating ethanol consumption. *J Neurosci*, *26* (5), 1457-64.

Joffe, R. T., A. J. Levitt, and S. T. Sokolov. (1996). Augmentation strategies: focus on anxiolytics. *J Clin Psychiatry*, *57* Suppl *7*, 25-31, discussion 32-3.

Joseph-McCarthy, D., J. C. Baber, E. Feyfant, D. C. Thompson, and C. Humblet. (2007). Lead optimization via high-throughput molecular docking. *Curr Opin Drug Discov Devel*, *10* (3), 264-74.

Judd, L. L. (2001). Major depressive disorder: longitudinal symptomatic structure, relapse and recovery. *Acta Psychiatr Scand*, *104* (2), 81-3.

Kar, S., and K. Roy. (2013). How far can virtual screening take us in drug discovery? *Expert Opin Drug Discov*, *8* (3), 245-61.

Kazius, J., R. McGuire, and R. Bursi. (2005). Derivation and validation of toxicophores for mutagenicity prediction. *J Med Chem*, *48* (1), 312-20.

Kessler, R. C. 2012. The costs of depression. *Psychiatr Clin North Am*, *35* (1), 1-14.

Khanna, I. (2012). Drug discovery in pharmaceutical industry: productivity challenges and trends. *Drug Discov Today*, *17* (19-20), 1088-102.

Khedkar, S. A. (2010). Current computational approaches in medicinal chemistry. *Curr Top Med Chem*, *10* (1), 1-2.

Kirchmair, J., S. Distinto, D. Schuster, G. Spitzer, T. Langer, and G. Wolber. (2008). Enhancing drug discovery through in silico screening: strategies to increase true positives retrieval rates. *Curr Med Chem*, *15* (20), 2040-53.

Kobayashi, M., and K. Naito. (2000). Pharmacological profiles of the potent carbonic anhydrase inhibitor dorzolamide hydrochloride, a topical antiglaucoma agent. *Nihon Yakurigaku Zasshi*, *115* (6), 323-8.

Koltun, D. O., N. I. Vasilevich, E. Q. Parkhill, A. I. Glushkov, T. M. Zilbershtein, E. I. Mayboroda, M. A. Boze, A. G. Cole, I. Henderson, N. A. Zautke, S. A. Brunn, N. Chu, J. Hao, N. Mollova, K. Leung, J. W. Chisholm, and J. Zablocki. (2009). Orally bioavailable, liver-selective stearoyl-CoA desaturase (SCD) inhibitors. *Bioorg Med Chem Lett*, *19* (11), 3050-3.

Kontoyianni, M., L. M. McClellan, and G. S. Sokol. (2004). "Evaluation of docking performance: comparative data on docking algorithms. *J Med Chem*, *47* (3), 558-65.

Krueger, B. A., A. Dietrich, K. H. Baringhaus, and G. Schneider. (2009). Scaffold-hopping potential of fragment-based de novo design: the chances and limits of variation. *Comb Chem High Throughput Screen*, *12* (4), 383-96.

Kulkarni, S. K., and A. Dhir. (2009). Current investigational drugs for major depression. *Expert Opin Investig Drugs*, *18* (6), 767-88.

Kutchukian, P. S., and E. I. Shakhnovich. (2010). De novo design: balancing novelty and confined chemical space. *Expert Opin Drug Discov*, *5* (8), 789-812.

Lahana, R. (1999). How many leads from HTS? *Drug Discov Today*, *4* (10), 447-448.

Lakatos, L., and Z. Rihmer. 2005. [1+1 or 2x1? Another form of dual antidepressive mechanism of action]. *Neuropsychopharmacol Hung* no, *7* (3), 118-24.

Lapidus, K. A., C. F. Levitch, A. M. Perez, J. W. Brallier, M. K. Parides, L. Soleimani, A. Feder, D. V. Iosifescu, D. S. Charney, and J. W. Murrough. (2014). A Randomized Controlled Trial of Intranasal Ketamine in Major Depressive Disorder. *Biol Psychiatry*, Doi: 10.1016/j.biopsych.2014.03.026.

Lauri, G., and P. A. Bartlett. (1994). CAVEAT: a program to facilitate the design of organic molecules. *J Comput Aided Mol Des*, *8* (1), 51-66.

Leggio, G. M., G. Camillieri, C. B. Platania, A. Castorina, G. Marrazzo, S. A. Torrisi, C. N. Nona, V. D'Agata, J. Nobrega, H. Stark, C. Bucolo, B. Le Foll, F. Drago, and S. Salomone. (2014). Dopamine D3 Receptor Is Necessary for Ethanol Consumption: An Approach with Buspirone. *Neuropsychopharmacology*, *39* (8), 2017-28.

Lewell, X. Q., D. B. Judd, S. P. Watson, and M. M. Hann. (1998). RECAP--retrosynthetic combinatorial analysis procedure: a powerful new technique for identifying privileged molecular fragments with useful applications in combinatorial chemistry. *J Chem Inf Comput Sci*, *38* (3), 511-22.

Li, Y., L. Han, Z. Liu, and R. Wang. (2014). Comparative Assessment of Scoring Functions on an Updated Benchmark: II. Evaluation Methods and General Results. *J Chem Inf Model*, *54* (6), 1717-36.

Li, Y., Z. Liu, J. Li, L. Han, J. Liu, Z. X. Zhao, and R. Wang. (2014). Comparative Assessment of Scoring Functions on an Updated Benchmark: I. Compilation of the Test Set. *J Chem Inf Model*, *54* (6), 1700-16.

Li, Z., Y. Yang, J. Zhan, L. Dai, and Y. Zhou. (2013). Energy functions in de novo protein design: current challenges and future prospects. *Annu Rev Biophys*, *42*, 315-35.

Lipinski, C., and A. Hopkins. (2004). Navigating chemical space for biology and medicine. *Nature*, *432* (7019), 855-61.

Liu, B., S. Li, and J. Hu. (2004). Technological advances in high-throughput screening. *Am J Pharmacogenomics*, *4* (4), 263-76.

Liu, Q., B. Masek, K. Smith, and J. Smith. (2007). Tagged fragment method for evolutionary structure-based de novo lead generation and optimization. *J Med Chem*, *50* (22), 5392-402.

Lloyd, D. G. (2013). Approaches to Scaffold Hopping. *Drug Discov Today Technol*, *10* (4), e451-2.

Lopez-Munoz, F., and C. Alamo. (2009). Monoaminergic neurotransmission: the history of the discovery of antidepressants from 1950s until today. *Curr Pharm Des*, *15* (14), 1563-86.

Loving, K., I. Alberts, and W. Sherman. (2010). Computational approaches for fragment-based and de novo design. *Curr Top Med Chem*, *10* (1), 14-32.

Lundstrom, K. (2009). An overview on GPCRs and drug discovery: structure-based drug design and structural biology on GPCRs. *Methods Mol Biol*, *552*, 51-66.

Maass, P., T. Schulz-Gasch, M. Stahl, and M. Rarey. (2007). Recore: a fast and versatile method for scaffold hopping based on small molecule crystal structure conformations. *J Chem Inf Model*, *47* (2), 390-9.

Maehr, H. (1997). Combinatorial chemistry in drug research from a new vantage point. *Bioorg Med Chem*, *5* (3), 473-91.

Manosso, L. M., M. Moretti, and A. L. Rodrigues. (2013). Nutritional strategies for dealing with depression. *Food Funct*, *4* (12), 1776-93.

Martelle, J. L., and M. A. Nader. (2008). A review of the discovery, pharmacological characterization, and behavioral effects of the dopamine D2-like receptor antagonist eticlopride. *CNS Neurosci Ther*, *14* (3), 248-62.

Martin, Y. C. (1992). 3D database searching in drug design. *J Med Chem*, *35* (12), 2145-54.

Martin, Y. C., M. G. Bures, E. A. Danaher, J. DeLazzer, I. Lico, and P. A. Pavlik. (1993). A fast new approach to pharmacophore mapping and its application to dopaminergic and benzodiazepine agonists. *J Comput Aided Mol Des*, *7* (1), 83-102.

Mauser, H., and W. Guba. (2008). Recent developments in de novo design and scaffold hopping. *Curr Opin Drug Discov Devel*, *11* (3), 365-74.

Mayr, L. M., and D. Bojanic. (2009). Novel trends in high-throughput screening. *Curr Opin Pharmacol*, *9* (5), 580-8.

Moal, I. H., M. Torchala, P. A. Bates, and J. Fernandez-Recio. (2013). The scoring of poses in protein-protein docking: current capabilities and future directions. *BMC Bioinformatics*, 14, 286.

Mogg, K., B. P. Bradley, B. O'Neill, M. Bani, E. Merlo-Pich, A. Koch, E. T. Bullmore, and P. J. Nathan. (2012). Effect of dopamine D(3) receptor antagonism on approach responses to food cues in overweight and obese individuals. *Behav Pharmacol*, *23* (5-6), 603-8.

Muench, J., and A. M. Hamer. (2010). Adverse effects of antipsychotic medications. *Am Fam Physician*, *81* (5), 617-22.

Murrough, J. W., D. V. Iosifescu, L. C. Chang, R. K. Al Jurdi, C. E. Green, A. M. Perez, S. Iqbal, S. Pillemer, A. Foulkes, A. Shah, D. S. Charney, and S. J. Mathew. (2013). Antidepressant efficacy of ketamine in treatment-resistant major depression: a two-site randomized controlled trial. *Am J Psychiatry*, *170* (10), 1134-42.

Nettles, J. H., J. L. Jenkins, A. Bender, Z. Deng, J. W. Davies, and M. Glick. (2006). Bridging chemical and biological space: target fishing using 2D and 3D molecular descriptors. *J Med Chem*, *49* (23), 6802-10.

Newman, A. H., T. Beuming, A. K. Banala, P. Donthamsetti, K. Pongetti, A. LaBounty, B. Levy, J. Cao, M. Michino, R. R. Luedtke, J. A. Javitch, and L. Shi. (2012). Molecular determinants of selectivity and efficacy at the dopamine D3 receptor. *J Med Chem*, *55* (15), 6689-99.

Newman, A. H., B. L. Blaylock, M. A. Nader, J. Bergman, D. R. Sibley, and P. Skolnick. (2012). Medication discovery for addiction: translating the dopamine D3 receptor hypothesis. *Biochem Pharmacol*, *84* (7), 882-90.

Newman, A. H., P. Grundt, and M. A. Nader. (2005). Dopamine D3 receptor partial agonists and antagonists as potential drug abuse therapeutic agents. *J Med Chem*, *48* (11), 3663-79.

Nishida, A., T. Miyaoka, T. Inagaki, and J. Horiguchi. (2009). New approaches to antidepressant drug design: cytokine-regulated pathways. *Curr Pharm Des*, *15* (14), 1683-7.

Nolan, T. L., D. J. Lapinsky, J. N. Talbot, M. Indarte, Y. Liu, S. Manepalli, L. M. Geffert, M. E. Amos, P. N. Taylor, J. D. Madura, and C. K. Surratt. (2011). Identification of a novel selective serotonin reuptake inhibitor by coupling monoamine transporter-based virtual screening and rational molecular hybridization. *ACS Chem Neurosci*, *2* (9), 544-552.

Nolen, W. A., J. J. van de Putte, W. A. Dijken, J. S. Kamp, B. A. Blansjaar, H. J. Kramer, and J. Haffmans. (1988). Treatment strategy in depression. I. Non-tricyclic and selective reuptake inhibitors in resistant depression: a double-blind partial crossover study on the effects of oxaprotiline and fluvoxamine. *Acta Psychiatr Scand*, *78* (6), 668-75.

O'Boyle, N. M., M. Banck, C. A. James, C. Morley, T. Vandermeersch, and G. R. Hutchison. (2011). Open Babel: An open chemical toolbox. *J Cheminform*, *3*, 33.

Opal, M. D., S. C. Klenotich, M. Morais, J. Bessa, J. Winkle, D. Doukas, L. J. Kay, N. Sousa, and S. M. Dulawa. (2013). Serotonin 2C receptor antagonists induce fast-onset antidepressant effects. *Mol Psychiatry*. Doi: 10.1038/mp.2013.144

Oprea, T. I. (2000). Property distribution of drug-related chemical databases. *J Comput Aided Mol Des*, *14* (3), 251-64.

Ou-Yang, S. S., J. Y. Lu, X. Q. Kong, Z. J. Liang, C. Luo, and H. Jiang. (2012). Computational drug discovery. *Acta Pharmacol Sin*, *33* (9), 1131-40.

Overington, J. P., B. Al-Lazikani, and A. L. Hopkins. (2006). How many drug targets are there? *Nat Rev Drug Discov*, *5* (12), 993-6.

P. Roy, Y. Leblanc, R. G. Ball, C. Birdeau, C. C. Chan, N. Chauret, W. Cromlish, D. Ethier, J. Y. Gauthier, R. Gordon, G. Greig, J. Guay, S. Kargman, C. K. Lau, G. O'Neill, J. Silva, M. Thérien, C. van Staden, E. Wong, L. Xu, P. Prasit. (1997). A new series of selective COX-2 inhibitors: 5,6-diarylthiazolo[3,2-b][1,2,4]triazoles. *Bioorganic & Medicinal Chemistry Letters*, *7* (1), 57-62.

Pacher, P., E. Kohegyi, V. Kecskemeti, and S. Furst. (2001). Current trends in the development of new antidepressants. *Curr Med Chem*, *8* (2), 89-100.

Palmeira, A., E. Sousa, M. H. Vasconcelos, M. Pinto, and M. X. Fernandes. (2012). Structure and ligand-based design of P-glycoprotein inhibitors: a historical perspective. *Curr Pharm Des*, *18* (27), 4197-214.

Pang, Y. P. (2007). In silico drug discovery: solving the target-rich and lead-poor imbalance using the genome-to-drug-lead paradigm. *Clin Pharmacol Ther*, *81* (1), 30-4.

Paul, S. M., D. S. Mytelka, C. T. Dunwiddie, C. C. Persinger, B. H. Munos, S. R. Lindborg, and A. L. Schacht. (2010). How to improve R&D productivity: the pharmaceutical industry's grand challenge. *Nat Rev Drug Discov*, *9* (3), 203-14.

Paykel, E. S. (1998). Remission and residual symptomatology in major depression. *Psychopathology*, *31* (1), 5-14.

Penn, E., and D. K. Tracy. (2012). The drugs don't work? antidepressants and the current and future pharmacological management of depression. *Ther Adv Psychopharmacol*, *2* (5), 179-88.

Perola, E., W. P. Walters, and P. S. Charifson. (2004). A detailed comparison of current docking and scoring methods on systems of pharmaceutical relevance. *Proteins*, *56* (2), 235-49.

Pinder, R. M. (1997). Designing a new generation of antidepressant drugs. *Acta Psychiatr Scand Suppl*, *391*, 7-13.

Pirard, B. (2011). The quest for novel chemical matter and the contribution of computer-aided de novo design. *Expert Opin Drug Discov*, *6* (3), 225-31.

Pratuangdejkul, J., B. Schneider, J. M. Launay, O. Kellermann, and P. Manivet. (2008). Computational approaches for the study of serotonin and its membrane transporter SERT: implications for drug design in neurological sciences. *Curr Med Chem*, *15* (30), 3214-27.

Quintus, F., O. Sperandio, J. Grynberg, M. Petitjean, and P. Tuffery. (2009). Ligand scaffold hopping combining 3D maximal substructure search and molecular similarity. *BMC Bioinformatics*, *10*, 245.

Rajamani, R., and A. C. Good. (2007). Ranking poses in structure-based lead discovery and optimization: current trends in scoring function development. *Curr Opin Drug Discov Devel*, *10* (3), 308-15.

Ramesha, C. S. (2000). How many leads from HTS? - Comment. *Drug Discov Today*, *5* (2), 43-44.

Rester, U. (2008). From virtuality to reality - Virtual screening in lead discovery and lead optimization: a medicinal chemistry perspective. *Curr Opin Drug Discov Devel*, *11* (4), 559-68.

Robinson, S. W., K. R. Jarvie, and M. G. Caron. 1994. High affinity agonist binding to the dopamine D3 receptor: chimeric receptors delineate a role for intracellular domains. *Mol Pharmacol*, *46* (2), 352-6.

Rosenzweig-Lipson, S., C. E. Beyer, Z. A. Hughes, X. Khawaja, S. J. Rajarao, J. E. Malberg, Z. Rahman, R. H. Ring, and L. E. Schechter. (2007). Differentiating antidepressants of the future: efficacy and safety. *Pharmacol Ther*, *113* (1), 134-53.

Russ, A. P., and S. Lampel. (2005). The druggable genome: an update. *Drug Discov Today*, *10* (23-24), 1607-10.

Sarah R. Langdon, Peter Erti and Nathan Brown. (2010). Bioisosteric replacement and scaffold hopping in lead generation and optimization. *Molecular Informatics*, *29* (5), 366-385.

Schacter, L. P., C. Anderson, R. M. Canetta, S. Kelley, C. Nicaise, N. Onetto, M. Rozencweig, L. Smaldone, and B. Winograd. (1992). Drug discovery and development in the pharmaceutical industry. *Semin Oncol*, *19* (6), 613-21.

Schneider, G. (2002). Trends in virtual combinatorial library design. *Curr Med Chem*, *9* (23), 2095-101.

Schneider, G., and U. Fechner. (2005). Computer-based de novo design of drug-like molecules. *Nat Rev Drug Discov*, *4* (8):649-63.

Schneider, G., T. Geppert, M. Hartenfeller, F. Reisen, A. Klenner, M. Reutlinger, V. Hahnke, J. A. Hiss, H. Zettl, S. Keppner, B. Spankuch, and P. Schneider. (2011). Reaction-driven de novo design, synthesis and testing of potential type II kinase inhibitors. *Future Med Chem*, *3* (4), 415-24.

Schneider, G., W. Neidhart, T. Giller, and G. Schmid. (1999). Scaffold-Hopping by Topological Pharmacophore Search: A Contribution to Virtual Screening. *Angew Chem Int Ed Engl*, *38* (19), 2894-2896.

Schuffenhauer, A., P. Ertl, S. Roggo, S. Wetzel, M. A. Koch, and H. Waldmann. (2007). The scaffold tree--visualization of the scaffold universe by hierarchical scaffold classification. *J Chem Inf Model*, *47* (1), 47-58.

SciFinder; Chemical Abstracts Service: Columbus, OH; carbon-13 NMR spectrum; https://scifinder.cas.org (accessed June 21, 2012).

Segall, M., E. Champness, C. Leeding, R. Lilien, R. Mettu, and B. Stevens. (2011). Applying medicinal chemistry transformations and multiparameter optimization to guide the search for high-quality leads and candidates. *J Chem Inf Model*, *51* (11), 2967-76.

Segall, M., E. Champness, O. Obrezanova, and C. Leeding. (2009). Beyond profiling: using ADMET models to guide decisions. *Chem Biodivers*, *6* (11), 2144-51.

Seifert, M. H., J. Kraus, and B. Kramer. (2007). Virtual high-throughput screening of molecular databases. *Curr Opin Drug Discov Devel*, *10* (3), 298-307.

Semba, J. (2004). [Functional role of dopamine D3 receptor in schizophrenia]. *Nihon Shinkei Seishin Yakurigaku Zasshi*, *24* (1), 3-11.

Service, SciFinder; Chemical Abstracts. June 21 (2012). Columbus, OH.

Shekhar, C. (2008). In silico pharmacology: computer-aided methods could transform drug development. *Chem Biol*, *15* (5), 413-4.

Shi, L., and J. A. Javitch. (2002). The binding site of aminergic G protein-coupled receptors: the transmembrane segments and second extracellular loop. *Annu Rev Pharmacol Toxicol*, *42*, 437-67.

Shoichet, B. K., S. L. McGovern, B. Wei, and J. J. Irwin. (2002). Lead discovery using molecular docking. *Curr Opin Chem Biol*, *6* (4), 439-46.

Singh, Y. P., and R. A. Singh. (2010). Insilico studies of organosulfur-functional active compounds in garlic. *Biofactors*, *36* (4), 297-311..

Slattery, D. A., A. L. Hudson, and D. J. Nutt. (2004). Invited review: the evolution of antidepressant mechanisms. *Fundam Clin Pharmacol*, *18* (1), 1-21.

Sliwoski, G., S. Kothiwale, J. Meiler, and E. W. Lowe, Jr. (2014). Computational methods in drug discovery. *Pharmacol Rev*, *66* (1), 334-95.

Sokoloff, P., B. Giros, M. P. Martres, M. L. Bouthenet, and J. C. Schwartz. (1990). Molecular cloning and characterization of a novel dopamine receptor (D3) as a target for neuroleptics. *Nature*, *347* (6289), 146-51.

Song, C. M., S. J. Lim, and J. C. Tong. (2009). Recent advances in computer-aided drug design. *Brief Bioinform*, *10* (5), 579-91.

Sourial, Alain Deschenes and Elizabeth. (2007). Ligand Scaffold Replacement using MOE Pharmacophore Tools. *Chemical Computing Group.*

Spankuch, B., S. Keppner, L. Lange, T. Rodrigues, H. Zettl, C. P. Koch, M. Reutlinger, M. Hartenfeller, P. Schneider, and G. Schneider. (2013). Drugs by numbers: reaction-driven de novo design of potent and selective anticancer leads. *Angew Chem Int Ed Engl*, *52* (17), 4676-81.

Stewart, K. D., M. Shiroda, and C. A. James. (2006). Drug Guru: a computer software program for drug design using medicinal chemistry rules. *Bioorg Med Chem*, *14* (20), 7011-22.

Strader, C. D., T. Gaffney, E. E. Sugg, M. R. Candelore, R. Keys, A. A. Patchett, and R. A. Dixon. (1991). Allele-specific activation of genetically engineered receptors. *J Biol Chem*, *266* (1), 5-8.

Sun, H., G. Tawa, and A. Wallqvist. (2012). Classification of scaffold-hopping approaches. *Drug Discov Today*, *17* (7-8), 310-24.

Taft, C. A., V. B. Da Silva, and C. H. Da Silva. (2008). Current topics in computer-aided drug design. *J Pharm Sci*, *97* (3), 1089-98.

Talele, T. T., S. A. Khedkar, and A. C. Rigby. (2010). Successful applications of computer aided drug discovery: moving drugs from concept to the clinic. *Curr Top Med Chem*, *10* (1), 127-41.

Tang, L., R. D. Todd, and K. L. O'Malley. (1994). Dopamine D2 and D3 receptors inhibit dopamine release. *J Pharmacol Exp Ther*, *270* (2), 475-9.

Thanos, P. K., J. M. Katana, C. R. Ashby, Jr., M. Michaelides, E. L. Gardner, C. A. Heidbreder, and N. D. Volkow. (2005). The selective dopamine D3 receptor antagonist SB-277011-A attenuates ethanol consumption in ethanol preferring (P) and non-preferring (NP) rats. *Pharmacol Biochem Behav*, *81* (1), 190-7.

Therrien, E., P. Englebienne, A. G. Arrowsmith, R. Mendoza-Sanchez, C. R. Corbeil, N. Weill, V. Campagna-Slater, and N. Moitessier. (2012). Integrating medicinal chemistry, organic/combinatorial chemistry, and computational chemistry for the discovery of selective estrogen receptor modulators with Forecaster, a novel platform for drug discovery. *J Chem Inf Model*, *52* (1), 210-24.

Trivedi, M. H., A. J. Rush, S. R. Wisniewski, A. A. Nierenberg, D. Warden, L. Ritz, G. Norquist, R. H. Howland, B. Lebowitz, P. J. McGrath, K. Shores-Wilson, M. M. Biggs, G. K. Balasubramani, and M. Fava. (2006). Evaluation of outcomes with citalopram for depression using measurement-based care in STAR*D: implications for clinical practice. *Am J Psychiatry*, *163* (1), 28-40.

Tsunoyama, K., A. Amini, M. J. Sternberg, and S. H. Muggleton. (2008). Scaffold hopping in drug discovery using inductive logic programming. *J Chem Inf Model*, *48* (5), 949-57.

Tversky, A. (1977). Features of similarity. *Psychological Review*, *84* (4), 28.

Uher, R., O. Mors, M. Rietschel, A. Rajewska-Rager, A. Petrovic, A. Zobel, N. Henigsberg, J. Mendlewicz, K. J. Aitchison, A. Farmer, and P. McGuffin. (2011). Early and delayed onset of response to antidepressants in individual trajectories of change during treatment of major depression: a secondary analysis of data from the Genome-Based Therapeutic Drugs for Depression (GENDEP) study. *J Clin Psychiatry*, *72* (11), 1478-84.

Vaino MJ, Thierry Kogej, Florian Raubacher, and Jens Sadowski. (2013). Scaffold Hopping by fragment replacement. *J Chem Inf Model*, *53* (7), 1825-35.

Vijayakrishnan, R. (2009). Structure-based drug design and modern medicine. *J Postgrad Med*, *55* (4), 301-4.

Vilar, S., R. Harpaz, L. Santana, E. Uriarte, and C. Friedman. (2012). Enhancing adverse drug event detection in electronic health records using molecular structure similarity: application to pancreatitis. *PLoS One*, *7* (7), e41471.

Vilar, S., R. Harpaz, E. Uriarte, L. Santana, R. Rabadan, and C. Friedman. (2012). Drug-drug interaction through molecular structure similarity analysis. *J Am Med Inform Assoc* no. *19* (6), 1066-74.

Wang, R., Y. Lu, and S. Wang. (2003). Comparative evaluation of 11 scoring functions for molecular docking. *J Med Chem*, *46* (12), 2287-303.

Warren, G. L., C. W. Andrews, A. M. Capelli, B. Clarke, J. LaLonde, M. H. Lambert, M. Lindvall, N. Nevins, S. F. Semus, S. Senger, G. Tedesco, I. D. Wall, J. M. Woolven, C. E. Peishoff, and M. S. Head. (2006). A critical assessment of docking programs and scoring functions. *J Med Chem*, *49* (20), 5912-31.

Westenberg, H. G. (1999). Pharmacology of antidepressants: selectivity or multiplicity? *J Clin Psychiatry*, *60* Suppl 17, 4-8; discussion 46-8.

Wildman, S. A., and G. M. Crippen. (2001). Evaluation of ligand overlap by atomic parameters. *J Chem Inf Comput Sci*, *41* (2), 446-50.

Willett, P. (2006). Similarity-based virtual screening using 2D fingerprints. *Drug Discov Today,* *11* (23-24), 1046-53.

Wilson, G. L., and M. A. Lill. (2011). Integrating structure-based and ligand-based approaches for computational drug design. *Future Med Chem*, *3* (6), 735-50.

Wong, D. T., K. W. Perry, and F. P. Bymaster. (2005). Case history: the discovery of fluoxetine hydrochloride (Prozac). *Nat Rev Drug Discov*, *4* (9), 764-74.

Yera, E. R., A. E. Cleves, and A. N. Jain. (2011). Chemical structural novelty: on-targets and off-targets. *J Med Chem*, *54* (19), 6771-85.

Zhao, H. (2007). Scaffold selection and scaffold hopping in lead generation: a medicinal chemistry perspective. *Drug Discov Today*, *12* (3-4), 149-55.